Engineering environments to prolong *in vitro* survival of human hematopoietic stem cells

A dissertation

submitted by

Dean Liang Glettig

In partial fulfillment of the requirements
for the degree of

Doctor of Philosophy

in

Biomedical Engineering

TUFTS UNIVERSITY

Date

May 2012

COMMITTEE:

David L. Kaplan, Ph.D.
Catherine K. Kuo, Ph.D.
Pamela C. Yelick, Ph.D.
Clifford J. Rosen, M.D.

ABSTRACT

Slight abnormalities in the bone marrow can have very severe consequences, which can be observed in many bone marrow-related diseases, the most well known one being leukemia. To date very limited treatment options exist for theses diseases and generally a stem cell transplant is required for a full cure. These transplants are not only risky but often fail at the stage of search for a compatible donor. A major reason for the absence of potent treatment alternatives is that many molecular and cellular interactions within the bone marrow are still unknown. To advance the cure of bone marrow-related diseases, several groups are trying to develop a sustainable and functional human bone marrow model that can serve two long-term purposes:

- Assess the effects of new drugs on bone marrow cells prior to human trials. This will not only remove xenogeneic risks, but likely also reduce the need for animal testing.
- Provide long-term proliferation of whole bone marrow *in vitro* as a practical and cost effective source of stem cells. These cells can be used for research but also help to establish a bank with a wide range of stem cells that will facilitate donor matching for transplants.

We have worked towards achieving these long-term goals by designing environments that extend hematopoietic stem cell (HSC) culture time *in vitro*. Specifically we increased HSC survival rate by:

- Determining an optimal medium for stem cell engraftment that supports both proliferation and quiescence.
- Adding adipocytes to currently established feeder layer models to inhibit stem cell differentiation.
- Creating a 3D construct and perfusion system that supports long-term culture.

Using our methods we concluded the following:

- There are two $CD34^+$ populations within the bone marrow that differ in size.
- The smaller cells are more quiescent and possibly more primitive than the larger cells.
- hMSCs differentiation potential rapidly declines when expanding using traditional culture methods.
- The use of the conventional markers for hMSCs does not suffice in the definition of a true stem cell.
- The use of the more novel markers CD146 and CD271 would more likely be appropriate markers of stemness.
- hASCs had an increased CD34 expression when compared to hMSCs.
- An improvement of $CD34^+$ *in vitro* survival rate was achieved when using a feeder layer containing adipocytes.
- Direct cell-cell contact is necessary for the expansion of the hHSCs.
- Long-term culture 2D is limited by the functionality or peeling of the feeder layers. Therefore a construct for 3D bone marrow culture is of great necessity.
- Using a multiple seeding method one can obtain a confluent 3D structure on a silk scaffold.
- A unidirectional slow perfusion bioreactor is a promising device to maintain *in vitro* 3D bone marrow culture.

ACKNOWLEDGMENTS

I would like to thank:

My committee members David Kaplan, Catherine Kuo, Pamela Yelick, and Clifford Rosen for their support and interest in my research.

Kelly Burke, Chris Cannizzaro, Tessa DesRochers, Michael House, Hyeon Joo Kim, Amanda Murphy, Michaela Reagan, Isabella Pallotta, William Rice, Philipp Seib and Sarah Sundelacruz for their inputs and assistance in this project.

Nicholas Bayhi, Eddie Hong, Kasey Mitchell, Kristina Papa, Emily Shaw, and Christina Thomas for the tremendous assistance with cell culture and pushing my knowledge by asking me questions that I couldn't always answer.

The NIH Tissue Engineering Resource Center for financial support of this research.

The many people of the Kaplan Lab and office 153, past and present, not only for the scientific support, but also making SciTech feel like a second home.

Allen Parmelee and Stephen Kwok for support with flow cytometric analysis and giving me a third home at the downtown campus.

David Kaplan, Carmen Preda, Milva Ricci, Keleigh Sanford and all the faculty members of the Department of Biomedical Engineering for supporting me during my PhD.

Lorenz Meinel and his group at ETHZ for establishing the connection to Boston.

Bertan Hallacoglu and Philipp Seib for being lunch-box buddies.

My parents and family for their constant support in all that I'm doing.

My amazing fiancée Kendra, for not only taking care of me but also constantly motivating me to achieve my goals.

TABLE OF CONTENTS

Abstract ii

Acknowledgments iv

Table of Contents v

List of Tables viii

List of Figures ix

Chapter I - The Bone Marrow Tissue 1

Hematopoietic cells 1

Stromal cells 2

Niche Theory 3

Red versus yellow bone marrow 5

Functionality of marrow fat 6

Medical relation 9

Current models 12

Hypothesis 13

Novel Approach 14

Chapter II – Tools in Human Hematopoietic Stem Cell Culture 16

Current knowledge 16

Culture medium 18

Cell sources 20

Isolation of HSCs 22

MSC feeder layer 39

Chapter III - Analysis of Feeder Layers 41

Introduction 41

Materials and Methods 44

Results 50

Discussion 57
Conclusions 61
Supplementary Data 62
Chapter IV - Extending HSC Survival *In Vitro* with Adipocytes 69
Introduction 69
Materials and Methods 71
Results 77
Discussion 83
Contact requirement of feeder cells 87
Materials and Methods 87
Results 88
Discussion 88
Varying the amount of adipocytes 89
Materials and Methods 90
Results 90
Discussion 91
Chapter V – 3D Yellow Bone Marrow Culture 93
Limitations of 2D studies 93
Silk as scaffold substrate 93
General Materials and Methods 94
Coating with bone matrix proteins 97
Coating with softer matrix proteins 102
Multiple seedings 111
Perfusion Culture 114
Comparison of the U-tube and the unidirectional perfusion bioreactor 120
Materials and Methods 121
Results 122

Discussion 123

Chapter VI – Conclusions and Future Directions 125

Abbreviations 128

Bibliography 131

LIST OF TABLES

Table 1.1.	Correlation of key elements in an *in vivo* bone marrow transplant with steps in *in vitro* HSC culture.	14
Table 2.1.	Comparison of surface markers defining hematopoietic stem cells (HSC) and multipotent progenitor cells (MPP) in mouse and human species (Seita and Weissman 2010).	17
Table 2.2.	Summary of shoe print region analysis of $CD34^{+}$ cells.	38
Table 3.1.	List of surface marker profiles used in the literature to define MSCs.	42
Suppl. Table 3.1.	List of flow cytometry markers included in this study. Descriptions extracted from NCBI RefSeq (Pruitt, Tatusova et al. 2009) and UniProt (Consortium 2011).	66
Suppl. Table 3.2.	Cell populations analyzed and cumulative time in culture before each passage in days. An additional 21 days should be added to determine the *in vitro* culture time of differentiated cells before analysis.	68

LIST OF FIGURES

Fig. 1.1.	Differentiation pathways of hematopoietic stem cells (adapted from (Tyler 2005)).	1
Fig. 1.2.	Diagram of the bone marrow niches (adapted from (Wilson and Trumpp 2006)).	4
Fig. 1.3.	Structural location of bone marrow (adapted from (Tyler 2005; Marieb 2009)).	5
Fig. 1.4.	Overview of the elements of the project.	14
Fig. 2.1.	Percentage of $CD34^+$ cells when expanded in different culture media.	19
Fig. 2.2.	Photo of a tube containing an aspirate of fresh human bone marrow.	20
Fig. 2.3.	Two common methods to remove RBCs.	22
Fig. 2.4.	Principles of flow cytometry.	25
Fig. 2.5.	Time-lapsed scatter plot of human bone marrow mononuclear cells.	27
Fig. 2.6.	Immunophenotyping the two cell populations.	28
Fig. 2.7.	Cell cycle analysis of the two cell populations (adapted from (Gothot, Pyatt et al. 1997).	30
Fig. 2.8.	Cell characterization of the two cell populations using an imaging flow cytometer.	31

Fig. 2.9.	Cell characterization of the two cell populations using an imaging flow cytometer.	33
Fig. 2.10.	CFC colony assay.	35
Fig. 2.11.	CFC and LTC-IC colony assays of shoe print regions.	37
Fig. 2.12.	Schematic of extraction procedure for MSCs.	39
Fig. 3.1.	Outline of the procedure.	44
Fig. 3.2.	Microscopic images of MSC1 cells at each passage pre- and post-differentiation.	51
Fig. 3.3.	Relative gene expression of MSC1 cells.	52
Fig. 3.4.	Flow cytometric analysis of MSC1 cells.	54
Fig. 3.5.	Flow cytometric profile of undifferentiated cells given in percentages of total population.	55
Fig. 3.6.	Autofluorescence of MSC1 cells.	56
Suppl. Fig. 3.1.	Microscopic images of MSC2 and ASC2 cells at each passage.	62
Suppl. Fig. 3.2.	Relative gene expression of adipogenic markers on ASC2 cells.	63
Suppl. Fig. 3.3.	Flow cytometric analysis of MSC2 and ASC2 cells.	64

Suppl. Fig. 3.4.	Autofluorescence of MSC2 and ASC2 cells.	65
Fig. 4.1.	Flow cytometric quantification of $CD34^+$ cells remaining in the feeder cultures in minimal medium.	78
Fig. 4.2.	Flow cytometric quantification of $CD34^+$ cells in both hMSC as well as adipogenic feeder cultures.	79
Fig. 4.3.	Photograph of a well with feeder cells contracting.	80
Fig. 4.4.	Microscope images of hMSCs after 3 weeks of adipogenic differentiation.	81
Fig. 4.5.	Percentage of $CD34^+$ cells in P0 and P2 derived feeder layers alone, compared to fresh bone marrow.	82
Fig. 4.6.	Flow cytometric quantification of $CD34^+$ cells cultured on P0 MSC feeder layers as well as adipogenic feeder layers derived from both P0 and P2 hMSCs.	83
Fig. 4.7.	Flow cytometric quantification of $CD34^+$ cells in both hMSC as well as adipogenic feeder cultures.	88
Fig. 4.8.	Flow cytometric quantification of $CD34^+$ cells in feeder cultures with varying amounts of adipocytes.	91
Fig. 5.1.	Confocal images of aqueous-derived silk scaffolds, pore-size: 300 - 400 μm, seeded once with hMSCs.	99

Fig. 5.2. Confocal image at 20x magnification of aqueous-derived silk scaffold, coated with 1mg/mL collagen I, pore-size: 300 - 400 μm, seeded once with P2 hMSCs. 100

Fig. 5.3. Time-lapsed, flow cytometric quantification of $CD34^+$ population in 3D silk scaffolds kept uncoated (blue), coated with collagen I (green), hydroxyapatite (red), and fibronectin (purple). 101

Fig. 5.4. Confocal images of aqueous-derived silk scaffolds, pore-size: 300 - 400 μm, seeded once with hMSCs. 106

Fig. 5.5. Time-lapsed, flow cytometric quantification of $CD34^+$ population in 3D silk scaffolds kept uncoated (blue), coated with collagen IV (red), matrigel (green), and tropoelastin (purple). 107

Fig. 5.6. Time-lapsed, CFC assay of $CD34^+$ population in 3D silk scaffolds kept uncoated (green), coated with collagen IV (yellow), matrigel (red), and tropoelastin (purple). 108

Fig. 5.7. Confocal images of aqueous-derived silk scaffolds, pore-size: 300 - 400 μm, seeded (A) twice and (B-D) three times with hMSCs. 112

Fig. 5.8. Diagram and photograph of U-tube perfusion bioreactor. 115

Fig. 5.9. Diagram of new unidirectional perfusion bioreactor. 119

Fig. 5.10. Photographs of new unidirectional perfusion bioreactor in incubator. 120

Fig. 5.11. Flow cytometric quantification of $CD34^+$ cells in 3D perfusion cultures. 122

CHAPTER I - THE BONE MARROW TISSUE

Situated in the medullary cavities of bones, bone marrow (Latin: *medulla ossium*) is a soft tissue comprised of many different cell types. The vast majority of these cell types can be assigned to either of two cell lines based on their functionality: hematopoietic and stromal cells.

Hematopoietic cells

The predominant cell types within the bone marrow are hematopoietic cells. These are mostly non-adherent cells, allowing them to circulate throughout the entire body and contribute to the various functions of blood, including gas exchange, immune response and hemostasis. This wide range of functionality is covered by an equally large number of blood cell types, each responsible for a specific task. However, every single one of these specialized cells is ultimately derived from a single cell type: the hematopoietic stem cell (HSC). Being a stem cell, this cell type not only has the capacity to self-renew, but may also differentiate into either lymphoid or myeloid progenitor cells, which will subsequently follow the differentiation pathway to become one of the several mature blood cell types (Fig. 1.1). This process of mature blood cell production is termed hematopoiesis.

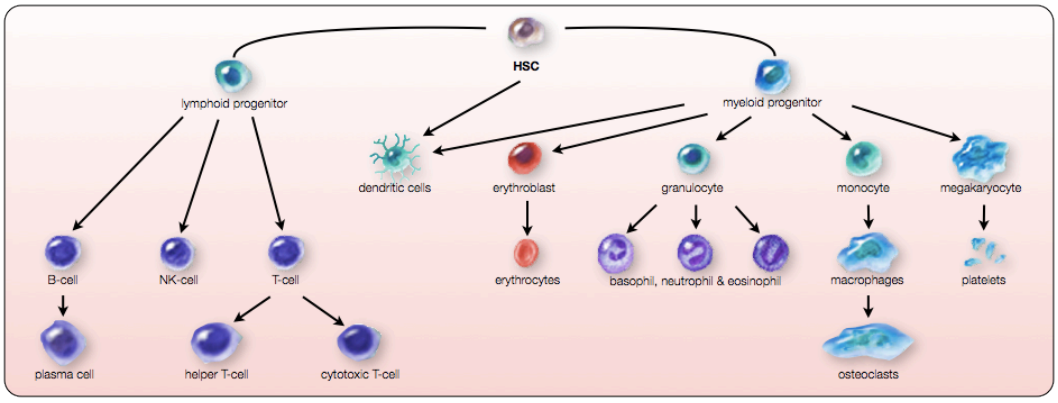

Fig. 1.1. Differentiation pathways of hematopoietic stem cells (adapted from (Tyler 2005)).

Erythrocytes - are the highly populated, 6 - 8µm small, red blood cells (RBC) that give the blood its distinct red color due to its coordinated heme-iron. The human body produces on average 2.5 billion erythrocytes per kilogram body weight every day (Vunjak-Novakovic 2010).

T-cells, B-cells, granulocytes and macrophages - are white blood cells that carry out multiple functions of the immune system. T- and B-cells produce antibodies in response to pathogens and are responsible for the adaptive immune system. Granulocytes develop into neutrophils, eosinophils, and basophils that actively target foreign cells and destroy these by oxidation of their cell membrane. Macrophages engulf the remains of pathogens and digest them enzymatically. The overall production rate of white blood cells is 1 billion per kilogram body weight every day.

Megakaryocytes - are the cells responsible for platelet production. Platelets play a key role in hemostasis, which is necessary in the process of normal wound healing. Though the abundance of megakaryocytes is fairly low, they still produce up to 2.5 billion platelets per kilogram body weight every day.

Therefore, not only do hematopoietic cells carry out very vital functions in the human body, but they are also produced at a very rapid rate, concluding that this tissue possesses a high metabolic activity (Lodish 2008).

Stromal cells

Stromal cells are dispersed throughout the bone marrow and, besides providing structural support, play a secondary yet equally important role in hematopoiesis. These cells support proliferation and differentiation of the hematopoietic cells by secreting cytokines. Stromal cells include osteoblasts, which are responsible for the dynamics in bone reorganization (D'Ippolito 1999), endothelial cells that line blood vessels and prevent immature hematopoietic cells from entering the blood stream (Travlos 2006),

and adipocytes, which historically had been suggested to be just space fillers, however more recently have been shown to play a role in regulation of hematopoiesis (Naveiras 2009).

Mesenchymal Stem Cells

In contrast to hematopoietic cells, stromal cells are all adherent cells, a property that led to the discovery of the mesenchymal stem cell (MSC). In 1976 Friedenstein and colleagues were able to isolate cells that formed colonies by culturing the cells on tissue culture plastic and harvesting the cells that adhered to the culture dish (Friedenstein 1976). At this time point the cells were referred to as colony-forming unit-fibroblasts (CFU-F), since they formed distinct colonies. It was only later when they were termed MSCs, derived from the fact that these cells develop from the mesoderm during embryonic development. In studies these stem cells have been successfully differentiated into adipocytes, chondrocytes, fibroblasts, myocytes and osteoblasts (Barry 2004). Within the bone marrow, MSCs are however suggested to follow a much less branched differentiation pathway towards only osteoblasts and adipocytes. These cells adhere to the bone matrix, where they form a confluent layer.

Niche Theory

The niche theory is a theory that evolved based on two observations: very early on it was shown that although the overall blood flow rate is relatively high through the entire bone marrow, there are localized flow variations within the same bone (Brookes 1967). More recently, improved imaging techniques have shown evidence that the HSCs are co-localized to the confluent layers lining the bone matrix (Mendez-Ferrer 2010). These observations imply that there are localized regions within the bone marrow that regulate proliferation and differentiation of the HSCs. These regions were defined as niches and resulted in the niche theory. It comprises of 2 distinct niches (Wilson 2006; Arai 2007) (Fig 1.2):

Endosteal/Osteoblastic niche - is suggested to be the location of the more quiescent HSCs. Specialized niche osteoblasts (SNO) and CXCL12-abundant reticular (CAR) cells line the endosteum where they provide an extracellular matrix (ECM) and secrete cytokines that regulate the cues for self-renewal and dormancy. The endosteal niche is also believed to be differentiated into quiescent storage niches and self-renewing niches that can either maintain a pool of quiescent HSCs or allow proliferation respectively.

Vascular niche - is located adjunct to the sinusoidal endothelial cells, which are also populated with CAR cells. Both a different cytokine composition as well as a slightly more elevated oxygen level are suggested to activate the HSCs and induce hematopoiesis.

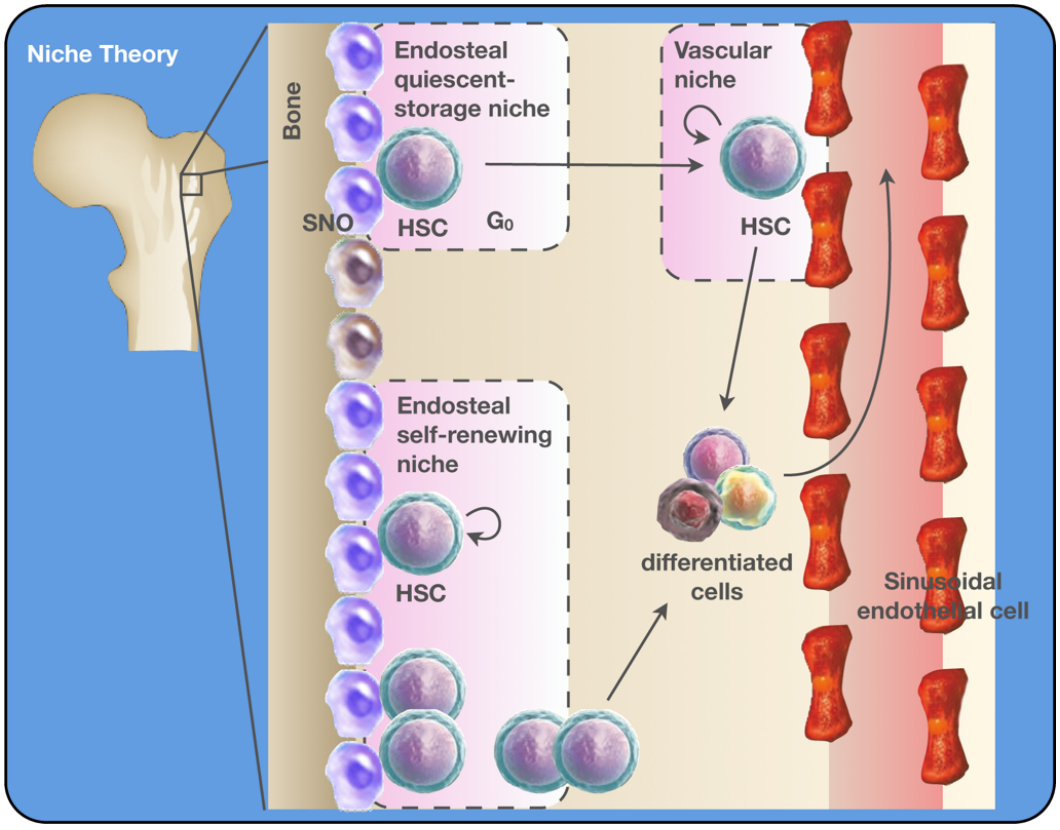

Fig. 1.2. Diagram of the bone marrow niches (adapted from (Wilson 2006)).

A recent publication however implies that these niches are likely more plastic than originally suggested (Bianco 2011). It is therefore unclear if the endosteal quiescent storage niche and the endosteal self-renewing niche are truly separate niches or instead can transition into each other. It is also believed that osteoblasts, adipocytes, sinusoidal endothelial cells and stromal cells interplay, creating a dynamic stem cell niche.

Red versus yellow bone marrow

The plasticity of the niche theory is further supported by the fact that all bone marrow is not equal. Anatomically, one can differentiate between red bone marrow (Latin: *medulla ossium rubra*) and yellow bone marrow (Latin: *medulla ossium flava*) based on appearance (Fig 1.3). Red bone marrow is the main location of hematopoiesis in the adult body. The massive production of mature red blood cells gives the tissue its distinct red color. On the other hand yellow bone marrow produces almost no mature blood cells. Instead it is filled with an abundance of adipocytes, which contribute to the yellow color.

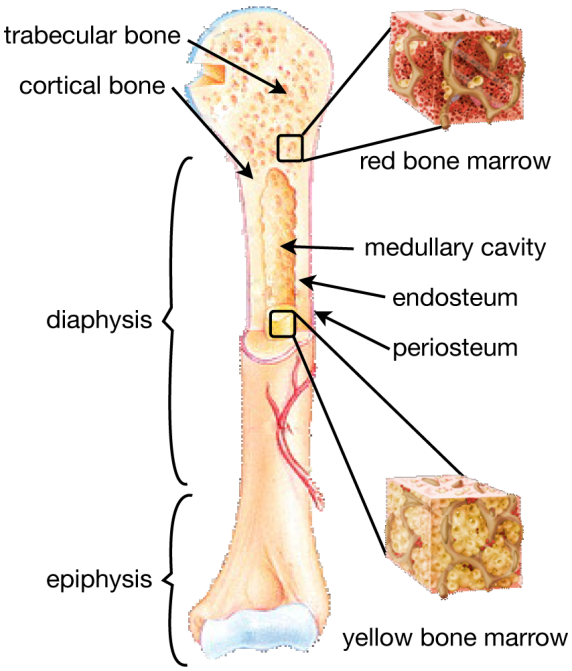

Fig. 1.3. Structural location of bone marrow (adapted from (Tyler 2005; Marieb 2009)).

Functionality of marrow fat

In 1882 Neumann reported that red bone marrow declined with age, and converted to yellow bone marrow from the periphery towards the axial skeleton. This observation derived from rodent models has since been referred to as Neumann's law (Tavassoli 1979; Tuljapurkar 2011). In newborn mammals there is close to no fat in the marrow and is only minimally localized at the tips of extremities. Using biopsies and magnetic resonance imaging (MRI) one has been able to show that the number of adipocytes present in the bone marrow compartment increases with age (Meunier 1971; Rozman 1989). The function of adipose tissue in the human body is generally believed to be for thermal insulation as well as energy storage, however the specific functionality of adipocytes within the bone marrow compartment is currently under debate. Due to the predominance of marrow fat in the extremities in the mouse model, the initial function of marrow fat was believed to be for heat generation (Beresford 1998). This observation is supported by the discovery that marrow adipocytes express uncoupling protein 1 (UCP-1), a mitochondrial protein that plays a key role in thermogenesis. Adding to this conclusion is the presence of both white adipose tissue (WAT) as well as brown adipose tissue (BAT) in the bone marrow compartment. BAT compared to WAT has a high abundance of mitochondria within the cells and therefore does not primarily function in energy storage, but instead is more involved in energy production linked to thermogenic regulators. In correlations with this, treatment of marrow fat with thiazolidinediones (TZD), drugs for treatment of type-II diabetes and known stimulants of adipogenesis through the peroxisome proliferator-activated receptor gamma (PPARγ) pathway (see Chapter III), upregulates BAT-specific gene markers.

More detailed analysis revealed that the infiltration of yellow bone marrow does not simply occur from the periphery towards the center of the body, but is also present in both epiphysis and diaphysis of long bones including the femur (Fig. 1.3) (Rosen 2009).

This conversion from red to yellow marrow is not purely age-related but occurs around the time of peak bone acquisition. This observation led to the conclusion that marrow fat might also be involved in the systemic energy metabolism (Lecka-Czernik 2012). There has been a recent suggestion that marrow fat acts as a localized energy storage depot that can be tapped on for osteogenic emergencies (Gimble 2006). This “internal” energy storage coincides with discoveries that marrow fat is more highly present in adolescent girls with anorexia nervosa (Ecklund 2010) a disease where the affected have very low body fat, yet show an early onset of osteoporosis and an increased risk of fracture. Another disease with an observed increase in marrow fat is diabetes (Botolin 2007). The correlation to systemic energy metabolism becomes evident when comparing states that show alterations in the fat volumes of bones: aging, malnutrition and diabetes all present alterations in the efficiency of energy metabolism (Lecka-Czernik 2012).

This however also raises another interesting aspect: there is no correlation between the amount of visceral and subcutaneous fat and the amount of marrow fat in a human being (Di Iorgi 2008). Although marrow adipocytes do express the same transcription factors as extramedullar adipocytes, they do possess a different unique function. Treatment of marrow adipocytes with TZDs upregulates the expression of genes essential for fatty acid metabolism however has no effect on expression of insulin-dependent glucose transporters (Shockley 2009). This suggests that marrow fat is more involved in lipid rather than glucose metabolism.

Other aspects of yellow bone marrow

The presence of adipocytes within the bone marrow compartment has generally been considered a negative effect. The link to diseases affecting energy metabolism is rather new, however in the past it was well established that a low bone mineral density is correlated to a high amount of adipocytes. This provides the link of marrow fat to yet another diseased state: osteoporosis. Another aspect is that marrow fat fills the void left

in the trabecular bone after radiation when a patient is being prepared for a bone marrow transplant (Casamassima 1989). More recently, in animal studies, marrow fat has been shown to down-regulate hematopoiesis (Naveiras 2009). Comparing bone marrow in the tail and thoracic vertebrae, they found a lower amount of hematopoietic activity and progenitor cells in compartments with a high abundance of adipocytes. Using a genetically modified fatless mouse, they showed a lower amount of adipocytes and a higher amount of red bone marrow present in the tail region, where marrow fat is normally predominant. Post irradiation and transplantation, the bone marrow more rapidly reconstituted hematopoietic activity in these fatless mice, presumably due to the lack of adipocytes. Finally using the PPAR$_{\gamma}$ inhibitor bisphenol A diglycidyl ether (BADGE), they suppressed adipocyte formation post radiation within the bone marrow cavity and showed a much higher increase in leukocyte and progenitor formation.

Though the aforementioned publication showed a clear inhibition of hematopoiesis by adipocytes, there was an equally interesting observation regarding the actual stem cells. Though there was less hematopoietic activity and fewer hematopoietic progenitor cells within the marrow cavities filled with adipocytes, these locations still had a siginificant amount of HSCs. In fact, multilineage long-term engraftment was significantly higher in HSCs extracted from a bone marrow compartment with a high abundance of adipocytes. Cell cycle analysis of the stem and progenitor cells within the marrow fat showed that these cells were more quiescent and in a G0 phase (similar to our observations in Chapter II). They also stated that though marrow fate does decrease hematopoietic activity, that the adipocytes might instead help to preserve the pool of stem cells through reduced production of growth factors such as granulocyte–macrophage colony-stimulating factor (GM-CSF) and granulocyte colony-stimulating factor (G-CSF), but also by the secretion of tumor necrosis factor-alpha (TNF-α) and adiponectin (Zhang 1995; DiMascio 2007).

Finally, there are also quite a few studies that provide evidence contradicting the common belief of marrow fat being solely linked to a diseased state: in humans older than 30 years of age, most of the femoral cavity is already occupied by adipose tissue even in healthy humans (Rosen 2009). Also the process of increased marrow fat can be reversed in times of increased blood cell demand, such as continuous physical training (Gurevitch 2007). Finally, certain studies have suggested that the presence of adipocytes in the niche is not inhibitory but instead necessary for the support of HSCs (Gimble 1990; Gimble 1996).

Medical relation

The importance of the bone marrow can be derived from the functions of its many cell types. In the same context, slight abnormalities within the bone marrow can have very severe consequences, which can be observed in many bone marrow-related diseases.

Leukemia

Probably being one of the most well known bone marrow disorders, leukemia occurs when any cell type of the white blood cell line is affected with cancer. These cancerous cells often lack properties of fully functional white blood cells and reduce the functionality of the patients immune system. The malfunctioning cells also disrupt the complex cell network within the marrow and inhibit the production of other blood cells. Symptoms are thus frequent infections, fatigue, bleeding, bruising, anemia, night sweats and bone and joint pains. Consequentially the spleen, the liver and the lymph nodes may become enlarged. Statistically, there are about 41,000 new leukemia patients registered every year in the United States alone (Howlader 2010). Though the disease is seen in all age groups, it is more predominant in people over the age of 60. Like most cancers, the causes are unknown and treatments generally involve subjecting the patient to chemotherapy. Imatinib mesylate is the only drug that was discovered to suppress chronic myelogenous leukemia (CML) (Moen 2007). It acts as a myeloid specific tyrosine

kinase inhibitor and therefore has other side effects. In most cases the only treatment to date to actually cure the disease requires an allogenic bone marrow transplant. This treatment is most successful in younger patients, but still requires a matched donor and is combined with very high risks.

Myeloproliferative neoplasms (MPN)

MPNs are a group of diseases that are characterized by the overproduction of one of the many cell precursors in the bone marrow (Tefferi 2011). This overproduction leads to an increase of the specific cell line and simultaneously reduces proliferation of other cell lines due to nutrient and space limitations. This results in symptoms related to blood cell overproduction or shortages. There is also a slight chance of MPNs developing into leukemia. MPNs are to date not curable, but clinical trials are being conducted using drugs that should retard the excessive cell proliferation.

Myelodisplastic Syndrome (MDS)

In MDS unlike with MPN, the affected blood cell types are produced at a normal rate however with abnormal features. This results in a deficiency of functional blood cells and can lead to anemia, infections and excessive bleeding and bruising. The several different MDS types are classified according to the morphology of the deformed cell types (Greenberg 1997). There is also a high risk of MDS transforming into acute myelogenous leukemia. The hypomethylating agents 5-azacytidine and decitabine and the immunomodulatory agent lenalidomide have recently been accepted by the food and drug administration (FDA) as drugs to reduce the need of blood transfusions.

Aplastic anemia

Defective stem cells can yield a total loss of precursors of one of the cell types and result in aplastic anemia. Causes can be due to exposure to mutagenic chemicals or radiation, in rare cases due to genetic abnormalities (e.g. Fanconi's anemia) or viral

illness (e.g. human parvovirus), but for most of the cases the cause is still unknown (Locasciulli 2007).

Other diseases

The diseases listed above are only a selection of the diseases directly related to bone marrow disorders of the hematopoietic cell line. There are also multiple disorders that are linked to the osteogenic cell line, with osteoporosis being the most predominant one. Very limited treatment options exist for theses diseases and generally a stem cell transplant is required for a full cure (Laubach 2009; Robak 2009). These transplants are not only risky but often fail at the stage of search for a compatible donor. A major reason for the absence of potent treatment alternatives is that many molecular and cellular interactions within the bone marrow are still unknown. Elucidation of these interactions has proven to be very difficult *in vivo* due to the thick cortical bone layer encapsulating the bone marrow cavity.

Context in research

To advance the understanding of diseases related to bone marrow failure, the research field is in desperate need of models. These models cannot only help advance the understanding of the complex interactions in the bone marrow, but also serve to:

- assess the effects of new drugs on bone marrow cells for drug screening.
- provide long-term proliferation of whole bone marrow *in vitro* and possibly yield a practical and cost effective source of stem cells. These can then not only be used for further research but can also be used to establish a bank with a wide range of stem cells that may facilitate donor matching for transplants.

Current models

Current models available are predominantly *in vivo* using mice (Pearson 2008) and in certain cases also zebrafish (de Jong 2005). Though these models provide insights in metabolism and developmental biology of the bone marrow, they are not easily translatable to the human body. This was again evident in a recently published study that demonstrated that aryl hydrocarbon receptor antagonists are able to promote expansion of human but not mouse HSCs (Boitano 2010). The gap between these models and human application illustrates the importance of an *in vitro* human bone marrow model. Ever since the isolation of the first hHSC (Weissman 2008) have groups been trying to culture human bone marrow *ex vivo* (Palsson 1993; Braccini 2005) albeit with limited success.

In vitro culture methods

Most human bone marrow experiments focus on maintaining or expanding a purified, CD34-positive ($CD34^+$) HSC population, as these cells are required for hematopoiesis. Long-term maintenance of these cells has however proven to be very challenging and is the reason behind the limited success of the *ex vivo* cultures. One problem is the determination of the appropriate concentration and combination of regulatory factors in the culture medium (see Chapter II - Culture Medium). Current cultivation methods vary strongly with respect to composition of the culture medium (Robinson 2005). To circumvent this problem, research groups have tried mimicking the stem cell-niche by culturing the bone marrow cells on a layer of feeder cells of mesenchymal origin (Goncalves 2006; Zhang 2006). The current standard in feeder layers that are even used for commercial expansion, are generally MSCs from either human (hMSC) or mouse (mMSC) origin. More recently, MSC feeder layers that have been differentiated towards osteoblasts have gained a lot of interest and are suggested to have improved expansion properties (Mishima 2010). Though studies with feeder layers have shown an

improvement in the expansion of bone marrow stem cells, they do not support maintenance of quiescent HSCs (Jang 2006). Therefore these culture environments are not able to sustain a long-term HSC culture.

Expansion versus quiescence

Comparison of current methods reveals a common element: many are focused on increasing the amount of HSCs *in vitro*. This is clearly a strong desire in stem cell transplants, where it is difficult to obtain a sufficient amount of HSCs from a single donor and a rapid increase in the stem cell population is of great desire. However with respect to long-term *in vitro* culture, pushing HSCs towards expansion might not be the most ideal strategy as it can likely override the cues maintaining dormant cells. The presence of dormant cells is crucial for long-term cell culture in an *in vitro* model.

Hypothesis

From these perspectives we hypothesized that **the inclusion of adipocytes in the feeder layer can aid in maintaining the HSC population *in vitro* by mimicking the niche of yellow bone marrow and suppressing differentiation**. The notion of adipocytes just acting as space fillers has long been taken over by the fact that adipose tissue functions as and endocrine organ and has effects on other cells (Kershaw 2004). The capability of adipocytes to down regulate hematopoiesis is suggested in part due to the reduced production of growth factors such as GM-CSF and G-CSF, but also by the secretion of TNF-α and adiponectin (Naveiras 2009). These inhibit hematopoietic progenitor expansion and therefore likely preserve the hematopoietic stem cell pool. By suppressing differentiation, less stress will likely be imposed on the HSCs, allowing more time for the cells to engraft in the feeder layer and recreate the niche.

Novel Approach

We therefore worked towards creating a three-dimensional (3D) human *in vitro* bone marrow model with an abundance of adipocytes (Fig. 1.4). Another way to view this is by considering *in vitro* HSC culture as an *in vitro* version of a bone marrow transplant. This is illustrated by comparison in Table 1.1.

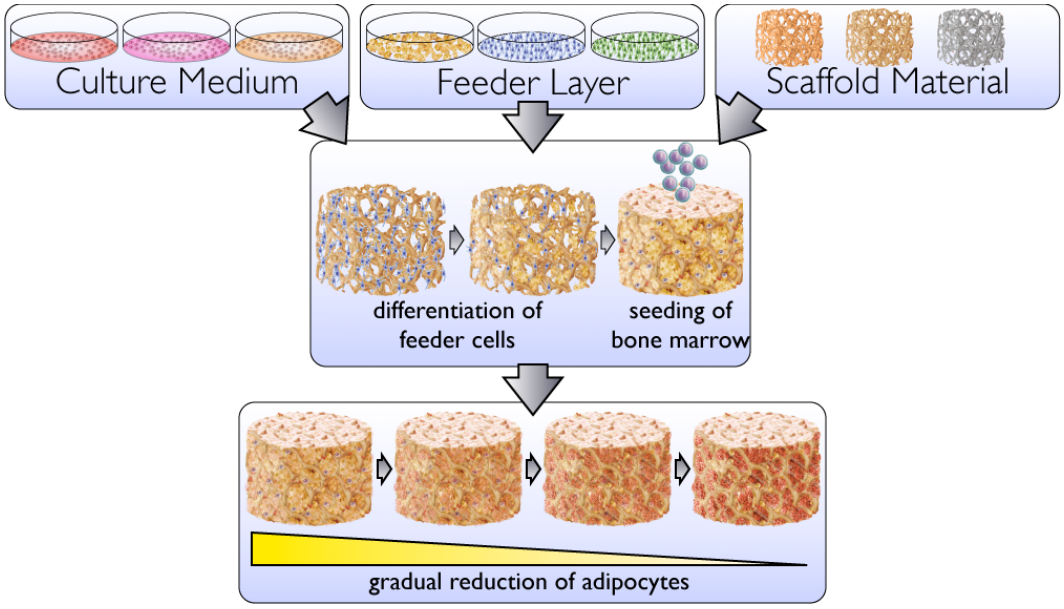

Fig. 1.4. Overview of the elements of the project.

Table 1.1. Correlation of key elements in an *in vivo* bone marrow transplant with steps in *in vitro* HSC culture.

***in vivo* bone marrow transplant**	***in vitro* HSC culture**
The cells from the recipient are ablated and removed by irradiation or chemotherapy leaving a bare bone marrow matrix.	Start with a bare substrate that allows adhesion of the endosteal cells.
Post-ablation the matrix is repopulated with endosteal cells that fill the void.	Feeder cells are grown to confluent layers that cover the substrate.
The stronger the intensity of irradiation the more adipocytes repopulate the matrix.	Inclusion of adipocytes in the feeder layer.
The bone marrow is injected into the body of the recipient where the stem cells engraft in the bone marrow matrix.	The bone marrow can be injected directly on the substrate with the feeder cells.

We identified 3 key elements needed towards creating this model that will be elaborated in the chapters of this dissertation:

- Determining an optimal medium for stem cell engraftment that supports both proliferation and quiescence.
- Adding adipocytes to a currently established feeder layer models.
- Creating a 3D construct and perfusion system that supports long-term culture.

CHAPTER II – TOOLS IN HUMAN HEMATOPOIETIC STEM CELL CULTURE

Current knowledge

HSCs have been extensively investigated and are commonly used in therapy for several years now (NIH 2001). No other type of stem cell, be it adult, fetal or embryonic, has attained such status to date. Despite the vast experience with HSCs, scientists face major roadblocks. The largest being the difficulty to proliferate or even maintain the stem cell *ex vivo*. Also controlled differentiation has not been fully achieved in comparison to MSCs. Still, many cues and characteristics of hematopoietic cells have been elucidated in more detail than in any other primary cell type, predominantly using the mouse model. However since the large realm of HSC research has been in animals and many of these properties are not translatable to human hematopoietic cells, research on human HSCs is clearly decades behind. An example of this knowledge gap is provided in Table 2.1, listing the surface markers on mouse HSCs and multipotent progenitor cells (MPP) in comparison with their respective human cells. Not only is one able to better differentiate between stem and progenitor cells in mice, but subgroups have also been introduced: dividing HSCs into long-term repopulating (LT-HSC) and short-term repopulating stem cells (ST-HSCs) and MPPs into early and late stages (Seita 2010). Recently, researchers have even started to include the definition of intermediate-term repopulating stem cells (ITRC) using additional surface markers (Benveniste 2010).

This chapter briefly describes methods that are commonly used in hematopoietic stem cell research, specifically limited to options available to human cells, with examples obtained throughout the time period of this dissertation.

Table 2.1. Comparison of surface markers defining hematopoietic stem cells (HSC) and multipotent progenitor cells (MPP) in mouse and human species (Seita 2010).

	Mouse	Human
HSC	***LT-HSC:*** $CD34^-$, $CD38^-$, $Sca1^+$, $Thy1.1^{+/low}$, $cKit^+$. Lin^-. $CD135^-$. $Slamf1^+$	$CD34^+$, $CD90^+$, $CD38^-$, $CD45RA^-$, Lin^-
	ST-HSC: $CD34^+$, $CD38^+$, $Sca1^+$, $Thy1.1^{+/low}$, $cKit^+$, Lin^-, $CD135^-$, $Slamf1^+$, Mac-1^{low}	
MPP	***Early MPP:*** $CD34^+$, $Sca1^+$, $Thy1.1^-$, $cKit^+$, Lin^-, $CD135^+$. $Slamf1^-$. Mac-1^{low}. $CD4^{low}$	$CD34^+$, $CD90^-$, $CD38^-$, $CD45RA^-$, Lin^-
	Late MPP: $CD34^+$, $Sca1^+$, $Thy1.1^-$, $cKit^+$, Lin^-, $CD135^{high}$, $Slamf1^-$, Mac-1^{low}, $CD4^{low}$	

CD34 antigen in human cells

The established phenotype of human HSCs is the expression of the CD34 surface protein. CD34 expression diminishes rapidly as the HSCs differentiate towards mature blood cells. Additionally this protein is a negative marker for MSCs. This yields a potent marker to differentiate between the two stem cell types in feeder layer cultures.

A drawback of using CD34 as quantitative marker is the fact that most myeloid and lymphoid progenitor cells still express CD34, despite being already lineage-committed (Seita 2010). To differentiate between HSCs and lineage-committed progenitor cells one can also stain the cells for the CD38 glycoprotein. This is suggested to be only expressed in the lineage committed progenitor cells. Therefore by double staining the bone marrow cells, the HSCs should be $CD34^+$ and $CD38^-$ whereas the progenitor cells will show up as $CD34^+$ and $CD38^+$.

Example

In extensive studies analyzing MSCs we have seen a very strong autofluorescence being emitted from the cells of this lineage, especially in the red channel (see Chapter III - Fig. 3.6). This makes it technically difficult to measure two labels simultaneously when using and MSC feeder layer.

Culture medium

Several different culture media have been published for HSC cultures (Murray 1999). The first culture conditions designed to specifically support *in vitro* proliferation of HSCs were published by the group of Thomas Michael Dexter in 1977 (Dexter 1977). The medium consisted of a common basal medium supplemented with horse serum and hydrocortisone, and its use was widely spread after publication. Many groups took on the use of this medium and it is still being used for certain long-term culture assays (see LTC-IC).

The discovery of the cytokines involved in regulating the cues of HSC differentiation, has led to the development of newer culture media. Norman Iscove developed in 1984 a novel basal medium designed for hematopoietic stem cells. It is a modification of Dulbecco's medium and is called Iscove's Modified Dulbecco's Medium (IMDM) (Iscove 1984). Commercial media have replaced the fetal bovine serum (FBS) in the cultures to reduce the variability between different batches. In human stem cell cultures, the medium is generally supplemented with recombinant proteins including fms-like tyrosine kinase 3 (Flt-3), stem cell factor (SCF), interleukin 6 (IL-6) and interleukin 3 (IL-3).

Example

In early experiments we tested our feeder cultures with 3 different media types: Dexter medium and IMDM containing a very low percent of FBS and was supplemented either with or without cytokines (Fig. 2.1). Results showed the greatest $CD34^+$ expansion after 7 days was achieved with IMDM supplemented with growth factors (GF), which is very similar to commercially available HSC expansion media. It has also been demonstrated that SCF enhances HSC engraftment in the stem cell niche, which would be beneficial for our studies (Dunbar 2001). In later experiments we showed again the requirement of the cytokines for these expansive properties over a time lapsed period (see Chapter IV - Fig 4.2).

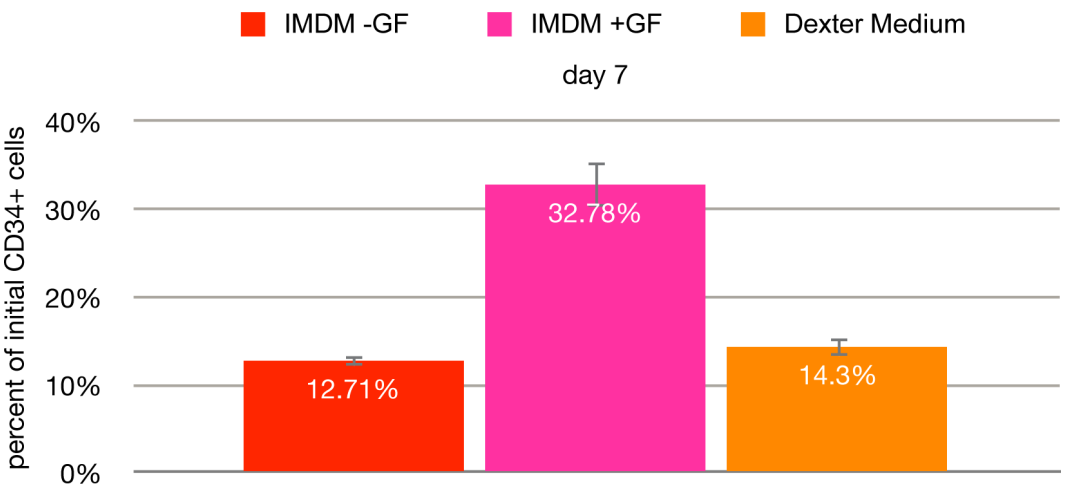

Fig. 2.1. Percentage of $CD34^+$ cells when expanded in different culture media: Dexter Medium contained 12.5% horse and 12.5% fetal bovine serum, 55 µM ß-mercaptoethanol and 100 nM hydrocortisone. IMDM -GF contained just 2% FBS. When supplemented with cytokines, 55 µM ß-mercaptoethanol, 10 ng/mL FLT-3, 10 ng/mL SCF, 10 ng/mL IL-6, and 2 ng/mL IL-3 were added. All are values obtained by flow cytometric analysis of > 200'000 events (n = 3, data displayed as mean ± SD).

One thing to keep in mind when analyzing this data, is that although these media have proven to expand the $CD34^+$ cell population, they reach a peak at 2 weeks, where after the $CD34^+$ population diminishes (see chapter IV - Fig 4.2). It has been observed that HSC expansion is almost always combined with differentiation (Boitano 2010). Therefore the increase in $CD34^+$ cells is likely not exclusively due to an increase in HSCs, but also in progenitor cells. Recently it has been discovered that the use of an aryl hydrocarbon receptor antagonist, StemRegenin, truly expands hHSCs.

With respect to the primary goal of this project, creating an environment that allows long-term culture of HSCs *in vitro*, the sole expansion of $CD34^+$ cells is not the main objective. Instead the persistence of cells with a $CD34^+$ phenotype over a longer time period will indicate the presence of a niche that supports the dormant HSCs that are crucial for long-term culture.

Cell sources

Bone marrow

As previously mentioned, the original source of extracting HSCs is through bone marrow aspirates extruded from within bones. The most common site of extraction is through the posterior iliac crest, located at the pelvic bone. This mainly for reasons of safety and ease of performance. Alternative sites include the tibia (infants only), anterior iliac crest (children and adults), and sternum (adults only, aspiration only) (Riley 2008). For this the site of extraction is first cleaned and desensitized by local injection of an anesthetic. Using a 16 gauge needle, a hole is bored through the bone and the bone marrow is extracted. Typically, for diagnostics, only a few milliliters are extracted, however up to 50 mL can be extracted from each pelvic bone side, without a drastic impact on the health of the patient. After extraction the wound is covered with gauze and generally heals completely within a few weeks. The aspirate is kept in a heparin solution and shipped for immediate use (Fig. 2.2).

Fig. 2.2. Photo of a tube containing an aspirate of fresh human bone marrow.

Peripheral blood

To avoid the use of a painful and highly invasive procedure, doctors are now predominantly extracting HSCs from peripheral blood. HSCs can naturally enter the blood stream and circulate throughout the entire body, however are present there in much lower concentrations: peripheral blood contains <0.1% HSCs whereas bone marrow contains ~2% HSCs (Van Epps 1994). Cytokine treatment using granulocyte-colony stimulating factor (GCSF) or cytotoxic therapy assist by releasing HSCs from the bone marrow and thereby increasing the level of HSCs in the blood to 0.6 - 2%. These can then be extracted from the peripheral blood by apheresis using the CD34-antigen.

Umbilical Cord Blood

Another common source of human HSCs is the extraction from the blood of umbilical cords. This tissue is usually discarded after birth and contains approximately 1% HSCs (Van Epps 1994). There is a substantial amount of research being conducted on umbilical cord blood to search for ways to expand the number of HSCs but also to compare and contrast the biological properties of cord blood with adult bone marrow stem cells. Umbilical cord blood represents a valuable resource for HSCs, research data have not conclusively shown qualitative differences in the differentiated cells produced between this source of HSCs and peripheral blood and bone marrow (Zhang 2012).

Cell source in this project

For this project the cell source of choice were fresh human bone marrow aspirates that were purchased commercially. In the clinic more and more transplants are performed using peripheral and cord blood. Former mainly because the extraction method is less invasive for the donor and still yields a high amount of HSCs. Latter is often used if it is hard to find a matching donor for the recipient, as it has been shown that the risk of graft-versus-host disease is lower when using cord blood stem cells (Rocha 2001).

In this project, the advantage of using bone marrow aspirates over other HSC sources overweighed: On one hand bone marrow aspirates are a good source for MSCs that are needed to form the feeder layers and MSCs not present in the other two cell sources. On the other hand, as previously stated, bone marrow aspirates provide the highest percentage of stem cells. On thing to keep in mind is that these cells are extracted fresh from a different donor for each experiment. This donor variability can occur in both the HSCs and MSCs and needs to be taken into consideration when comparing results from different experiments.

Isolation of HSCs

Removal of RBCs

To reduce the amount of blood clots, bone marrow aspirates are not utilized directly for *in vitro* long term stem cell culture, but are instead treated to remove the red blood cells prior to their application. Figure 2.3 outlines two common procedures for removal of the RBCs.

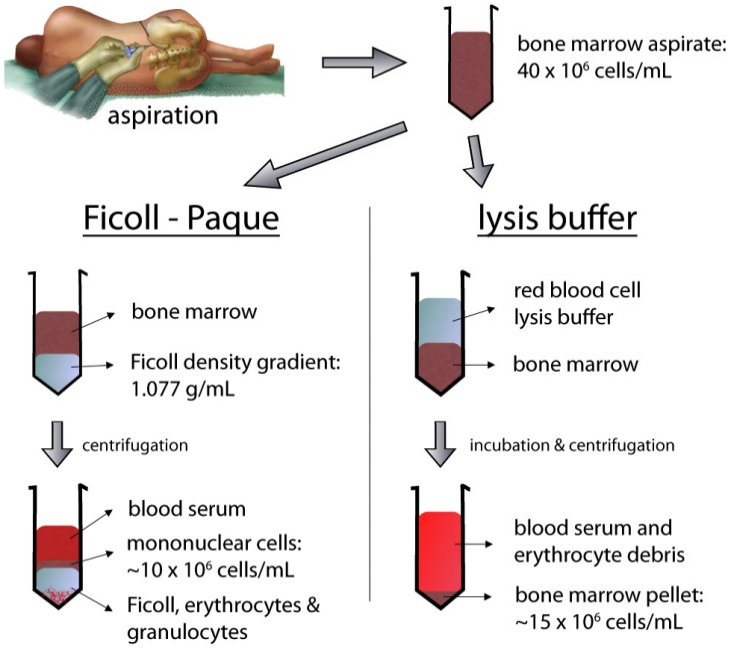

Fig. 2.3. Two common methods to remove RBCs.

Ficoll-Paque

Ficoll is a neutral, highly branched, high-mass, hydrophilic polysaccharide which can be easily used to prepare solutions of a very defined density. For a Ficoll-Paque treatment of bone marrow, one generally adds the viscous Ficoll-solution to the bottom of a tube and layers the whole bone marrow on top. By centrifugation the bone marrow is split into its components according to their densities: the liquid blood serum will float on top of the Ficoll section whereas mononucleated cells will compact as a layer directly above the Ficoll. The smaller and more compact erythrocytes and densely granulated granulocytes show a higher density than the Ficoll solution and will pellet at the bottom of the tube. The mononuclear cells can be easily isolated by harvesting the compacted cell layer above the Ficoll (Boyum 1968). The disadvantage of this method is the lack of cell-specificity: not only red blood cells are removed, but also granulocytes and in general cells with an altered density e.g. with an elevated protein production when undergoing mitosis.

Lysis buffer

The active component of the red blood cell lysis buffer is ammonium chloride. Ammonium is readily taken-up by red blood cells (Sass 1979). Because of this, the cytosol of the red blood cells has a higher ionic strength than the surrounding solution and due to this osmotic imbalance, water rushes into the cells until they burst. Compared to Ficoll, the lysis buffer has the advantage of being more specific toward erythrocytes, yielding a higher amount of mononuclear cells. However the buffer components might still have a side-effect on the remaining cells, e.g. induce differentiation.

In this project we chose to use the Ficoll method for the isolation of the mononuclear cells. Though the yield was slightly lower, we saw the benefit in the less harsh environment when compared to an ammonium chloride lysis buffer.

Flow cytometry

In order to determine the amount of HSCs present in the cultures a highly quantitative analytical method is needed. The current gold standard of obtaining accurate quantitative numbers of a sample with a large number of cells is flow cytometry. It allows simultaneous multiparametric analysis of the physical and/or chemical characteristics of individual cells.

Principle

Before measurements can be carried out on cells, they must be first disaggregated and suspended in solution. Antibodies are added that bind specifically to a targeted surface marker. To each of these antibodies is also a fluorophore attached (Fig. 2.4A). Fluorophores are fluorescent molecules that emit an optical signal at a defined wavelength after being excited by an energy source. The addition of these fluorescent antibodies to a cell suspension assigns a defined fluorophore to a specific cell: the cells are being “labeled”. The suspended cells are then injected into the flow cytometer where they pass through a capillary in a narrow fluid stream. This capillary is so narrow that ideally only a single cell can pass through at a time (Fig. 2.4B). A laser beam of a defined wavelength is directed towards this hydro-dynamically focused stream and excites every passing fluorophore. In return the fluorophores emit a light signal according to their defined emission wavelength. The intensity of this emission is then detected by a detector (FL-1). A number of other detectors are aimed at the point where the stream passes through the light beam: one in line with the light beam named forward scatter (FSC), and one perpendicular to it named side scatter (SSC). FSC correlates with the cell volume since the bigger the cell, the more light is scattered in the forward direction. SSC relates to the inner complexity of the particle, e.g. shape of the nucleus, the amount and type of cytoplasmic granules and/or the membrane roughness. The more complex a cell is built up, the more the focused laser beam is scattered in all directions.

Another factor that needs to be taken into account is autofluorescence (intrinsic fluorescence). Because almost everything yields fluorescence to a certain extent after being excited, even unlabeled cells can emit a signal. Therefore, even though autofluorescence is generally weaker than the fluorescence emitted by an added fluorophore (extrinsic fluorescence), the actual extrinsic fluorescence of a labeled cell has to be calculated from the difference of total fluorescence and the autofluorescence.

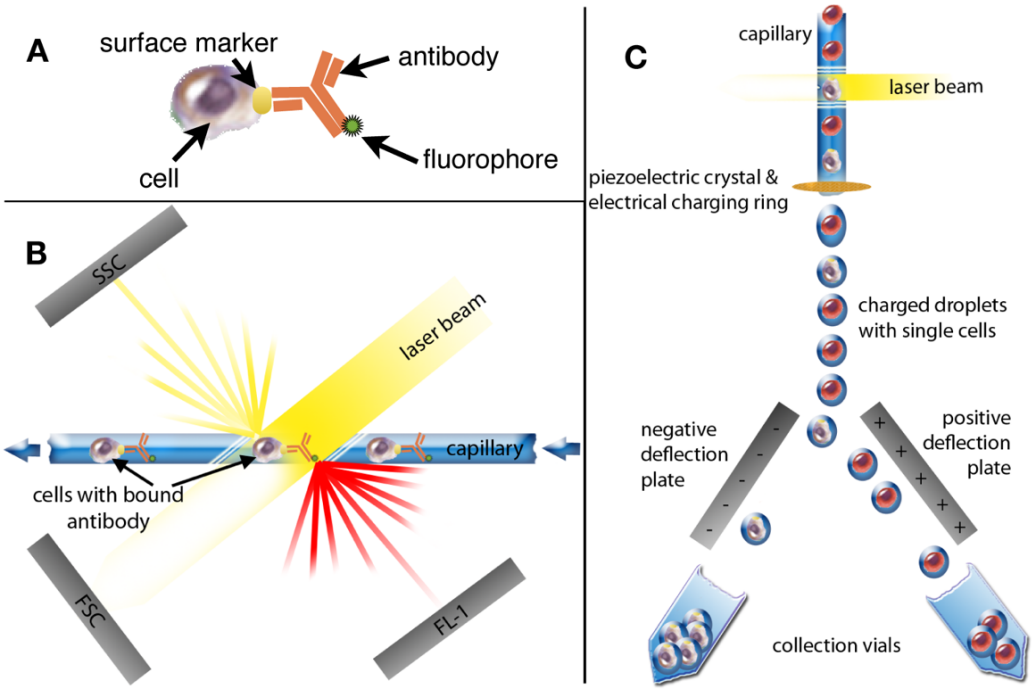

Fig. 2.4. Principles of flow cytometry.

Data Analysis

The data set obtained by a flow cytometry measurement contains the FSC, SSC, and fluorescence values of each detector for each individual cell. These data sets are generally displayed in two variations: histograms and dot-plots.

Histogram

Here the fluorescence intensity is plotted against the amount of cells: the higher the peak in a histogram, the more cells there are that exhibit fluorescence at this intensity.

Fluorescence intensities are generally plotted at a logarithmic scale to display the wide range of intensities. This is mainly because fluorescence differences that are several orders of magnitude are of greater interest than just small variances. Histograms are very easy to read and are commonly used in publications. However they are only able to display a the fluorescence of a single parameter, a restriction that becomes very apparent when strong autofluorescence inhibits the clear distinction between labeled and unlabeled cells.

Dot-Plots

Dot-plots are a combination of several parameters in one plot. The intensities of each parameter define the axes. The amount of cells with same intensities is given in a color scheme, which can be defined by the data processing program. A commonly used dot plot is the scatter plot that is obtained by plotting FSC against SSC. The scatter plot can give insight in the morphological status of a cell. Dot-plots are also made to illustrate bi-parametric fluorescence. Because fluorophores only emit a signal at a defined wavelength, one can attach different fluorophores to different antibodies. By adding multiple types of fluorescent antibodies to the cell solution, cells can be analyzed based on a combination of surface markers. These surface markers can be either on the same cell, for multiparametric determination of a single cell type, or on different cell types, for enumeration of different cell populations. To detect the different fluorophores the device has different detectors for the individual wavelengths.

Examples

As described at the beginning of this chapter, human HSC research is decades behind, and very few markers are known that can differentiate between stem and progenitor cells. Therefore we made an attempt to further describe HSCs based on the scatter plot in flow cytometric analysis.

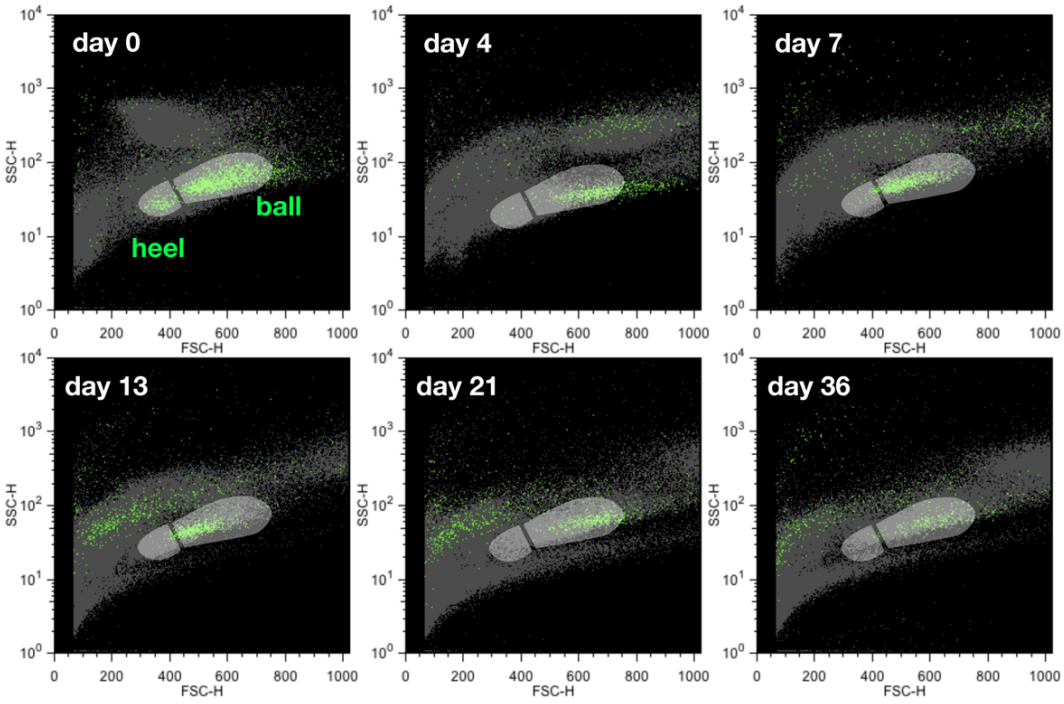

Fig. 2.5. Time-lapsed scatter plot of human bone marrow mononuclear cells.

The idea came from the observation that the $CD34^+$ population of fresh bone marrow always showed two distinct populations (Fig. 2.5): a smaller one (heel) and larger one (ball). For tracking purposes these populations were gated using the template of a shoe print, defining the regions of the two populations as heel and ball respectively. When cultured on tissue culture plastic (TCP) using IMDM +GF, we observed that the $CD34^+$ cells in the heel region rapidly disappeared after 1 week, however that the cells in the ball region more slowly diminished over 1 month. Since there is little information on the size distribution of human HSCs, adding this parameter for distinction would provide very useful as it would not require the use of any additional antibodies, and could be performed simultaneously during regular flow cytometric analysis. We therefore proceeded to further characterize the cells of each region using different techniques.

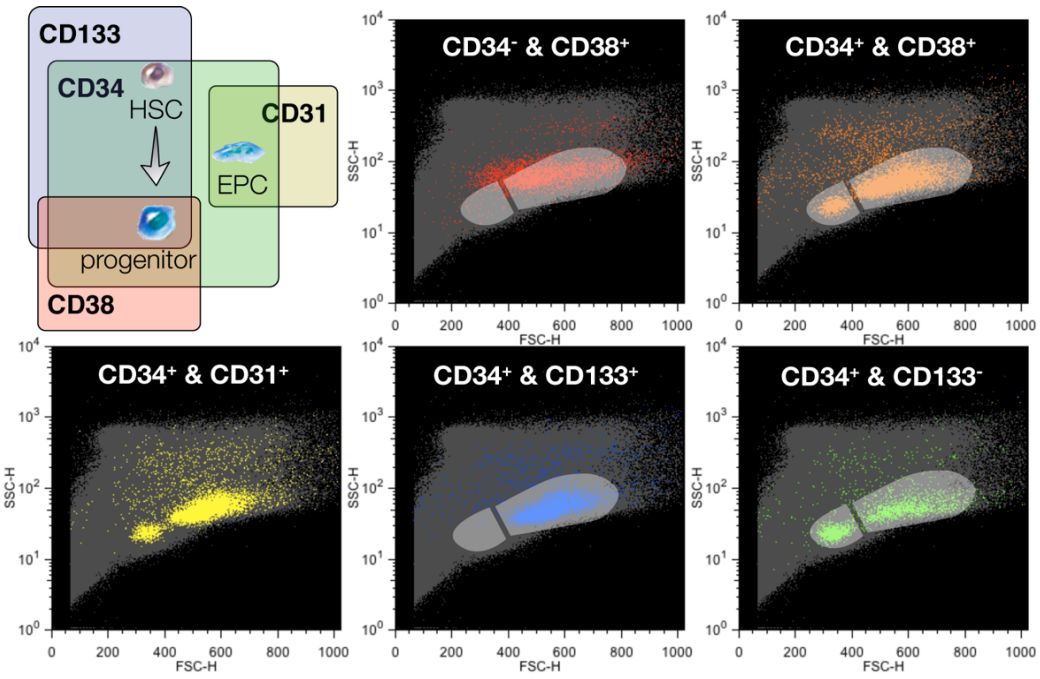

Fig. 2.6. Immunophenotyping the two cell populations.

Immunophenotype

In a first experiment we performed a multi-parametric characterization of the individual stem cells using markers used in human HSC culture (Fig. 2.6). Next to the common CD34 labeling, that is known to label both HSCs and progenitor cells, we used CD38 which should only label progenitor cells. Additionally CD133 was introduced, a marker that is present on both HSCs and pluripotent progenitor cells and can be considered an alternative to CD34 (Yin 1997). CD31 was introduced due to the knowledge that fresh bone marrow aspirates can also contain endothelial progenitor cells, which are expected to be both $CD34^+$ and $CD31^+$.

Though $CD34^-$ and $CD38^+$ were located within the ball region, the main center of the cell population was shifted towards a slightly higher SSC. $CD34^+$ and $CD38^+$ did coincide with both regions, included however also a lot of other cells at higher SSC. Using the CD133 label yielded cells that were $CD34^+$ but $CD133^-$ within both regions, however cells that were positive for both markers showed up only within the ball region. The

CD31 labeling showed cell populations in both regions and overall morphologies very similar to those of $CD34^+$ and $CD38^+$ cell populations.

Given that the $CD38^+$ marker is an established progenitor cell marker, and that the $CD34^+$ subpopulation of the $CD38^+$ cells were predominantly within the two regions, confirmed that the shoe print region is indeed the region where hematopoietic cells in earlier stages reside. When looking at the CD133 staining, no cells were double positive in the heel region. A publication by de Wynter et al. has noted that $CD34^+$ and $CD133^+$ populations are highly enriched in long-term repopulating cells (de Wynter 1998). Unfortunately this did not give us much insight on the functionality of the smaller cells. CD31 staining was not-conclusive, as it seemed to stain almost all $CD34^+$ cells. A recent study showed that CD31 is indeed present on many hematopoietic stem and progenitor cells, and that the surface marker composition and role of endothelial progenitor cells within the bone marrow is still unclear (Kim 2010).

Cell cycle analysis

Since the differences between the two populations couldn't be determined based on phenotype, we wanted to see if we could discern between them based on their status in the cell cycle. As outlined in the niche theory, HSCs can be in either a proliferative or quiescent state, progenitor cells however are considered non-quiescent, as they need to undergo rapid differentiation for hematopoiesis (Fig. 2.7A). General cell cycle analysis using flow cytometry is based on measuring the DNA content of a cell with the Hoechst 33342 stain. A cell undergoing mitosis will have double the amount of DNA, than a cell in the G1 phase. This is however insufficient to discern between proliferative cells that are in the G1 phase, and quiescent cells in G0. Using pyronin Y, one can also stain for the RNA in the cells. G0 cells are believed to have a lower amount of RNA than G1 cells since they're in a quiescent stage and have a lower metabolism (Gothot 1997).

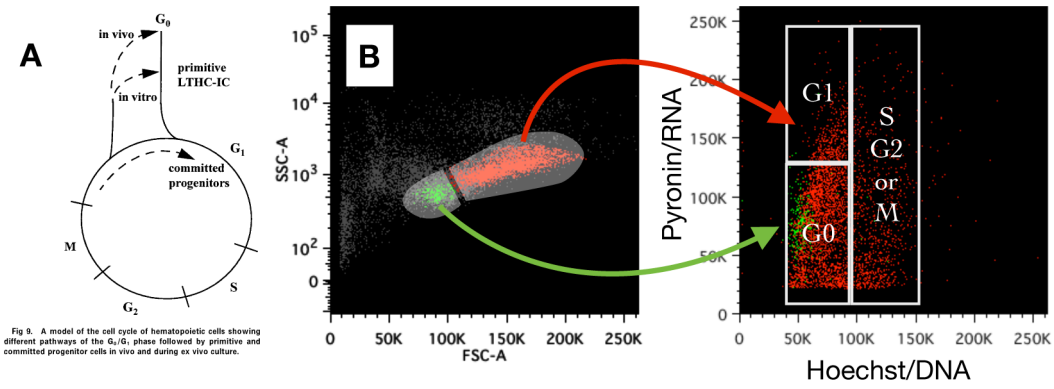

Fig. 2.7. Cell cycle analysis of the two cell populations (adapted from (Gothot 1997)).

Using the technique as described by Gothot et al. we stained our $CD34^+$ cells and observed that the smaller cells in the heel region did indeed possess a lower amount of both DNA and RNA when compared to the cells within the ball region (Fig. 2.7.B). This suggests that these cells were likely in the less proliferative G_0 phase.

Imaging flow cytometer

Next we wanted to see if morphology provided another marker to discern between the two populations. As previously mentioned, morphological analysis in flow cytometry is traditionally carried out using scatter plots. Imaging flow cytometers however posses the ability to take actual images and not just measure the scattering properties of every single cell in a cell suspension. This provides the additional benefit of comparing detailed morphological structures within a large cell population.

In this experiment we chose to stain for $CD34^+$ cells and also label the cells with CD45, a marker that is present on all leukocytes and can be therefore taken as a measure for the amount of differentiation of a hematopoietic cell.

Figure 2.8 shows an excerpt of the large amount of data. Analysis was not highly conclusive, however did show that smaller $CD34^+$ cells were less complex and had a lower CD45 labeling when compared to larger $CD34^+$ cells.

Fig. 2.8. Cell characterization of the two cell populations using an imaging flow cytometer.

Fluorescence-activated cell sorting (FACS)

Flow cytometry is not only limited to analysis of different cell types but also allows physical separation of the cells based on fluorescent markers. This technology is termed fluorescence-activated cell sorting (FACS) (Fig. 2.4C). Similar to flow cytometers, a fine stream of cells passes through a capillary where the fluorophores are excited by a laser beam. At the end of the capillary there is an oscillating piezoelectric crystal. When the laminar stream of cells exits the capillary, the piezoelectric crystal breaks the stream into individual droplets. Each droplet ideally contains no more than one single cell. At the position where the stream breaks into droplets there is also an electrical charging ring. This ring places a charge on each droplet containing a cell. The assignment of the charge is based on the fluorescence profile of the cell when it passes through the laser beam. The droplets then pass through an electrical field between a negative and positive deflection plate. Droplets with a negative charge will move towards the positive plate and vice-versa. Collection vials at the end of these streams will catch the droplets of the respective charge, and thus yield cell populations of a defined fluorescence profile.

This isolation method has been well established over the past decades. There are however some drawbacks: on one hand the utilization of fluorescent antibodies, as well as the operation of a FACS machine is very costly. On the other hand, the environmental surrounding the cells during measurment, e.g. the sheer stress within the capillary or the charge imposed on the cell droplet, may have a negative side-effect, e.g. induce differentiation or apoptosis.

Magnetic-activated cell sorting (MACS)

MACS, is a technique using similar principles as FACS. MACS also uses antibodies that bind to surface markers, however instead of binding fluorophores to them, iron beads are used. By holding a magnet to the vial with the cell solution, the cells bound to a magnetic bead are retained in the vial and the residual cell solution can be washed out.

Due to this simplicity, the cells can be kept in more natural conditions, which gives MACS the advantage of being a more gentle procedure. A major drawback however is the low fidelity of cell separation.

Example

Cell tracking

Using FACS we wanted to see if we could track the changes in the cell populations *in vitro*, as we had previously noted that the smaller cells rapidly disappear from the heel region, but we were unable to follow where they went.

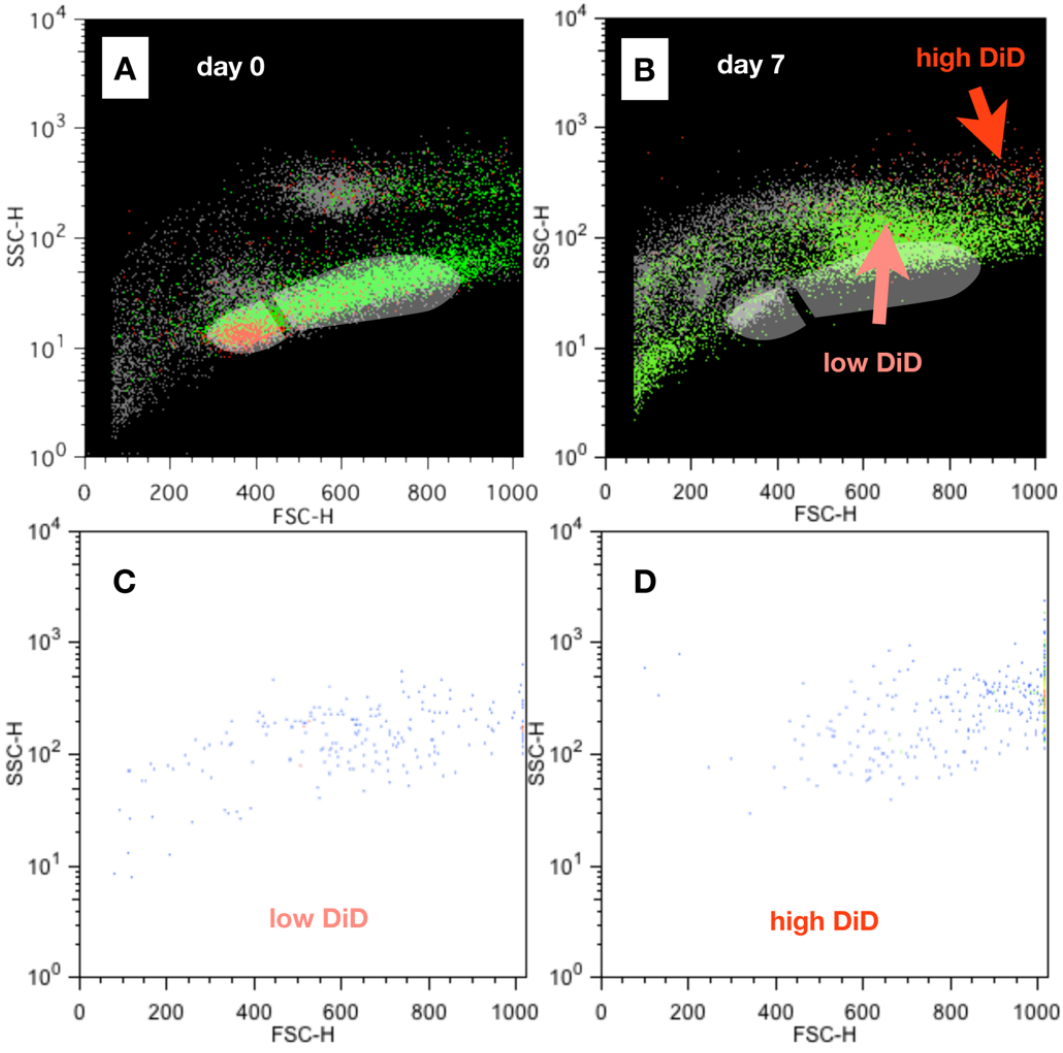

Fig. 2.9. Cell characterization of the two cell populations using an imaging flow cytometer.

After labeling with CD34, we isolated the cells in the heel region using FACS and labeled them with the surface membrane dye DiD (Fig. 2.9A). These labeled cells were then recombined with the residual cell population and kept on TCP using IMDM +GF. After 1 week, we extracted the cells, labeled them with CD34 again and measured their fluorescence on the flow cytometer.

Day 7 did show again that the heel region was devoid of $CD34^+$ cells, and that most cells were within the ball region (Fig. 2.9B). The DiD labeled cells showed up at a much higher FSC and SSC than the heel region. Cells that had strong DiD fluorescence (DiD^{high}) had also a much higher FSC (Fig. 2.9D) when compared to cells the had a lower DiD fluorescence (DiD^{low}) (Fig. 2.9C).

These observations showed an interesting fact: the smaller $CD34^+$ cells within the heel region rapidly increased in size. Since DiD decreases in intensity when a cell starts to divide, the relative DiD intensity can be correlated to the amount of cell doublings a cell has undergone. Therefore one can also make the assumption that the larger DiD^{high} cells had not proliferated, but only increased in size. Given that there were also DiD^{low} cells present, one can assume that there were also a few cells that had undergone proliferation. Interestingly these DiD^{low} cells appeared in a similar region as the ball cells. Based on these conclusions one might setup the hypothesis that the cells initially within the heel region rapidly increased in size after seeding *in vitro*, and then underwent proliferation and possibly even differentiation.

Functional Assays

All the methods previously described, are characterizations of cells based on specific markers. However these markers, though related, don't explicitly conclude that the cell is a true stem cell. This is especially the case with human HSCs where the current definitions include a range of stem and progenitor cells. This is where functional assays can give more insight.

Colony-forming cell (CFC) assay

The CFC assay is the current gold standard in analyzing hematopoietic progenitor cells. The concept behind colony assays is that under defined culture conditions only specific cell types proliferate and form colonies (Mayani 1993). In this assay, cells are plated at a low density in a medium containing a cocktail of growth factors. These growth factors push the stem and progenitor cells down their differentiation pathway yielding erythrocyte-, megakaryocyte- and granulocyte-forming cells. Because most hematopoietic cells are non-adherent, the medium used is a viscous solution of methylcellulose preventing the differentiating cells from dispersing evenly throughout the culture dish, and clustering them in colonies when they proliferate. These colonies are distinguishable based on morphology and quantified after 2 weeks using a microscope (Fig. 2.10). One thing to note here is that the assay is targeted primarily towards progenitor cells. The reason primitive progenitor and stem cells might not produce colonies has to do with the fact that the cells are only exposed to the medium for 2 weeks which is insufficient time for them to reach full differentiation. Medium changes to allow longer differentiation are not possible because the cells are embedded within the methylcellulose medium.

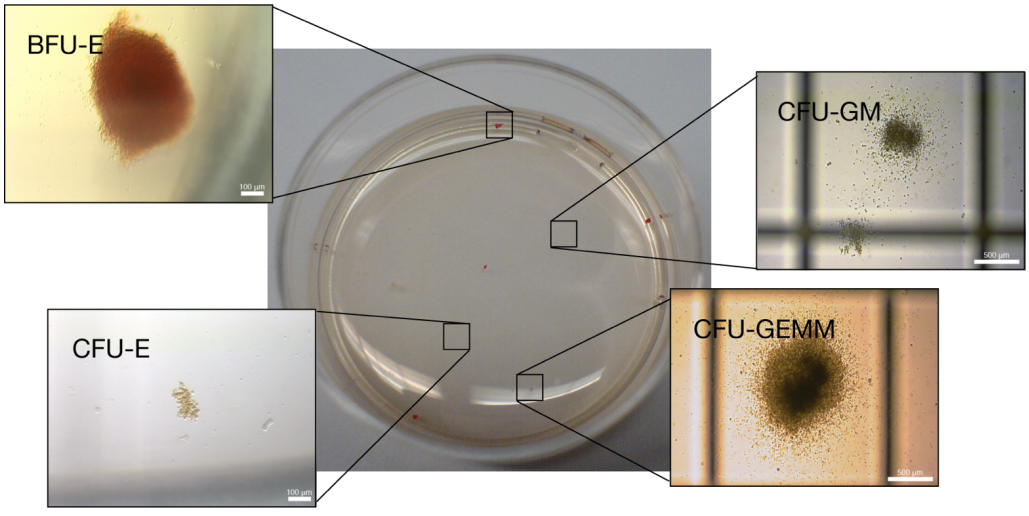

Fig. 2.10. CFC colony assay.

Long-term culture-initiating cell (LTC-IC) assay

The LTC-IC assay is the equivalent of the CFC assay for less committed stem and progenitor cells. Cells detected with this assay share phenotypic and functional properties with *in vivo* repopulating cells (Petzer 1996). First a feeder layer is setup that supports the proliferation of long-term repopulating cells. Then hematopoietic cells are seeded and maintained in this culture for 5-6 weeks using Dexter's medium. During this time, progenitor cells will have already fully differentiated, whereas the more primitive stem and progenitor cells will have only started to proliferate and differentiate. After this time period, all cells are extracted and then plated again at a low density in a methylcellulose medium and maintained in a very similar fashion to the CFC assay. After 2 weeks, the colonies are analyzed and counted. The LTC-IC assay is based on the assumption that the more primitive cells will have reached the same state of differentiation as the progenitor cells that differentiate in CFC assays.

Humanized mouse model

HSCs are defined by their ability to give rise to all the kinds of blood cells in the body. This means that a single HSC is capable of regenerating the entire hematopoietic system, which is the principle behind bone marrow transplants. Therefore to see if a cell is truly a stem cell that can reconstitute hematopoiesis, one injects stem cells into non-obese diabetic (NOD) / severe combined immunodeficiency (SCID) mice that have been irradiated to destroy their own bone marrow (Ito 2002). If the injected cells contain true stem cells, they will engraft in the bone marrow cavity and regenerate hematopoiesis. One note of caution here is that a positive outcome is based on the survival of the mouse after injection. Therefore engraftment of the cell within the bone marrow is correlated to the functionality of the stem cell. If however the stem cell engrafts within the bone marrow cavity and for some reason remains quiescent, this will yield a negative outcome, despite the cell possibly still being a HSC.

Examples

Using the two functional *in vitro* assays we wanted to see at which state of differentiation the cells are within the two shoe print regions. Using FACS we isolated the $CD34^+$ cells from both the heel and the ball regions but also $CD34^-$ cells that were not within those two regions (named "other"). The cells of each region were seeded at same densities using both the CFC and the LTC-IC assays and colonies were correlated to seeding density.

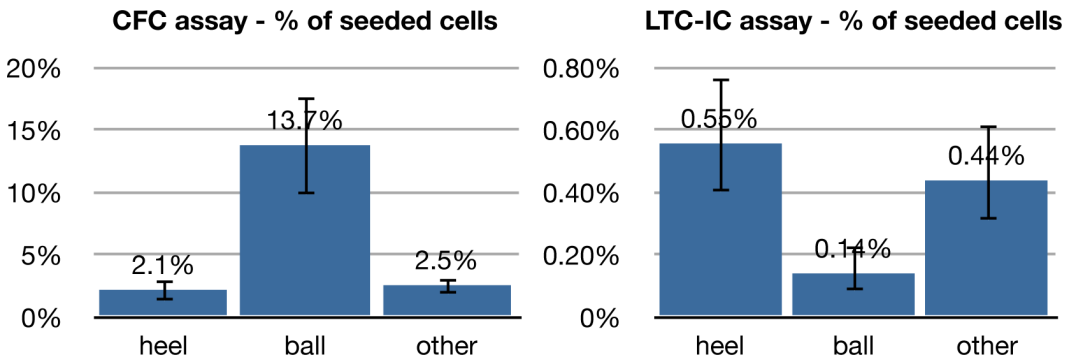

Fig. 2.11. CFC and LTC-IC colony assays of shoe print regions.

Both assays showed an overall very low amount of colonies formed from the seeded cells, however the LTC-IC colonies were an order of magnitude lower. In the CFC assays the cells in the ball region showed the highest percentage of colonies at 13.7%. In the LTC-IC assay, the cells in the ball region produced the lowest amount of colonies. Both the heel and the cells outside of the shoe print region had a significantly higher percentage over the cells in the ball region.

Results showed that the $CD34^+$ population in bone marrow did contain a mixture of cells at varying stages of differentiation. The lower amount of colonies produced in the LTC-IC assay, proved there were in fact very few primitive stem cells present. Given that the small cells in the heel region did not produce many CFC colonies, but instead were higher in the LTC-IC assay, led to the conclusion that these cells were more primitive and less differentiated. The opposite observation regarding the cells in the ball region

led to the conclusion that these cells are more differentiated progenitor cells that more rapidly produced colonies in the CFC assay. Interestingly, the $CD34^-$ cells outside of the shoe print regions also produced LTC-IC colonies. This might be explained by reports that certain $CD34^-$ cells also can induce hematopoiesis (Yin 1997; Boxall 2008) and that these cells were selectively expanded in the LTC-IC assay.

Conclusions

Table 2.2 summarizes the findings of the multiple analytical methods performed on the $CD34^+$ cells. Based on these findings we setup the hypothesis that the cells in the heel region are HSCs in a quiescent state and that the cells in the ball region are more proliferative stem and progenitor cells. Ultimately though these are all *in vitro* assays. To further investigate this hypothesis we would have to inject the cells of the different regions into NOD/SCID mice. As noted though this might still not be truly conclusive, especially given the fact that the cells are all in the G_0 phase. Another explanation for these observations might be the possibility that these smaller $CD34^+$ cells are part of the newly discovered very small embryonic-like (VSEL) stem cells that have also been discovered in the bone marrow (Sovalat 2011).

Table 2.2. Summary of shoe print region analysis of $CD34^-$ cells.

Assay	**heel cells**	**ball cells**
Scatter plot	diminished rapidly after 1 week	diminished slowly over 1 month
Immunophe-notype	$CD31^+$, $CD34^+$, $CD38^+$, $CD133^-$	$CD31^+$, $CD34^+$, $CD38^+$, $CD133^+$
Cell cycle analysis	only G_0 phase	all phases
Cell tracking	rapid increase in size after seeding	-
CFC & LTC-IC	more primitive stem cells	more progenitor cells

MSC feeder layer

As outlined before, the underlying hypothesis of feeder cultures is to provide an environment that mimics the stem cell niche. Therefore the use of MSCs is of high interest.

Extraction

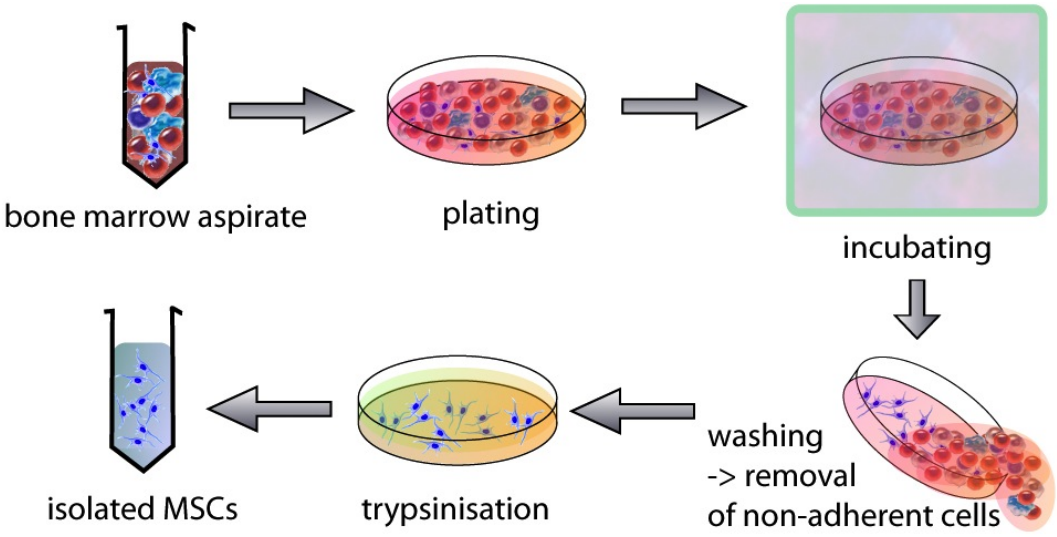

Fig. 2.12. Schematic of extraction procedure for MSCs.

Extraction procedure of MSCs nowadays is still fairly similar to the original extraction method described by Friedenstein et al. (Friedenstein 1976) (Fig. 2.12). In most cases hMSCs are extracted from bone marrow aspirates that are taken from the posterior iliac crest. Mostly these bone marrow aspirates are seeded without any pretreatment, however if blood clotting is an issue the aspirates can also be treated with a Ficoll-Paque density gradient or a RBC lysis buffer before plating. 24 hours after plating, the hMSCs will have adhered to the TCP and the remaining hematopoietic cells can be washed away during medium exchanges. The hMSCs will expand till confluence is reached and can be harvested using trypsin.

This extraction method holds two caveats: 1. Isolation is purely based on adhesion to TCP. Therefore any other adherent (stem) cell types in the tissue will likely be mixed in with the extracted population. 2. TCP is a very stiff non-natural substrate and the longer the MSCs are exposed to it the more they loose their stem cell properties (Izadpanah 2008). However since only very few MSCs are prevalent in the initial tissue, expansion and subsequent passaging are necessary to obtain sufficient cells for a feeder layer.

Therefore we performed extensive analysis on the cell composition and differentiation potential of both hMSCs and hASCs with respect to passage number (see Chapter III) and also tried to alter the matrix on which the cells were cultures (see Chapter V).

CHAPTER III - ANALYSIS OF FEEDER LAYERS

Since the stromal cells comprising the feeder layers will play a very important role in recreating the stem cell niche, we conducted an extensive study developing a method to characterize stem cells from different sources with respect to their differentiation potential.

Introduction

In the rapidly evolving field of tissue engineering and regenerative medicine, many approaches utilize stem cells that can be differentiated *ex vivo* to recreate specific types of tissues. Human bone marrow-derived mesenchymal stromal cells (hMSCs) have been extensively studied with respect to their differentiation potential towards adipocytes and osteoblasts, among other tissues, and provide an essential source for these tissue outcomes (Gregory 2005). In many cases, hMSCs are also being used due to their reported immunosuppressive functions (Le Blanc 2003; Helmy 2010). More recently, studies have shown that adipose-derived stem cells (hASCs) show similar differentiation properties (Tapp 2009).

The stem cells used in most of these studies are routinely obtained by plating the cells on tissue culture plastic (TCP) and extracting the adherent cells. This isolation method is often chosen because it is gentle to the cells as well as relatively inexpensive and easy to perform (Beyer Nardi 2006). In contrast, isolation by adherence is not stringent when compared with fluorescence-activated cell sorting (FACS) and generally yields a heterogeneous population. Studies using mixed cell populations can be both useful, as well as misleading, as it is often unknown which specific cell type responds to the culture conditions used (Charbord 2010). Also a mixed population might not behave in the same manner as a pure isolated cell population, such as due to cell-cell signaling factors.

The predominant use of the facilitated adhesion extraction method is also related to the fact that there is no unique phenotypic marker that defines a true hMSC. To circumvent this problem, many groups, most recently the Mesenchymal and Tissue Stem Cell Committee of the International Society for Cellular Therapy (Dominici 2006), have listed a combination of surface marker profiles in an attempt to define this population of cells. Table 3.1 shows both the range, but also the variety, of markers being used to define these stem cells. Unfortunately, these definitions do not agree on a single distinguishable marker. This large variation in profile definition has not only led to confusion as to which profile combination defines the optimal stem cell, but subsequently different groups use different combinations as their definition of hMSCs. This approach impairs comparison of results between different research groups, as there is already a large variance due to donor variability and culture conditions (Ho 2008; Vater 2011). Further, looking ahead to clinical needs, without clear methods to generate consistent assessments of stem cell populations, variability in clinical trial outcomes would be problematic.

Table 3.1. List of surface marker profiles used in the literature to define MSCs.

Study	**Immunophenotype**	**Year**
(Dominici 2006)	CD105+, CD73+, CD90+, CD45-, CD34-, CD14-, CD19-	2006
(Romanov 2005)	CD105+, CD54+, CD106+	2005
(Wagner 2005)	CD10+, CD14-, CD24-, CD31-, CD34-, CD36+, CD38+, CD45-, CD117-, CD133-, CD13+, CD29+, CD44+, CD73+, CD90+, CD105+, CD166+	2005
(Suva 2004)	CD45-, CD14-, CD34-, CD90+	2004
(Quirici 2002)	NGFR+, CD34-, CD113+, CD90+	2002
(Pittenger 1999)	CD29+, CD44+, CD71+, CD90+, CD106+	1999

Another issue is that researchers are unable to define the “state” of the hMSCs that are being used. Since only a few MSCs are prevalent in the tissue, expansion and subsequent passaging is often necessary to obtain sufficient cells. However, hMSCs gradually alter their stem cell properties with extended culture time *in vitro* (Izadpanah 2008). In the best case the *in vitro* “age” of a stem cell is given by its passage number (P), which is influenced by many different factors (e.g. seeding density, growth rate, culture medium) and therefore does not help in defining the “state” of the stem cells before their application.

Finally, current differentiation studies with hMSCs and hASCs are limited due to the lack of true quantitative analysis. Endpoint analysis of differentiated cells is generally based on RNA quantification of cell specific genes using quantitative polymerase chain reaction (qPCR), as well as staining methods to determine the presence of tissue-specific components, e.g. calcium phosphate staining with Alizarin red for osteogenesis (Mitchell 2006). These supposedly quantitative methods should be regarded as qualitative methods as they only provide information regarding the overall population but do not reflect how many cells responded to a specific treatment and therefore how many stem cells were present before and after differentiation. A more quantitative analytical method is therefore of high interest with respect to the decreasing differentiation potential of stem cells with increasing time in culture.

In an attempt to standardize MSC definition and with it improve stem cell extraction, characterization, and streamline outcomes, we have developed methods to correlate the quantitative analytical strength of flow cytometry to the qualitative outcomes of functional assays. For this, cells were passaged several times post extraction and differentiated at each passage towards adipocytes and osteoblasts (Fig. 3.1). The differentiated and undifferentiated cells were analyzed with both qualitative and quantitative analytical tools such as flow cytometry, qPCR and staining.

If this relatively inexpensive and simple method was utilized for MSCs in research, a large database could be assembled that would allow researchers to compare results and determine the "state" of stem cells before use. Ideally one could also back-correlate the definitions of the stem cells in the database to the different parameters of cell source (e.g., gender, age, site) and also better determine the influence of different culture conditions on cell outcomes. This approach has direct implications for studies in regenerative medicine as well as for clinical therapies that involve the use of stem cells.

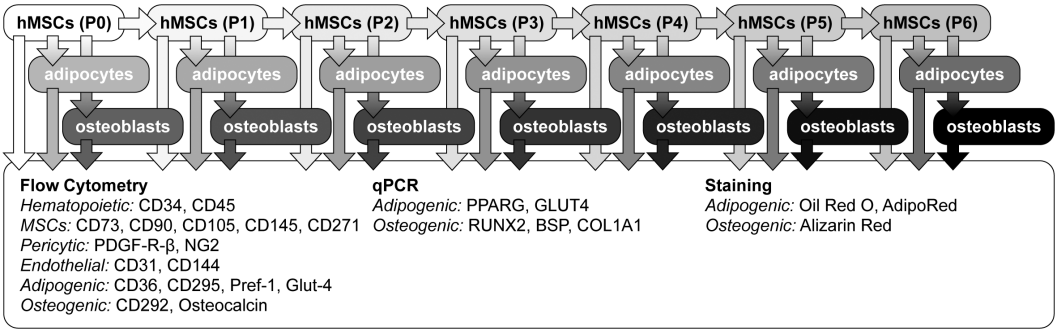

Fig. 3.1. Outline of the procedure.

Materials and Methods

Bone marrow derived human MSC extraction

hMSCs were extracted from two different donors (MSC1 and MSC2) from a commercially obtained fresh human bone marrow aspirate (Lonza). Aspirate donors were male, under 25 years of age and free of HIV, hepatitis B and hepatitis C. The aspirate was diluted 10-fold with MSC expansion medium consisting of DMEM:F12 basal medium (DMEM:F12) supplemented with 10% fetal bovine serum (FBS), antibiotics-antimycotics (100 U/mL penicillin, 100 µg/mL streptomycin, 0.25 µg/mL fungizone), 0.1 mM nonessential amino acids and 1 ng/mL bFGF (Invitrogen). This diluted bone marrow was plated on tissue culture treated plastic (TCP) T-185 flasks at an average seeding density of 350,000 bone marrow mononuclear cells/cm^2. After 10

days the non-adherent cells were removed and the adherent cells were kept in expansion medium to reach confluence.

Adipose tissue derived MSC extraction

hASCs were extracted from two different donors (ASC1 and ASC2) following a standard procedure from human subcutaneous adipose tissue from elective surgeries under approved protocols (Dubois 2008). Briefly, primary isolation of the hASCs was conducted by first homogenizing the extracted adipose tissue to obtain smaller tissue masses. These masses were then washed three times to remove excess blood cells as well as non-adipogenic tissue. After the washes the adipogenic tissue was digested with equal volumes of 1 mg/mL collagenase type I in pre-warmed phosphate buffered saline (PBS) for one hour. This dissociated the tissue, releasing the hASCs from the adipocytes. Centrifugation at 300 g for 10 min allowed the hASCs to pellet, which were then washed twice in PBS and defined as SVF. These cells were then plated on TCP at a density of 0.16 mL original tissue volume per cm^2. hASCs were then expanded to confluence using DMEM:F12 medium with 10% FBS and 1% antibiotics-antimycotics.

Osteoblasts

Human osteoblasts derived from healthy adults (NHOst) were purchased commercially (Lonza). These were used as controls to measure as standards in comparison to MSC2 cells differentiated to osteoblasts.

Expansion and Passaging

Continuous expansion was performed using the same expansion medium, although without bFGF as this has been reported to play a negative role on hMSCs (Sotiropoulou 2006) and should therefore be avoided in cultures that are intended for tissue implants. Upon reaching confluence, the expanded cells from each flask were passaged using 0.25% trypsin-EDTA (Invitrogen) and expanded in 4 new T-185 flasks. An average of $5x10^6$ cells per flask at confluence yielded a passaging seeding density of 6,750

cells/cm^2, suggesting a 2-fold cell doubling to reach confluence. This expansion was carried out continuously for up to 6 passages (Fig. 3.1).

Differentiation

Additional flasks were differentiated towards either adipocytes or osteoblasts (Fig. 3.1). The medium of the confluent flasks was exchanged with a differentiation medium. In the case of adipogenic differentiation the medium consisted of DMEM:F12 with 3% FBS, 1% antibiotics-antimycotics (100 U/mL penicillin, 100 µg/mL streptomycin, 0.25 µg/mL fungizone) (Invitrogen) supplemented with 33 µM biotin, 17 µM D-pantothenic acid hemicalcium salt, 1 µM human insulin, 1 µM dexamethasone, 50 mM 3-isobutyl-1-methylxanthine and 5 µM 2,4-thiazolidinedione (Sigma). For osteogenic differentiation the medium was DMEM:F12 with 10% FBS, 1% antibiotics-antimycotics (100 U/mL penicillin, 100 µg/mL streptomycin, 0.25 µg/mL fungizone) (Invitrogen) supplemented with 10 mM glycerol-2-phosphate disodium salt hydrate, 400 µM L-ascorbic acid 2-phosphate sesquimagnesium salt hydrate, 10 nM 1α,25-dihydroxyvitamin D3 and 10 nM dexamethasone (Sigma). The cells of each passage were kept in the respective differentiation medium for 3 weeks to allow full differentiation and medium was fully replenished biweekly.

Microscope images and staining

Changes in cell morphology pre- and post-differentiation were observed using an inverted microscope. To determine successful differentiation, cells were also stained with Oil Red O (Sigma) in the case of adipogenic differentiation or Alizarin Red (Sigma) for osteogenic differentiation. Additionally, AdipoRed (Lonza) staining was used after hASC differentiation as it is faster and more quantifiable due to fluorescence measurements.

RNA isolation, purification, and qPCR

RNA was isolated from 6 samples of cells both before and after differentiation using Trizol reagent (Invitrogen) following the single step acid-phenol guanidinium method, and purified using the Qiagen RNEasy kit (Qiagen). To synthesize cDNA, reverse transcription was performed on the purified RNA using the High Capacity cDNA Archive kit (Applied Biosystems). Osteoblast differentiation markers include runt-related transcription factor 2 (RUNX2), bone sialoprotein (BSP) and collagen type I (COL1A1). Adipogenic differentiation markers include perixosome proliferator-activated receptor γ (PPARG) and insulin-responsive glucose transporter 4 (GLUT4). Primers and probes for the bone-related and adipose-related genes above were obtained from TaqMan® Gene Expression Assay kits (Applied Biosystems). Transcript expression levels were quantified with a Stratagene Mx3000P QPCR System (Stratagene). Expression levels were normalized to glyceraldehyde 3-phosphate dehydrogenase (GAPDH) and reported relative to values of P0 undifferentiated cells. We have previously reported PCR reaction conditions and primers (Meinel 2006; Mauney 2007).

Flow cytometry

Phenotypic markers

Flow cytometric analysis was performed on cells of each passage, both after reaching confluence and after 3 weeks of differentiation. Cells were labeled with antibodies pre-conjugated with either fluorescein isothiocyanate (FITC), phycoerythrin (PE), peridinin chlorphyll protein (PerCP) or allophycocyanin (APC). Two phenotypic cell markers were selected for each of the following cell types: hematopoietic stem cells (CD34, clone: 581, BD Biosciences; CD45, clone: MEM-28, Abcam), adipocytes (CD36, clone: 255606, R&D Systems; CD295, clone: 52263, R&D Systems; Pref-1, clone: 211309, R&D Systems, Glut-4, clone EP930(2)AY), osteoblasts (CD292, R&D Systems; osteocalcin, clone: 190125, R&D Systems), endothelial cells (CD31, clone: WM59, Abcam; CD144, clone

16B1, eBioscience) and pericytes (PDGFR-ß, clone: PR7212, R&D Systems; NG2, clone: LHM-2, R&D Systems). Additionally 3 commonly cited MSC markers (CD73, clone: AD2, BD Biosciences; CD90, clone: 5E10, Biolegend; CD105, clone: 166707, R&D Systems) as well as 2 more novel MSC markers (CD146, clone: 128018, R&D Systems; CD271, clone: ME20.4-1.H4) were included. Hematopoietic cell markers were chosen based on their high abundance in the extracted tissues. Endothelial cell markers were chosen as it has been reported that endothelial cell progenitor cells are also present in bone marrow (Reyes 2002) and can be co-extracted with hMSCs. Especially since many of the MSC markers are proteins expressed for cell adhesion (Supplementary Table 3.1) it is important to be certain that the extracted cells do not include endothelial cells. For future studies where endothelial cells may be included in co-cultures with hMSCs for regenerative medicine, distinguishing the survival of these respective cell populations would be useful. Pericyte markers were included due to recent suggestions that both hMSCs and hASCs are located in proximity to blood vessels *in vivo*, where they exert the function of pericytes by supporting blood vessel structure and wound repair (da Silva Meirelles 2008). Due to a lack of commonly used adipogenic or osteogenic markers for flow cytometry, a few selected markers were chosen for each cell type.

Cell extraction

For flow cytometric analysis, growth medium was aspirated from 3 confluent T-185 flasks. After washing with PBS, 5 mL of 0.25% trypsin/EDTA (Invitrogen) was added to each flask and kept in an incubator for 10 min at 37 °C. Trypsinization was halted by adding 10 mL serum containing medium and the cell suspension was collected into a 50 mL conical tube. The conical tube was centrifuged for 10 min at 450 g and 4 °C. After removing the supernatant, the pellet was resuspended in 2 mL of FACS-buffer, consisting of PBS supplemented with 0.5% FBS (Invitrogen) and 5 mM EDTA (Sigma).

Intracellular staining - osteocalcin sample

A 200 µL aliquot of the original 2 mL suspension was separated and fixed in 10% formalin solution for 10 min. The fixed cells were centrifuged for 10 min at 450 g and 4 °C. Following centrifugation, the supernatant was removed and the cells were re-suspended in 2 mL PBS. After another centrifugation step, the supernatant was removed and the cell pellet was re-suspended in 2 mL 0.1% Triton-X in PBS solution, to perforate the lipid bilayer, allowing the stain to enter the cell. Subsequent washes always included Triton-X to maintain lipid bilayer perforation.

Sample labeling and measurement

The cell suspension was split into samples in 2 mL Eppendorf tubes. Then 10 µg of human IgG (Sigma) was added to each of the samples to block any nonspecific receptors before adding the respective antibody to each sample. Unstained samples were included for autofluorescence background reduction. Each sample was incubated at 4 °C for 30 min in the dark. After incubation 1 mL of FACS-buffer was added to each sample and centrifuged for 10 min at 450 g and 4 °C. The supernatant was removed and the pellets were re-suspended in 1 mL FACS-buffer. After a second centrifugation at the same settings, the samples were re-suspended in 250 µL FACS-buffer, transferred into their respective FACS-tubes and kept on ice until measurement. Flow cytometric analysis was performed on a FACSCalibur (Becton Dickinson). A minimum of 50,000 events was recorded for each sample. Analysis was performed using FlowJo (TreeStar) on dot plots to obtain a more accurate quantification as compared to histogram analysis.

Statistics

Statistically significant differences between two conditions in qPCR were determined by performing a two-tailed Student's t-test. Differences were considered significant if $P < 0.05$, unless otherwise noted.

Results

hMSCs extracted from the two different donors were labeled MSC1 and MSC2, respectively. Likewise the hASCs extracted from two different donors were labeled ASC1 and ASC2, respectively. Due to the limited amount of cells obtained directly after extraction, the stromal vascular fraction (SVF) of ASC1 was used entirely for flow cytometric analysis. Likewise insufficient cells were available at P0 of the ASC2 cells, such that full analysis commenced at P1.

Expansion

Following the procedure outlined in Figure 1, the experimental setup allowed the same seeding density at each passage, and confluence was reached in most cases 3 weeks post expansion. The cumulative time of culture for the cells *in vitro* is listed in Supplementary Table 3.2.

Microscopic analysis

Microscopic analysis of the MSC1 cells (Fig. 3.2) showed that both adipogenic and osteogenic differentiation was the highest at P0. Despite treating cells at each passage for the same period of time with differentiation medium, different levels of matrix deposition were observed. Figure 3.2 also shows that in comparison to P0, the P1 cells had a lower amount of differentiated cells. This drop in differentiation potential decreased gradually with each passage. This is especially visible in adipogenic differentiation, where at P0 adipocytes were highly abundant with large lipid vacuoles compared to P5 where adipocytes were not only scarce but also showed very small lipid vacuoles. The same trends were observed in both MSC2 and ASC2 cells (Suppl. Fig. 3.1).

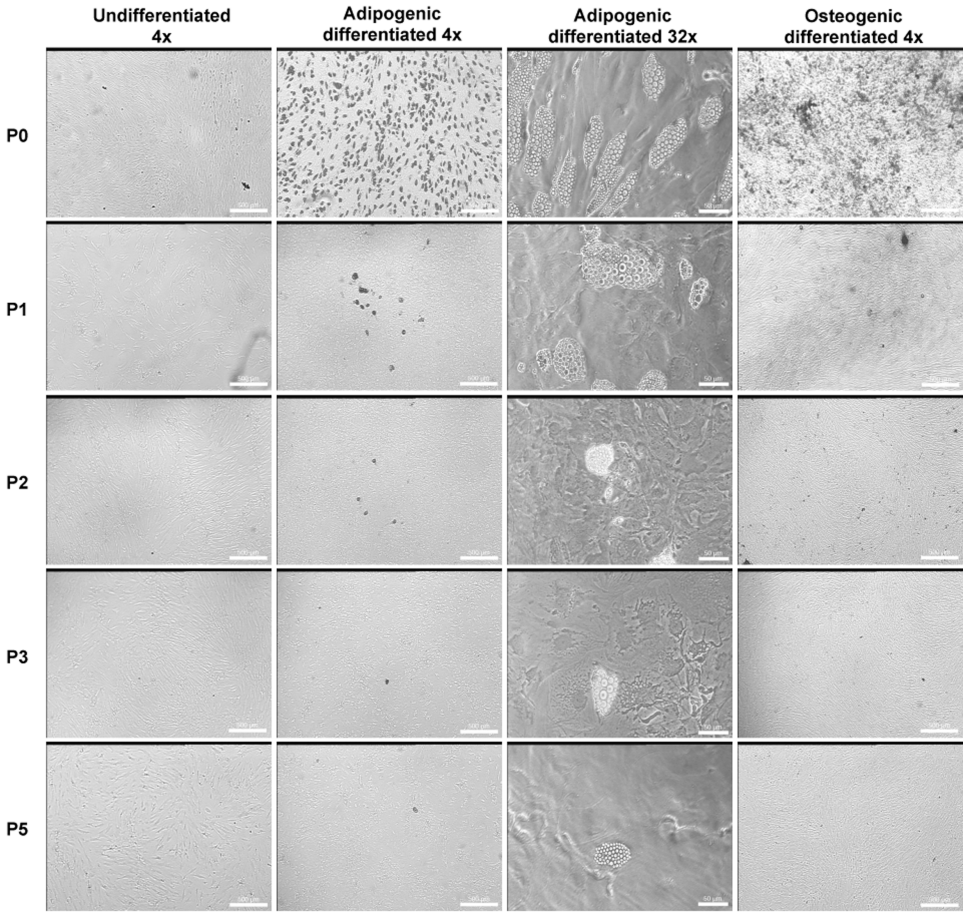

Fig. 3.2. Microscopic images of MSC1 cells at each passage pre- and post-differentiation. Rows are images of cells from the same passage (P0 - 5) shortly before extraction for flow cytometric and qPCR analysis. Columns are images of undifferentiated, adipogenic and osteogenic differentiated cells measured at 4x and 32x magnification for a population overview or detailed cell morphology respectively. Scale bars in all 4x images are equal to 500 µm. In 32x images, scale bars are equal 50 µm.

qPCR

Adipogenic differentiation was confirmed with qPCR analysis with an increase of perixosome proliferator-activated receptor γ (PPARG) at all passages (Fig. 3.3 and Suppl. Fig. 3.2). Additionally, the PPARG levels of undifferentiated hMSCs gradually decreased with each passage. An increase in PPARG was also observed at all passages after osteogenic differentiation. Glucose transporter 4 (GLUT4) expression followed no

distinct trend. With regard to osteogenic differentiation, the same gradual baseline decrease of all markers was measured with the undifferentiated cells at each passage. In each case runt-related transcription factor 2 (RUNX2) levels and bone sialoprotein (BSP) levels increased after 3 weeks of differentiation, however collagen type I (COL1A1) levels showed no clear trend.

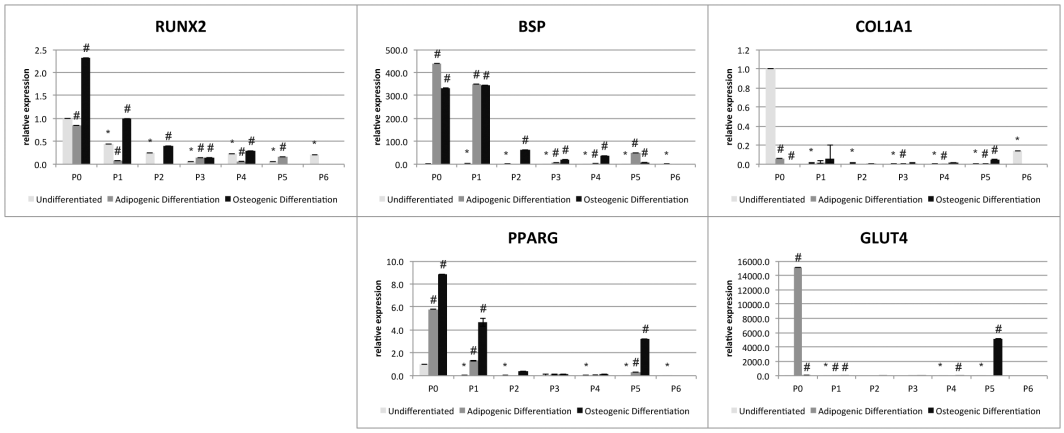

Fig. 3.3. Relative gene expression of MSC1 cells. Top row: osteogenic markers runt-related transcription factor 2 (RUNX2), bone sialoprotein (BSP) and collagen type I (COL1A1). Bottom row: adipogenic markers: perixosome proliferator-activated receptor γ (PPARG) and glucose transporter 4 (GLUT4). Data is grouped by passage number (P0 - 6) showing data from undifferentiated, adipogenic and osteogenic differentiated cells. Data points are mean relative expression ± standard deviation (n = 6). Marked samples are statistically different, * relative to undifferentiated P1 samples ($P < 0.05$), # relative to undifferentiated samples of same passage number ($P < 0.05$).

Flow cytometric analysis

The two hematopoietic markers CD34 and CD45 showed almost no positive labeling at any passage of hMSCs (Fig. 3.4A and Suppl. Fig. 3.3A). hASCs instead showed a significant $CD34^{+}$ labeling. This was initially observed with the SVF of the ASC1 cells (Fig. 3.5A). These cells showed slightly lower labeling percentages of the most common hMSC markers, slightly higher percentages of CD45 and CD31 and a significantly higher percentage of CD34 cells as compared to hMSCs. Subsequent measurement of the

ASC2 cells showed similar surface marker profiles for P0 cells as compared to MSC1 cells (Fig. 3.5B). $CD34^+$ labeling decreased rapidly after the initial 14 days in culture and gradually diminished in undifferentiated cells after 2 passages (Suppl. Fig. 3.3C). These low CD34 percentages increased over 33% after adipogenic differentiation, which was not observed in hMSC cells.

CD73 and CD90 labeled almost the entire cell population over all passages in all hMSC and hASC sources. This labeling remained high also after adipogenic and osteogenic differentiation. CD105 labeling remained at a relatively high rate on undifferentiated MSC1 cells, however had a similar trend on MSC2 and ASC2 cells, where following an initially low labeling the percentages increased gradually to a peak at P3-5 and dropped at P6 again. After differentiation the average labeling decreased in general to the $CD105^+$ level of early passages. CD146 showed a similar pattern to the CD105 labeling, however at much lower levels and a relatively similar trend was also observed on CD271, although again at even lower levels.

Of the pericyte markers, PDGFR-ß showed an overall very high labeling pre- and post-differentiation on MSC1 cells (Fig. 3.4B). Only undifferentiated MSC2 cells had the same high labeling percentage (Suppl. Fig. 3.3B). This percentage dropped significantly on differentiated cells of early passages and gradually increased proportionally to passage number. On the other hand NG2 levels were very low in all passages and all sources.

Endothelial markers CD31 and CD144 were present at a very low level with an outlier at P0 of undifferentiated MSC1 cells.

CD36 showed very low labeling at early passages with a gradual increase with passages. This was the only marker that exhibited this pattern consistently over all cell sources. CD295 showed no apparent correlation with respect to passage, differentiation

or cell source. The same was observed in surface marker staining of Pref-1 and Glut-4 on ASC2 cells (Suppl. Fig. 3.3D).

Similar to CD36, CD292 had a very low gradual increase with each passage. Osteocalcin on the other hand was very high in all passages and showed a gradual increase in labeling on undifferentiated MSCs. On osteogenically differentiated MSC2 cells a pattern was noted that was inversely proportional to the differentiation potential observed under the microscope.

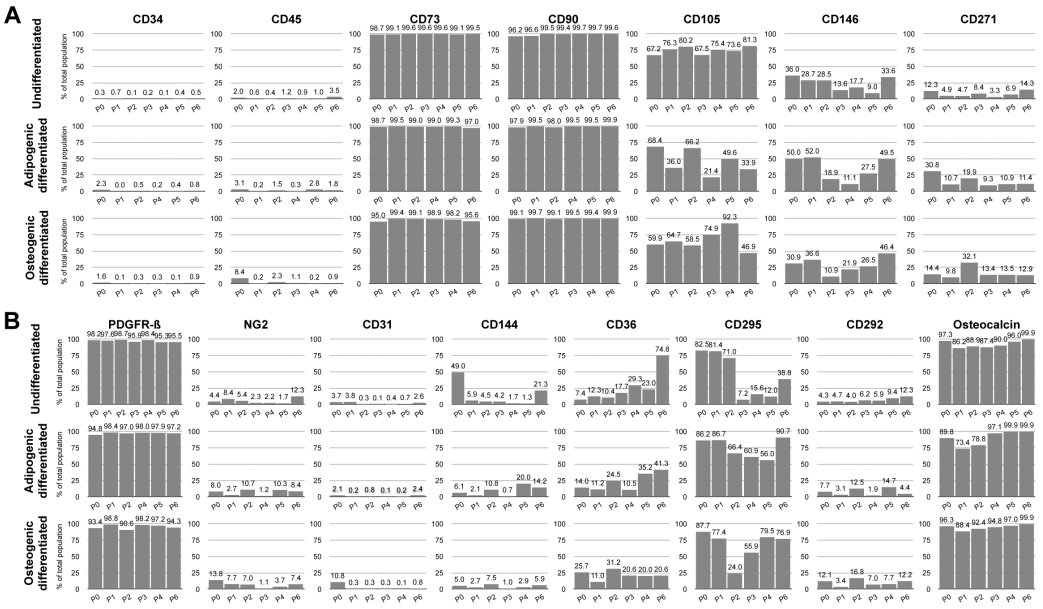

Fig. 3.4. Flow cytometric analysis of MSC1 cells. A minimum of 50,000 events was recorded for each sample. Data is given in percentages of total population of undifferentiated (top row), adipogenic differentiated (middle row) and osteogenic differentiated cells (bottom row). Data is ordered by passage number (P0 - 6) and grouped in each column by marker type. (A) Analysis of MSC markers with CD34 and CD45 as common negative, CD73, CD90 and CD105 as common positive and CD146 and CD271 as novel positive MSC markers. (B) Analysis of pericyte (PDGFR-β and NG2), endothelial cell (CD31 and CD144), adipocyte (CD36 and CD295) and osteoblast (CD292 and osteocalcin) markers.

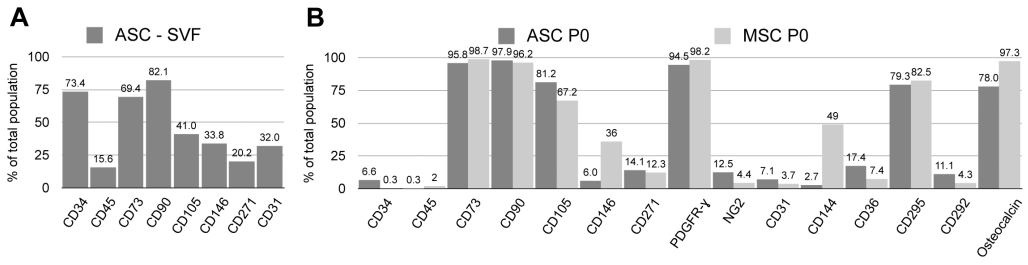

Fig. 3.5. Flow cytometric profile of undifferentiated cells given in percentages of total population. (A) Common MSC markers of ASC1 cells derived from the SVF. (B) Comparison of MSC, pericyte, endothelial cell, adipocyte and osteoblast markers on unpassaged (P0) cells of ASC2 and MSC1 cells. A minimum of 50,000 events was recorded for each sample.

Another observation derived from flow cytometric analysis was a gradual increase of autofluorescence with increasing passage (Fig. 3.6 and Suppl. Fig. 3.4). After an initial increase in fluorescence when excited by a 488 nm laser and detected at 530/30 nm (FL1-H), fluorescence gradually also increased when excited by a 635 nm laser and detected at 661/16 nm (FL4-H).

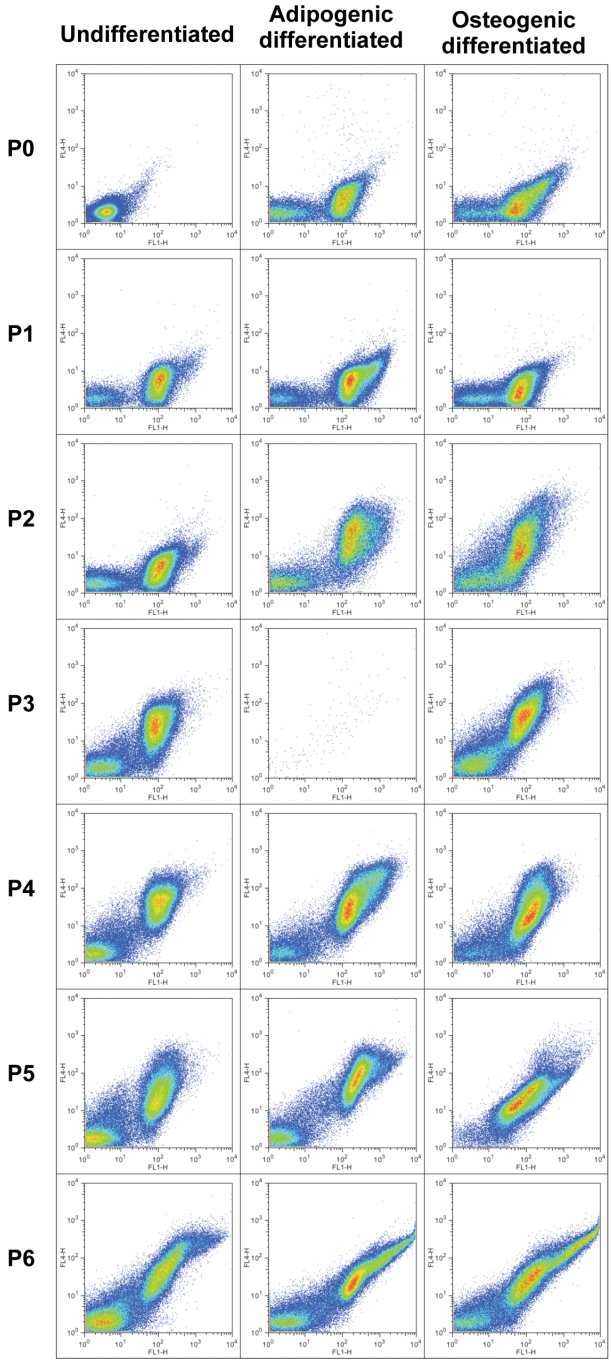

Fig. 3.6. Autofluorescence of MSC1 cells. Rows are log-scale dot plots of cells from the same passage (P0 - 6), and columns list undifferentiated, adipogenic differentiated and osteogenic differentiated conditions respectively. X-axis: FL1-H (ex: 488 nm; em: 530/30 nm). Y-axis: FL4-H (ex: 635 nm; em: 661/16 nm).

Discussion

An initial reaction to this method may be the need for a lot of cells, predominantly for flow cytometric analysis, such that insufficient cells were available for full analysis of early passages of hASCs. This concern can be put in perspective in that we used up to 15 markers to cover a broad spectrum of phenotypes. Using the same doubling rates, we calculated that only $0.5x10^6$ cells are needed at initial seeding of each cell source to investigate 1 surface marker, perform osteogenic and adipogenic differentiation and commence continuous passaging. Thus, the majority of stem cell sources should be readily amenable to the methods described in the present paper.

The lack of using basic fibroblast growth factor (bFGF) for this study was visible in the relatively long times it took to reach confluence at each passage. Interestingly, there was generally no change in the expansion rate of the cells even after several months *in vitro*. Considering the rapid drop in differentiation potential after P1, one can therefore conclude that expansion rate is not linked to differentiation potential. This adds to the debate regarding the use of bFGF in regenerative medicine (Sotiropoulou 2006).

The rapid drop in differentiation potential was very evident and should be greatly taken into consideration when determining the optimal balance between retaining stem cell properties and passaging cells.

The low increase in early gene markers (PPARG, RUNX) and large increase of a late marker (BSP), largely overlaps with the microscope data showing again that differentiation occurs predominantly only in early passages. Additionally, we are not aware of any study that shows the gradual decrease in the baseline of gene markers pre-differentiation. This might be an interesting aspect of the results with regard to determining the state of stem cells. However herein also lies the limitation of qPCR data: it is unclear if differentiation has been fully completed, or whether individual stem cells are still undifferentiated in culture.

The lack of hematopoietic and endothelial cell markers (CD45, CD31, CD144) in passaged cultures is explainable with the fact that the culture medium used was not targeted towards these cell types, and that they died off or were washed out during the extended culture period. This is especially obvious in the ASC-SVF culture where a comparably high percentage of cells was present and labeled positive for these markers, and are likely contaminants of other cells

With regard to CD34 labeling, this still proves to be a negative marker for hMSCs, which is especially important as it is a positive marker for hematopoietic stem cells (HSC). Though the presence of CD34-positive cells in the hASC population raises an interesting question. Hematopoiesis is predominantly localized within the bone marrow, hence one would not expect a high percentage of $CD34^+$ hematopoietic stem cells (HSC) in adipose tissue. Though these are present in bone marrow aspirates during extraction, they survive only for short periods *in vitro*. This makes the presence of $CD34^+$ cells in hASC cultures a potential positive marker, of which it's function is still being discussed (Festy 2005; Suga 2009). It is also very interesting to see the increase of $CD34^+$ cells in hASC cultures after adipogenic differentiation. Though further studies will be necessary, this adds fuel to the discussion of the relationship between adipocytes and HSCs (Sera 2009).

With regards to traditional MSC markers, it is striking that CD73 and CD90 labeled almost all cells, not only in hASC and hMSC cultures, but also over the entire time in culture. Based on the qPCR and microscope data, one can assume that only very few cells still possess full differentiation potency at later passages, it must be concluded that these two markers are not very useful to define true MSCs. This is especially the case considering their rate does not decrease at all after 3 weeks of differentiation. CD105 showed a slightly lower labeling percentage and when using the definition of a hMSC being $CD34^-$, $CD45^-$, $CD73^+$, $CD90^+$ and $CD105^+$, one can rather safely rely on CD105 as

single marker as it is the least common denominator. However we still have strong doubts that CD105 is a valuable stem cell marker, as it again did not follow the differentiation pattern observed under the microscope. Based on the amount of cells visibly undergoing differentiation, we would suggest relying rather on more novel hMSC markers such as CD146 and CD271. This could be verified by sorting out these cells individually using FACS and performing differentiation studies on the isolated cell type.

The high frequencies of PDGFR-ß likely has origins from the fact that it is not specific for pericytes but instead is reported to be present on a wide range of cells of mesenchymal origin (Andrae 2008). On the other hand NG2 is believed to be more specific for pericytes. The low amount of labeling should not necessarily refute the suggestion of hMSCs being pericyte-like, especially considering the observed low amount of differentiating cells.

The labeling percentages of adipogenic markers CD36, CD295, Pref-1 and Glut-4 provided no apparent correlation between the differentiation levels observed in the microscopic images. CD36 was the only marker that consistently increased with passage and may prove to be a potential marker of stem cell aging. Though the expression of the selected adipogenic proteins on the surface membrane is required for activation of important metabolic pathways of adipocytes, they do carry out many different functions (Fruhbeck 2006; Huang 2007; Jing 2009; Sul 2009; Glatz 2010). The diversity of the metabolic pathways may be a possible reason behind the lack of a clear pattern, as the cells might be in very different stages of differentiation. In a recent publication, high levels of CD295 were correlated to the aging and dying of MSCs (Laschober 2009). This could not be verified in our results. Since the chosen adipocyte markers did not lead to any conclusive results, more research needs to be done to discover adipogenic markers for flow cytometry. Possible new markers include AdipoRed staining and measuring the ratio of intracellular vs. surface expression of Glut-

4 (Watson 2001). Here it should be mentioned that the lack of flow cytometric data on adipocytes is due to the fact that they are difficult to measure in a flow cytometer. The strong shear forces can easily rupture the fragile lipid filled cells, though it has been shown in the past though that this can be counteracted by fixation (Smyth 1992). This also leads to the importance of finding a true stem cell marker. If this could be found, flow cytometric analysis of differentiated cells would still allow accurate quantification of differentiation by counting the amount of remaining stem cells post differentiation.

Similar to the suggestions for CD36, CD292 could be a potential tool for determining the state of a stem cell. The lack of high expression after osteogenic differentiation may be understood in that it is not a requirement for differentiation and is only necessary for extracellular matrix (ECM) deposition of osteoblasts (ten Dijke 2003). If osteoblasts secrete large amounts of ECM they may be difficult to label with flow cytometric markers. This might explain the inversely correlated relationship in differentiated MSC2 cells as well.

The use of osteocalcin, as the only intracellular marker, circumvented this issue and showed a very high, gradually increasing labeling in hMSCs. Future experiments should include other osteogenic markers, most notably CD106, which has recently been suggested to quantify osteogenic differentiation (Liu 2008).

Finally the increase in autofluorescence may be due to accumulation of flavoproteins and lipofuscin (Reyes 2006; Rice 2010). Accumulation of these compounds is suggested to be related to oxidative stress and aging of cells cultured *in vitro* and therefore provides an additional marker for the state of stem cells. The hypothesis here would be that the higher the autofluorescence the lower the differentiation potential. This would be a relatively simple analytical tool to prescreen MSCs for a more generalized assessment of differentiation potential.

Conclusions

Our method of correlating quantitative flow cytometric data with current standard qualitative assays displays a straightforward and relatively inexpensive approach for detailed characterization of a batch of stem cells. To our knowledge this is the first collection of such detailed analysis of hMSCs and hASCs in long-term *in vitro* culture and will be helpful to aid other researchers in planning future experiments. Not only were we able to disqualify certain makers for true stem cell characterization (CD73 and CD90), but also highlight a marker with significant difference between hMSCs and hASCs (CD34). Since no stem cell marker followed the differentiation pattern observed under the microscope, the discovery of a unique stem cell marker remains to be identified. Since most non-MSC markers labeled the cell populations at very different levels, it is clear that standard isolation methods yield heterogeneous populations that also change during extended culture. However considering most traditional MSC markers used in this experiment labeled either almost everything or almost nothing, one must conclude that these markers are not very useful as they do not define a true stem cell, but given their origin, rather just an adherent stromal cell. Therefore MSCs remain an undefined cell type. Though the data presented here might not directly help in discovering a unique stem cell marker, by using this method we were able to disqualify the reliability of certain markers with regard to stemness and gradually allow one to zone in on the profile of a true stem cell. This approach should also allow one to define different stages of stemness as it is known with HSCs (Kondo 2003). In the context of the project, the discovery that hASCs had an increased CD34 expression over hMSCs, especially after adipogenic differentiation makes it a very impractical cell type to use as a feeder layer. Despite suggestions that ASCs have a proliferative advantage over MSCs in mice (Nakao 2010), the quantification of HSCs in human cultures would be greatly impaired if the feeder cells were expressing CD34 as well.

Supplementary Data

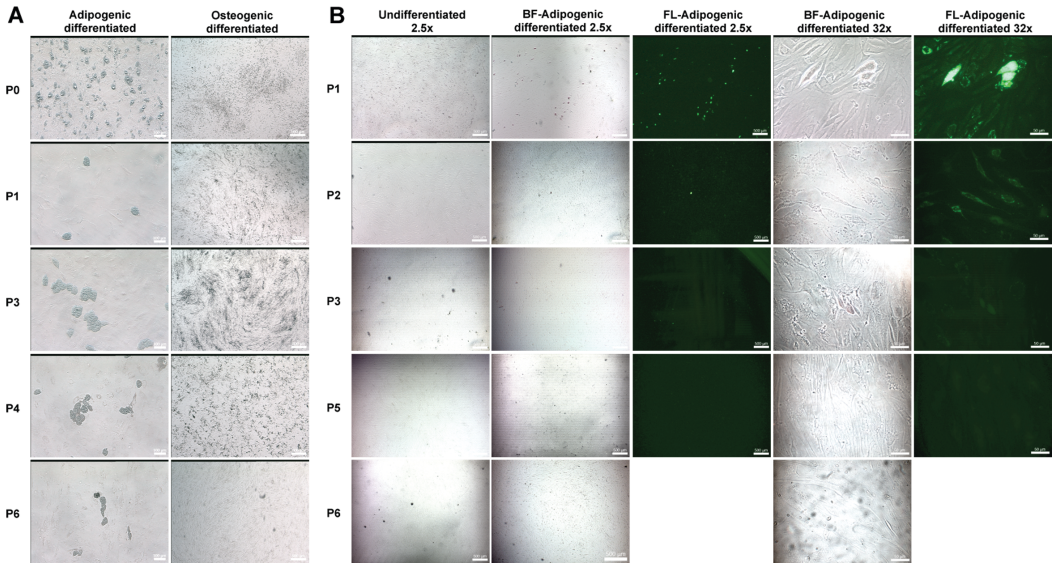

Suppl. Fig. 3.1. Microscopic images of MSC2 and ASC2 cells at each passage. (A) Rows are images of MSC2 cells from the same passage (P0 - 6) shortly before extraction for flow cytometric and qPCR analysis. Columns are images of adipogenic and osteogenic differentiated cells respectively. Scale bars in images of adipogenic cells are equal to 100 µm. In images of osteogenic cells, scale bars are equal 500 µm. (B) Rows are images of ASC2 cells from the same passage (P1 - 6) shortly before extraction for flow cytometric and qPCR analysis. Columns are either brightfield (BF) or 525 nm fluorescence (FL) images of undifferentiated and adipogenic differentiated cells measured at 2.5x and 32x magnification for a population overview or detailed cell morphology respectively. Scale bars in all 2.5x images are equal to 500 µm. In 32x images, scale bars are equal 50 µm.

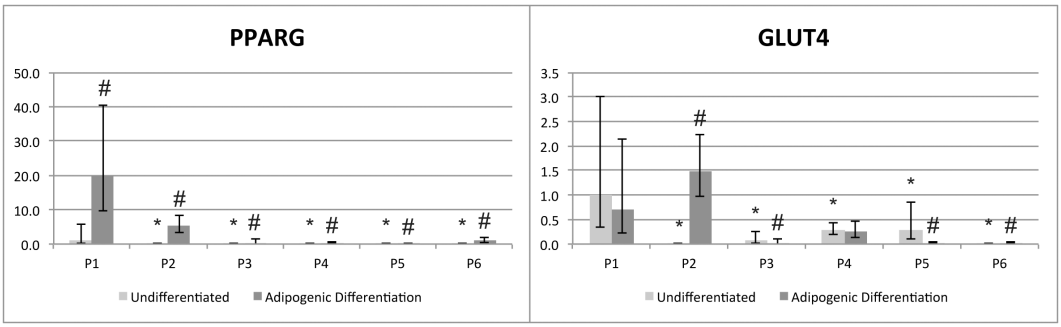

Suppl. Fig. 3.2. Relative gene expression of adipogenic markers on ASC2 cells. Perixosome proliferator-activated receptor γ (PPARG) and glucose transporter 4 (GLUT4). Data is grouped by passage number (P1 - 6) showing data from undifferentiated and adipogenic differentiated cells. Data points are mean relative expression ± standard deviation (n = 6). Marked samples are statistically different, * relative to undifferentiated P1 samples ($P < 0.05$), # relative to undifferentiated samples of same passage number ($P < 0.05$).

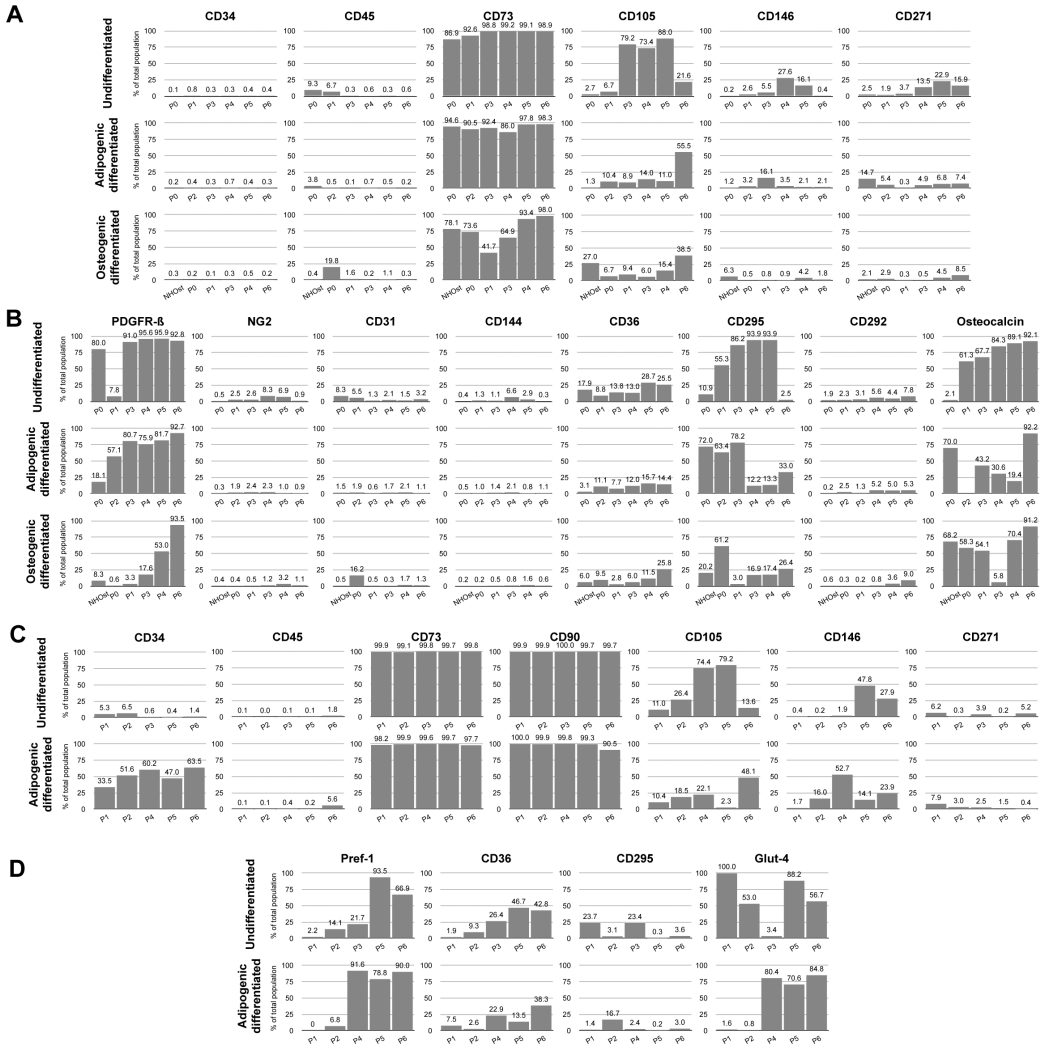

Suppl. Fig. 3.3. Flow cytometric analysis of MSC2 and ASC2 cells. A minimum of 50,000 events was recorded for each sample. Data is given in percentages of total population of undifferentiated (top row), adipogenic differentiated and osteogenic differentiated cells. Data is ordered by passage number (P0 - 6) and grouped in each column by marker type. (A) Analysis of MSC2 cells using MSC markers with CD34 and CD45 as common negative, CD73 and CD105 as common positive and CD146 and CD271 as novel positive MSC markers. (B) Analysis of MSC2 cells using pericyte (PDGFR-β and NG2), endothelial cell (CD31 and CD144), adipocyte (CD36 and CD295) and osteoblast (CD292 and osteocalcin) markers. (C) Analysis of ASC2 cells using MSC markers with CD34 and CD45 as common negative, CD73 , CD90 and CD105 as common positive and CD146 and CD271 as novel positive MSC markers. (D) Analysis of ASC2 cells using adipogenic cell markers.

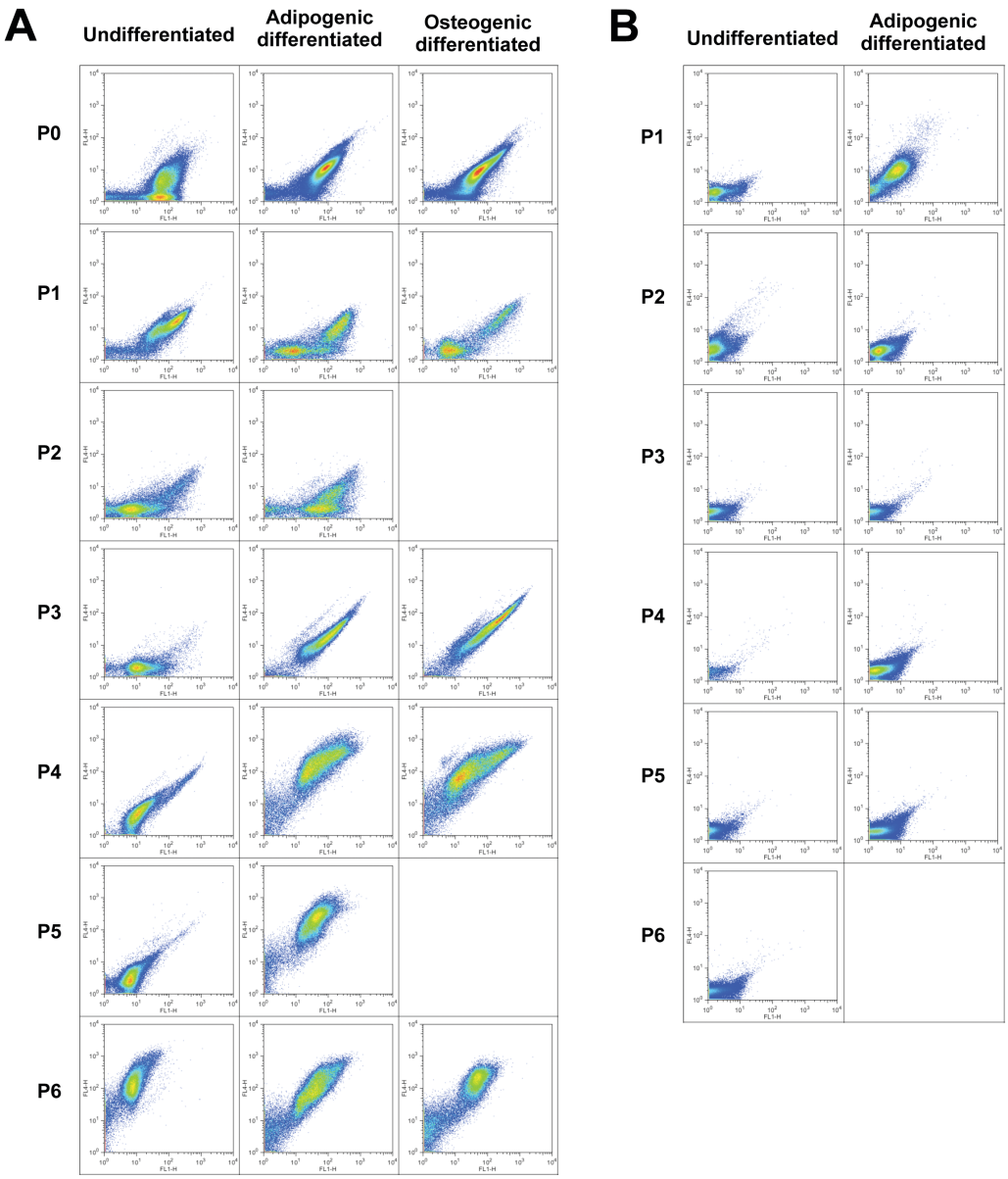

Suppl. Fig. 3.4. Autofluorescence of MSC2 and ASC2 cells. Rows are log-scale dot plots of cells from the same passage (P0 - 6), and columns list undifferentiated, adipogenic differentiated and osteogenic differentiated conditions respectively. X-axis: FL1-H (ex: 488 nm; em: 530/30 nm). Y-axis: FL4-H (ex: 635 nm; em: 661/16 nm). Autofluorescence of (A) MSC2 cells and (B) ASC2 cells.

Supplementary Table 3.1. List of flow cytometry markers included in this study. Descriptions extracted from NCBI RefSeq (Pruitt 2009) and UniProt (Consortium 2011).

CD34 – a cell surface glycoprotein and cell-cell adhesion factor. Has been found to mediate stem cell adhesion to bone marrow ECM or stromal cells. Expression is most common on early hematopoietic cells.
CD45 – or protein tyrosine phosphatase receptor type C (PTPRC). PTPs are known to regulate various cellular processes such as cell growth, differentiation, mitotic cycle, and oncogenic transformation. Expressed on differentiated hematopoietic cells with the exception of erythrocytes and plasma cells.
CD73 – or 5'nucleotidase ecto (NT5E). Expressed on endothelial cells, pericytes, osteoblasts, and MSCs. A membrane bound enzyme catalyst of AMP to adenosine.
CD90 – or thymocyte differentiation antigen 1 (Thy-1). An anchored cell surface protein expressed on MSCs, HSCs, and a subset of $CD34^+$ bone marrow cells.
CD105 – or Endoglin. A membrane antigen that recognizes adhesion receptors of the integrin family. Found on endothelial cells and is believed to be involved in the TGF-beta1 receptor complex.
CD146 – or melanoma cell adhesion molecule (MCA). A marker for endothelial cell lineages and newly recognized as a marker for MSCs.
CD271 – or low-affinity nerve growth factor receptor (LNGFR). A protein involved in the development, survival and differentiation of cells. MSCs are believed to have CD271 on their surface.
CD31 – or platelet/endothelial cell adhesion molecule (PECAM). Serves as an endothelial marker and can be expressed on the surface of platelets.
CD144 – or vascular endothelian cadherin (VE-cadherin). A calcium dependent cell-cell adhesion glycoprotein composed of cadherin repeats. Plays an important role in endothelial cell biology.
PDGFR-ß – platelet-derived growth factor receptor–ß. Implicated in cellular processes such as proliferation, survival and migration and is expressed during blood vessel formation.
NG2 – or chondroitin sulfate proteoglycan 4 (CSPG4). A proteoglycan associated with development of pericytes.
Pref-1 – or delta-like 1 homolog (DLK1). A transmembrane protein that is involved in the differentiation of several cell types, including adipocytes.
CD36 – or platelet glycoprotein 4. An integral membrane protein that binds collagen, lipoproteins, phospholipids and fatty acids. Expressed by platelets, erythrocytes, monocytes and differentiated adipocytes.
CD295 – or leptin receptor protein (LEPR). Serves as a receptor for leptin, a hormone specific to fat cells.

Glut4 – or solute carrier family 2, facilitated glucose transporter member 4 (SLC2A4). An insulin-regulated glucose transporter expressed on skeletal and cardiac muscles as well as brown and white fat.
CD292 – or bone morphogenetic protein receptor, type 1A (BMPR1A). Necessary for extracellular matrix deposition by osteoblasts.
Osteocalcin – or bone gamma-carboxyglutamic acid-containing protein (BGLAP). A protein found in bone and dentin and believed to be solely secreted by osteoblasts. Osteocalcin directs fat cells to release the hormone adiponectin.

Supplementary Table 3.2. Cell populations analyzed and cumulative time in culture before each passage in days. An additional 21 days should be added to determine the *in vitro* culture time of differentiated cells before analysis.

	P0	**P1**	**P2**	**P3**	**P4**	**P5**	**P6**
MSC 1	14	35	56	77	98	119	140
MSC 2	21	33	55	76	97	111	125
ASC 2	14	35	56	77	98	119	140

CHAPTER IV - EXTENDING HSC SURVIVAL *IN VITRO* WITH ADIPOCYTES

Introduction

Many bone marrow related diseases have limited treatment options and generally require a bone marrow transplant for a full cure. To foster progress in the field of treating such diseases, *in vitro* tissue models are needed in order to test novel drugs. However current strategies for culturing bone marrow *ex vivo* are still limited. A major issue is the difficulty in culturing hematopoietic stem cells (hHSC) (Clark 1997). The difficulty lies in the fact that the cues are not known to maintain both self-renewal and differentiation of the stem cells. Using a cocktail of growth factors researchers have been successful in stimulating self-renewal divisions of hHSCs (Murray 1999), which are generally quantified by their expression of the surface protein CD34 (Kondo 2003). This rapid expansion has been the focus of many studies that aim to increase the percent of hHSCs for bone marrow transplants, however is not necessarily beneficial in the long-term maintenance of the stem cells *in vitro*. Though the accelerated expansion of the stem cells does rapidly multiply the amount of $CD34^+$ cells *in vitro*, this proliferation is also accompanied by differentiation (Boitano 2010). In recent years better stem cell survival was achieved in co-cultures of mesenchymal stem cells (hMSC) and hHSCs by culturing the bone marrow cells on a layer of feeder cells of mesenchymal origin (Gersbach 2006). Because hMSCs line the inner cavities of the bone structure *in vivo*, they are suggested to help reconstitute the natural stem cell niche environment by providing the appropriate growth factors. Though recent studies with feeder layers have shown an improvement in initial proliferation, they still do not allow long-term *in vitro* bone marrow culture, as they are not able to sustain cultures beyond 2-3 weeks and therefore do not mimic a niche that maintains the quiescence of the hHSCs (Jang 2006;

Hofmeister 2007). A comparison of current feeder layer culture methods reveals a common property; they are all focused on replicating the highly complex and metabolically active red bone marrow. This may be the reasoning behind the limitation of long-term stem cell culture, since directly after seeding the hHSCs are not only required to repopulate the stem cell niche, but also have to perform hematopoiesis/differentiation. If these steps could occur sequentially instead of concurrently, less stress would likely be imposed on the stem cells, allowing more cells to remain in a quiescent state and reconstitute a hematopoietic stem cell niche *in vitro*.

The culture method suggested here uses a novel approach by culturing the bone marrow cells in an environment of MSC feeder layers containing adipogenic cells, mimicking the yellow bone marrow or marrow fat. Anatomically, yellow bone marrow is closely related to red bone marrow with the former obtaining the color from an abundance of adipocytes. In newborn mammals there is no yellow bone marrow, however the number of adipocytes increases with age in the marrow. Therefore a high abundance of adipocytes in the bone marrow is generally considered as negative, since down-regulation of hematopoiesis results (Naveiras 2009). Of notice though is that even in healthy humans over 30 years of age, most of the femoral cavity is occupied by adipose tissue. Also the process of bone marrow adipogenesis can be reversed by long-term physical training due to the increased blood cell demand (Gurevitch 2007). In addition, marrow fat becomes a filler for the void left by trabecular bone after radiation during the process of a bone marrow transplant that only gradually regains hematopoietic activity (Casamassima 1989).

With this in mind the adipocytes can be beneficial and be used as a “tool” for the suggested approach. Though the inclusion of the adipocytes in the feeder layer may inhibit rapid hHSC expansion it might allow a slower reconstitution of the stem cell niche, by delaying the additional stress of differentiation on the hHSCs. Essentially a

culture of bone marrow cells *ex vivo* can be considered an *in vitro* bone marrow transplant, for which we should design an environment that mimics the host tissue. Additionally, certain studies have suggested that the presence of adipocytes in the niche is necessary for the support of hHSCs (Gimble 1990; Gimble 1996). Ultimately the goal is to verify the hypothesis that *in vitro* cultures of hHSCs in the presence of adipocytes allow for a prolonged hHSC survival.

Materials and Methods

Extracting hMSCs for feeder layers

To test the hypothesis, feeder layers were derived from either undifferentiated or differentiated hMSCs. For each new experiment fresh human bone marrow aspirates were obtained commercially (Lonza, Walkersville, MD) and shipped overnight for next day processing. Aspirate donors were male, under 25 years of age and free of HIV, hepatitis B and hepatitis C. The aspirate was diluted 10-fold with hMSC expansion medium consisting of DMEM supplemented with 10% fetal bovine serum (FBS), antibiotics (100 U/mL penicillin, 100 µg/mL streptomycin, 0.25 µg/mL fungizone), 0.1 mM nonessential amino acids and 1 ng/mL basic fibroblast growth factor (bFGF). This diluted bone marrow was plated on TCP in T-185 flasks for hMSC expansion. After 14 days the non-adherent cells were removed and the adherent cells kept in expansion medium for an additional 7 days to reach confluence. These expanded cells were then passaged using 0.25% trypsin-EDTA and expanded in new T-185 flasks using the same culture medium for an additional week until confluence. These cells were extracted again using 0.25% trypsin-EDTA and seeded at 200,000 cells per well in a 6-well plate and kept in expansion medium for additional 7 days until confluence. In general feeder layers were formed using twice-passaged (P2) hMSCs, except for the unpassaged (P0) cells, where the feeder layers were formed directly in 6-well plates.

Compared to other feeder cultures, it no irradiation was used for the feeder cells for several reasons: A. irradiation should only inhibit mitotic activity of the feeder cells, however little has been documented about the effects of this treatment on adipocytes. Since adipocytes are known to inhibit HSC differentiation and proliferation *in vivo*, we wanted to avoid altering them as much as possible for the *in vitro* experiments. 2. The lack of mitotic activity in irradiated cells has additional side effects, especially in long-term cultures. The inability to proliferate leads eventually to apoptosis of the feeder cells and depletion of cytokines released by the feeder layer cells. Therefore experiments using irradiated feeder layers rarely go beyond 14 days (Jang 2006; Hofmeister 2007). Given that the experiment is designed to analyze long-term effects of the feeder cells we wanted to use proliferative feeder layers that can also release cytokines long-term.

Seeding BMMNC on feeder layers

After preparation and differentiation of the feeder layers bone marrow mononuclear cells (BMMNC) were seeded on top. For each experiment new BMMNCs were obtained from freshly isolated human bone marrow aspirates with the same properties as described for the aspirates used for hMSC extraction. After a 4-fold dilution with Iscove's Modified Dulbecco's Medium (IMDM) the BMMNCs were extracted over a Ficoll density gradient and counted with a hemocytometer before seeding. Each individual well of a 6-well plate received a plating of $1x10^6$ BMMNCs. Due to the lack of adherence of hematopoietic cells, culture medium was replenished bi-weekly by slowly exchanging half of the medium from the top of each well. Also cultures were kept in a 5% oxygen environment, to mimic the lower oxygen tension in native bone marrow, and to maintain a quiescent state (Koller 1992; Yin 2006).

Flow cytometric quantification of $CD34^+$ cells

After culture in low oxygen, all the cells were extracted from 4 wells of each condition. For this the medium of each well was extracted into a 15 mL conical tube. Each well was

then washed with 2 mL PBS and the washes were also collected. Five hundred µL 0.25% trypsin-EDTA was added to each well and kept in the incubator for 10 min until all adherent cells were detached. To ensure a single cell solution the cells were then mixed with a micropipette and extracted into the same conical tube to inhibit the trypsin. A final wash of each well with 2 mL PBS ensured complete extraction. The cells were then pelleted by centrifugation at 450 g and 4°C for 10 min. The pellet was resuspended in 100 µL FACS buffer that consisted of PBS supplemented with 0.5% bovine serum albumin (BSA) and 5 mM EDTA. To each cell suspension 10 µg human Immunoglobulin G (IgG) (Sigma, Saint Louis, MO) was added to block binding of nonspecific receptors. Subsequently 10 µL of CD34-FITC antibody (BD Biosciences, San Diego, CA) was added to label the hHSCs from the three wells per condition The cells from the remaining well were left unlabeled as a negative control. After incubation in the refrigerator for 30 min the cells were washed twice with 1 mL FACS buffer and finally resuspended in 250 µL FACS buffer for flow cytometric analysis on a standard two-laser FACSCalibur (BD Biosciences, San Jose, CA).

Data analysis was performed using 2D dot plot gating with FlowJo analytical software (Tree Star, Inc., Ashland, OR). This allowed quantification of labeled cells to compare to histological analysis. Since the total cells per well varied depending on the manipulation of the feeder cells, the percentage of $CD34^+$ cells in each well was not an ideal comparison between the different conditions. Therefore the data was plotted as percent of seeded $CD34^+$ cells remaining in each well at each time point, with 100% being the initial amount of $CD34^+$ cells in the fresh bone marrow.

Effects of feeder cells alone

Initially, cultures were set up in four different feeder cultures. Besides a control of no feeder cells, BMMNCs were also seeded on undifferentiated hMSCs as well as hMSCs differentiated towards adipocytes or osteoblasts, all cell types present in the bone

marrow. After expansion of the hMSCs in the 6-well plates the hMSC feeder layers were kept undifferentiated using a maintenance medium. This medium consisted of DMEM:F12 supplemented with 3% FBS, and antibiotics (100 U/mL penicillin, 100 µg/mL streptomycin, 0.25 µg/mL fungizone). For adipogenic differentiation the maintenance medium was additionally supplemented with 33 µM biotin, 17 µM D-pantothenic acid hemicalcium salt, 1 µM human insulin, 1 µM dexamethasone, 50 mM 3-isobutyl-1-methylxanthine (IBMX) and 5 µM 2,4-thiazolidinedione (TZD). For osteogenic differentiation the maintenance medium was instead supplemented with 10 mM glycerol-2-phosphate disodium salt hydrate, 400 µM L-ascorbic acid 2-phosphate sesquimagnesium salt hydrate, 10 nM 1α,25-dihydroxyvitamin D3, 10 nM dexamethasone and 10% FBS instead of 3% FBS.

The feeder layers were kept in 3 mL maintenance or differentiation medium respectively and medium was fully replenished biweekly. After 3 weeks $1x10^6$ BMMNCs from a new human bone marrow aspirate were plated in each well. In this experiment the co-cultures were kept in a minimal culture medium consisting of IMDM supplemented with only 2% FBS and antibiotics (100 U/mL penicillin, 100 µg/mL streptomycin, 0.25 µg/mL fungizone). The reasoning behind this minimal medium was to avoid masking the effects of the cytokines released by the feeder cells with a cocktail of growth factors generally added to hHSC expansion media. After culture under hypoxic conditions (5% O2, 5% CO2, 95% relative humidity) the cells were extracted at 7, 13, 21 and 36 days for flow cytometric quantification of $CD34^+$ cells.

Combination of adipocytes and growth factors

In a second experiment using new bone marrow aspirates, the hMSC feeder layers were again compared to the adipogenic feeder layers, however this time cultures also included using a common hHSC expansion medium. The omission of the no-feeder and osteogenic feeder layer and focus on MSC feeder layers cultures was based on two

reasons: A. The amount of BMMNCs available in each bone marrow aspirate limited the amount of wells available to test different culture conditions. B. MSC feeder layers are the current standard in *in vitro* hHSC culture, and therefore the hypothesis should be compared against them. As described in the previous experiment, the hMSC feeder layers were kept in maintenance medium and the adipogenic feeder layers in adipogenic differentiation medium for 3 weeks, respectively. Then again $1x10^6$ BMMNCs of a new human bone marrow aspirate were seeded on the feeder layers and each condition was additionally cultured in either a minimal or a hHSC expansion medium. In this experiment the minimal medium consisted of IMDM supplemented with 15% FBS and antibiotics. The HSC expansion medium was additionally supplemented with 55 µM ß-mercaptoethanol, 10 ng/mL Flt-3, 10 ng/mL IL-6, 10 ng/mL SCF 10 ng/mL and 2 ng/mL IL-3. After culture under hypoxic culture conditions (5% O2, 5% CO2, 95% relative humidity) the cells were extracted at 1, 3, 5, 7, 10, 14, 17, 21, 24, 28 and 42 days for flow cytometric quantification of the $CD34^+$ cells.

Comparison of unpassaged vs. passaged feeder cells

Since the amount of adipocytes visibly detectable in feeder layers derived from P2 hMSCs is low, we made an attempt to increase the amount of adipocytes in a feeder layer by using unpassaged (P0) hMSCs from a new bone marrow aspirate. Since P0 hMSCs are subjected a lot shorter time to *in vitro* culture conditions than passaged cells, and are therefore more “stem-like”. Differentiation of P0 hMSCs has therefore led to a higher percentage of adipocytes than P2 hMSCs. These adipocytes also exhibit larger lipid vacuoles than adipocytes derived from P2 hMSCs, after the same amount of time in differentiation medium.

To form P0 feeder layers 100 µL of a fresh undiluted human bone marrow aspirate was plated per well in 6-well plates. The same hMSC expansion medium was used to expand the hMSCs as in previous experiments for hMSC extraction. After 2 weeks the

non-adherent cells were removed and the feeder layers were kept an additional week in expansion medium to reach confluence. In parallel P2 hMSCs from a different bone marrow aspirate were expanded to new feeder layers using the same method as described in the aforementioned experiments. In this experiment three different conditions were set up: hMSC and adipogenic feeder layers were obtained from the P0 hMSCs, by keeping the feeder layers for 3 weeks in the respective hMSC maintenance or adipogenic differentiation medium, as previously described. To consider the effects of the lower passage number, an additional adipogenic feeder layer was generated by differentiation of the P2 hMSCs feeder layers. After differentiation, again $1x10^6$ BMMNCs of a new human bone marrow aspirate were seeded on the feeder layers and each condition was kept in the hHSC expansion medium with the cocktail of growth factors described in the previous experiment. After culture under hypoxic culture conditions (5% O2, 5% CO2, 95% relative humidity) the cells were extracted at 7, 14, 21, 28, 35 and 42 days for flow cytometric quantification of the $CD34^+$ cells.

In addition the feeder layers themselves were analyzed for $CD34^+$ cells before the seeding of BMMNCs to determine the amount of hHSCs remaining in the feeder layers. This was thought to be especially important in this experiment as the P0 feeder layers were extracted from fresh bone marrow and without passaging, could have trapped HSCs in the feeder layer.

Statistical analysis

All data are expressed as means ± SD and a minimum of three replicates were performed for each assay. Using GraphPad Prism (GraphPad Software, San Diego, CA) a two-way analysis of variance (ANOVA) was used for statistical analysis of multiple comparisons. Statistical difference between experimental groups was considered to be significant when the p value was < 0.05.

Results

Effects of feeder cells alone

In comparison of the BMMNCs cultured in minimal medium, the percent of $CD34^+$ cells remaining in culture dropped rapidly to less than a fifth after 7 days, regardless of the type of feeder layer (Fig. 4.1A). This decrease continued gradually, though less rapidly over time. Magnification of the lower 20% of the graph allows a better comparison of the feeder layers (Fig. 4.1B). Here it is evident that the hMSC feeder layer had no significant difference over TCP alone. The osteogenic feeder layer showed a slight improvement over both TCP and hMSC feeder layers, that was only statistically significant at day 7. Adipogenic feeder layers had a $CD34^+$ cell survival of 19% after 7 days down to 4% after 35 days. This improvement was significant over MSC and no feeder layers throughout the experiment, with an average of an almost two-fold higher $CD34^+$ cell survival. Due to fungal contamination, measurement of the osteogenic feeder layers as well as the MSC feeder layers was halted after 2 and 3 weeks respectively.

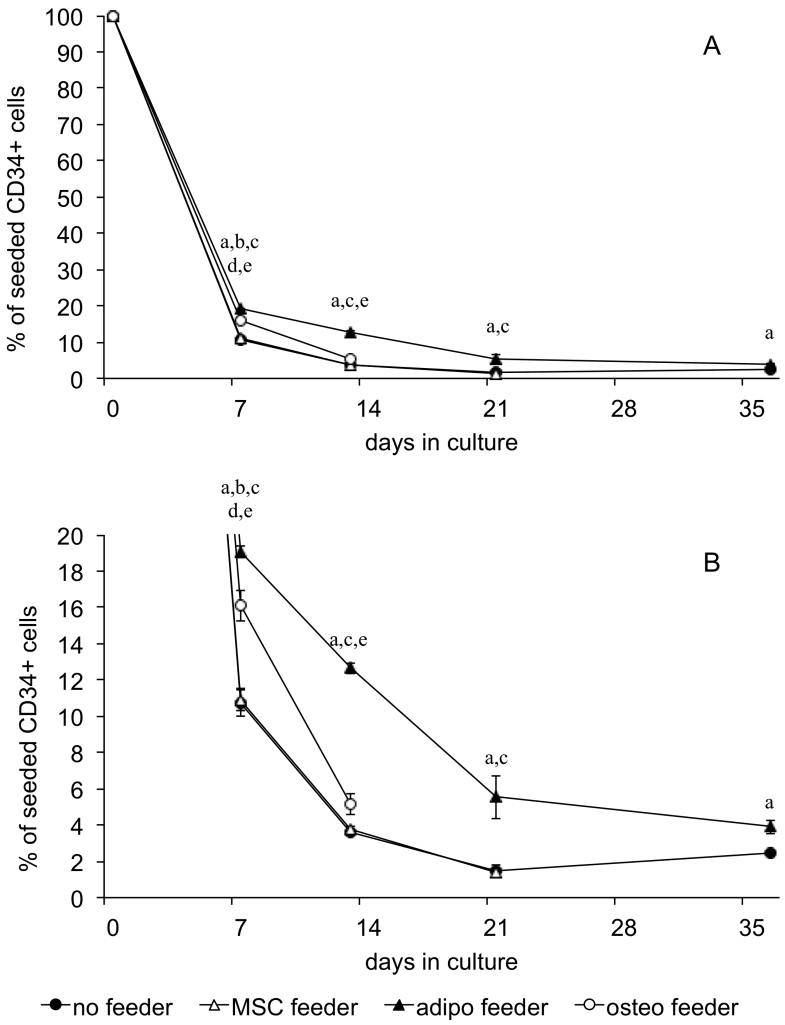

Fig. 4.1. Flow cytometric quantification of $CD34^+$ cells remaining in the feeder cultures in minimal medium. hMSC, adipogenic and ostegenic feeder layers are compared with TCP alone. (A) Entire view and (B) magnified view of the same graph. Data are given as means ± SD (n ≥ 3) and a statistically significant difference is denoted by a letter above the respective time point (a = no feeder vs. adipo feeder, b = no feeder vs. osteo feeder, c = MSC vs. adipo feeder, d = MSC vs. osteo feeder, e = adipo vs. osteo feeder).

Combination of adipocytes and growth factors

Flow cytometric data of cultures in minimal medium compared to cultures in medium supplemented with growth factors for hHSC expansion again showed a gradual decrease in $CD34^+$ cell survival in minimal medium (Fig. 4.2). Addition of the growth

factors induced a highly significant ($p < 0.0001$) rapid increase in the $CD34^+$ cell proliferation, reaching a maximum at two weeks. In these cultures hMSC feeder layers exhibited slightly higher, albeit insignificant, proliferation over adipogenic feeder layers up to two weeks. After three weeks however the remaining $CD34^+$ cell population was significantly higher in the presence of adipocytes than with undifferentiated hMSCs. Ultimately the edges of the feeder layers started peeling off the wells after 3 weeks and started rolling up towards the center of the well while contracting (Fig. 4.3). The $CD34^+$ population diminished almost completely after 42 days.

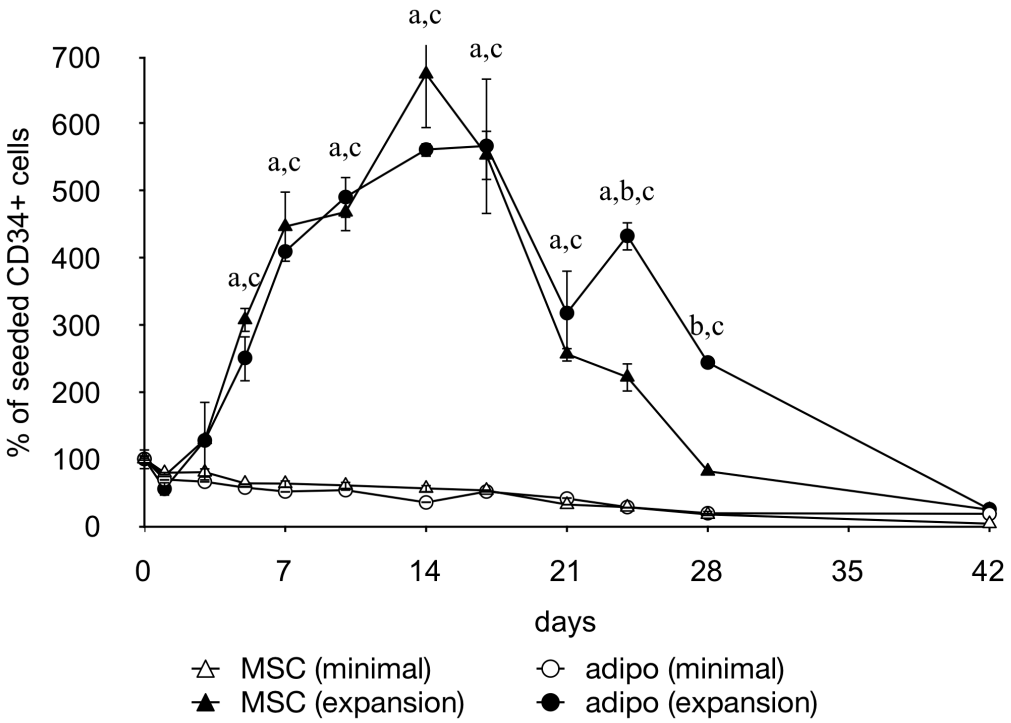

Fig. 4.2. Flow cytometric quantification of $CD34^+$ cells in both hMSC as well as adipogenic feeder cultures. Feeder cultures were additionally maintained in either minimal medium (minimal) or a medium supplemented with a cocktail of growth factors (expansion). Data are given as means ± SD ($n \geq 3$) and a statistically significant difference is denoted by a letter above the respective time point (a = MSC (minimal) vs. MSC (expansion), b = MSC (expansion) vs. adipo (expansion), c = adipo (minimal) vs. adipo (expansion).

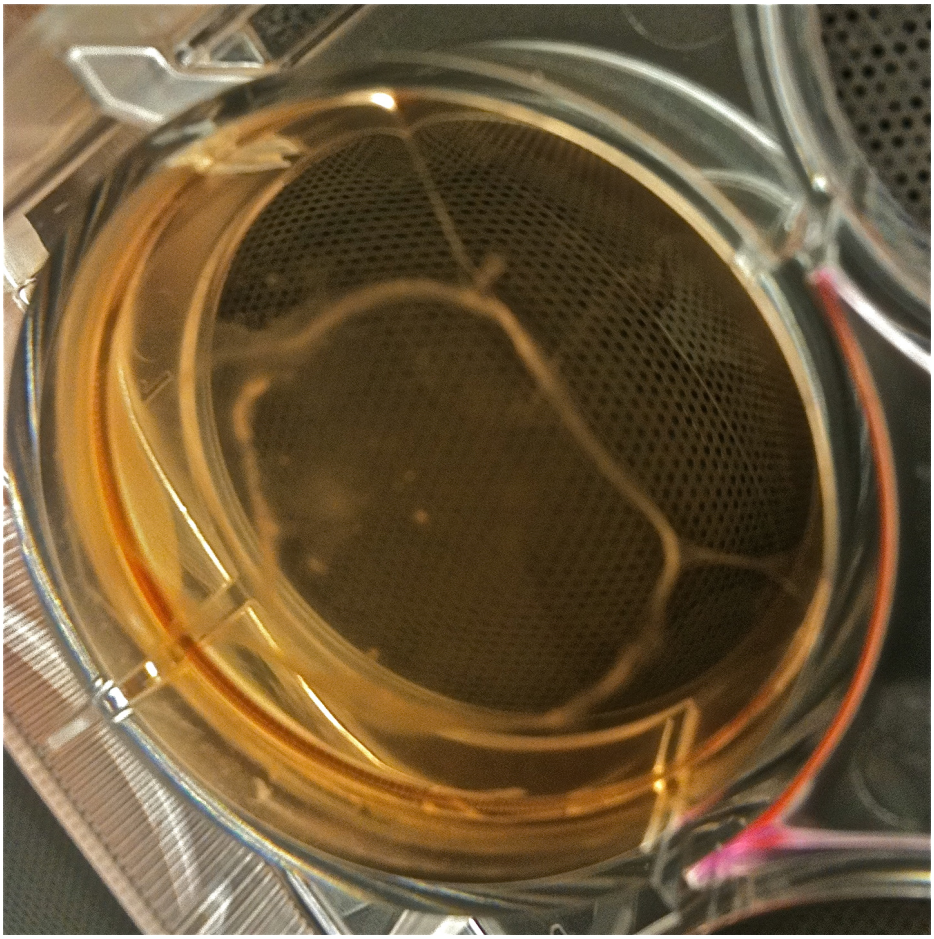

Fig. 4.3. Photograph of a well with feeder cells contracting. The picture was take 6 weeks post seeding of the BMMNCs.

Comparison of unpassaged vs. passaged feeder cells

The P0 hMSCs were utilized to obtain feeder layers with a higher adipogenic differentiation. Figure 4 shows the hMSCs after 3 weeks of adipogenic differentiation. Simple comparison of the microscope images illustrates that the P0 cells have a higher abundance of adipocytes (darker cells in Fig. 4.4B) and that these cells also exhibit larger lipid vacuoles (round intracellular droplets in Fig. 4.4D).

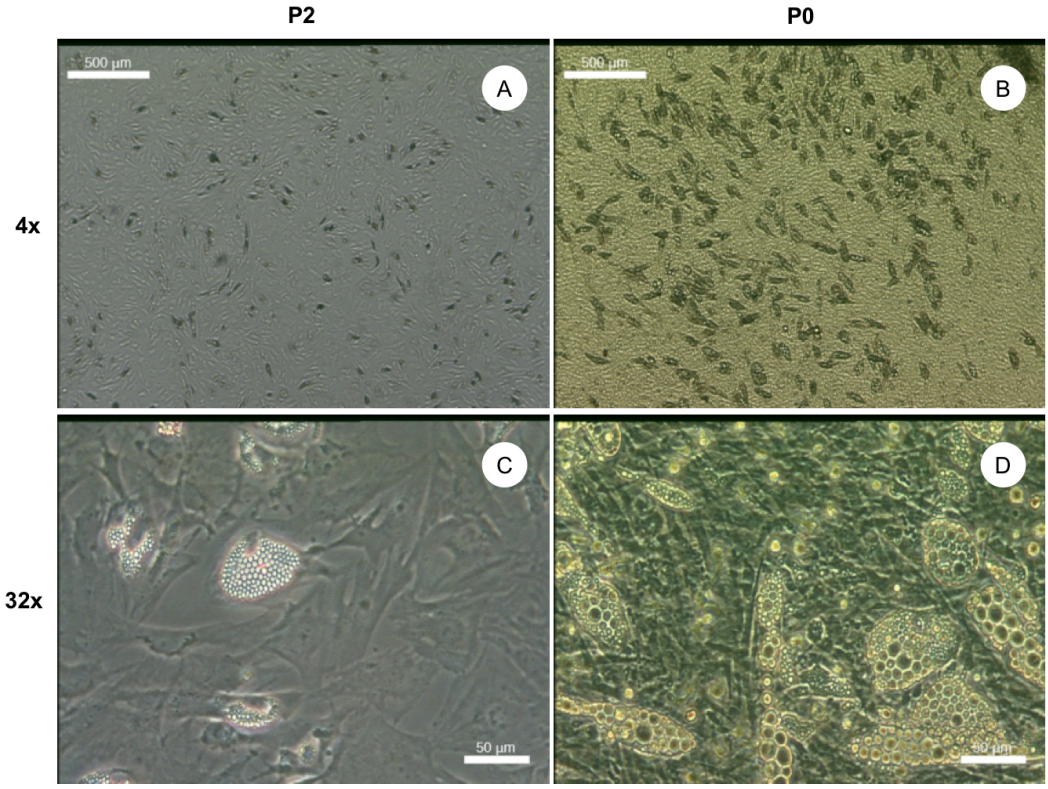

Fig. 4.4. Microscope images of hMSCs after 3 weeks of adipogenic differentiation. P2 feeder layers at lower (A) and higher (C) magnification. P0 feeder layers at lower (B) and higher (D) magnification. Scale bars are 500µm (A, B) and 50µm (C, D) respectively.

$CD34^+$ cell quantification of the feeder layers alone showed a very low percentage of $CD34^+$ cells compared to the initial percentage in fresh bone marrow of 2.19% ± 0.4% (Fig. 4.5). Additionally, the difference in $CD34^+$ was very small between P0 and P2 cells as well as undifferentiated and differentiated feeder layers. Therefore the amount of $CD34^+$ cells contributing from the feeder layers alone was minimal and could be neglected in the time-lapsed quantification (Fig. 4.6).

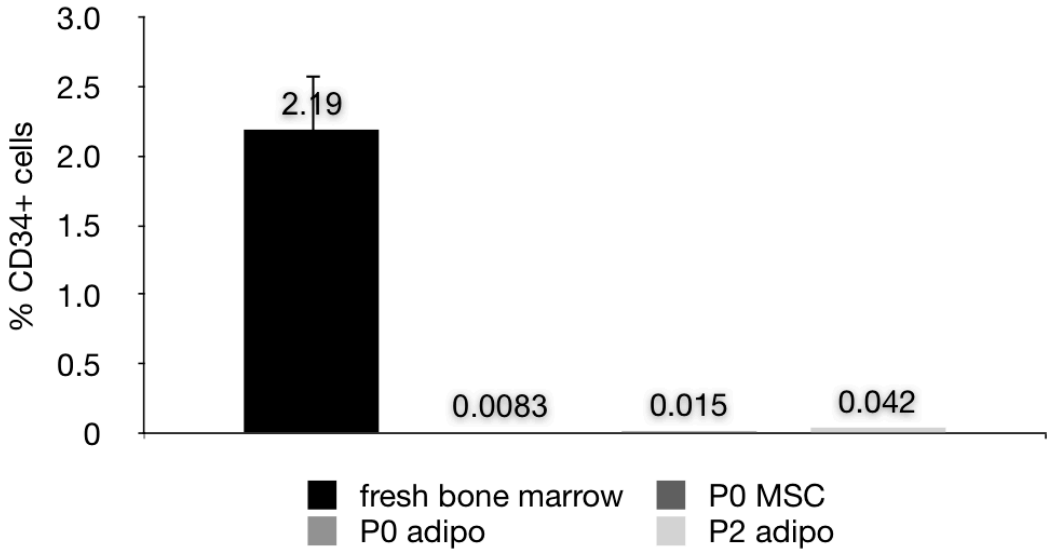

Fig. 4.5. Percentage of CD34$^+$ cells in P0 and P2 derived feeder layers alone, compared to fresh bone marrow. All are values obtained by flow cytometric analysis of > 200'000 events from a single sample, except for the fresh bone marrow (n = 3, data displayed as mean ± SD).

The time-lapsed flow cytometric quantification of the CD34$^+$ cells showed again a rapid initial proliferation in the cultures using P2 hMSC (Fig. 4.6). This rapid increase peaked at an almost 3-fold expansion around 1-2 weeks and subsequently declined. Comparing these data with the cultures on P0 feeder cells, shows however a significantly lower initial expansion in both undifferentiated as well as adipogenic differentiated feeder layers. Of notice is that the mean value of the P2 adipogenic feeder layers remained higher up to 28 days.

Though statistical significance diminished, a few additional tendencies can be noted based on the mean values: The initial proliferation of the CD34$^+$ cells was slightly higher on P0 hMSC than on P0 adipogenic feeder layers, but after three weeks to the end of the experiment the mean CD34$^+$ cell population was again higher in the presence of adipocytes than with undifferentiated hMSCs. As in the previous experiment the feeder layers started peeling off the wells at already 3 weeks.

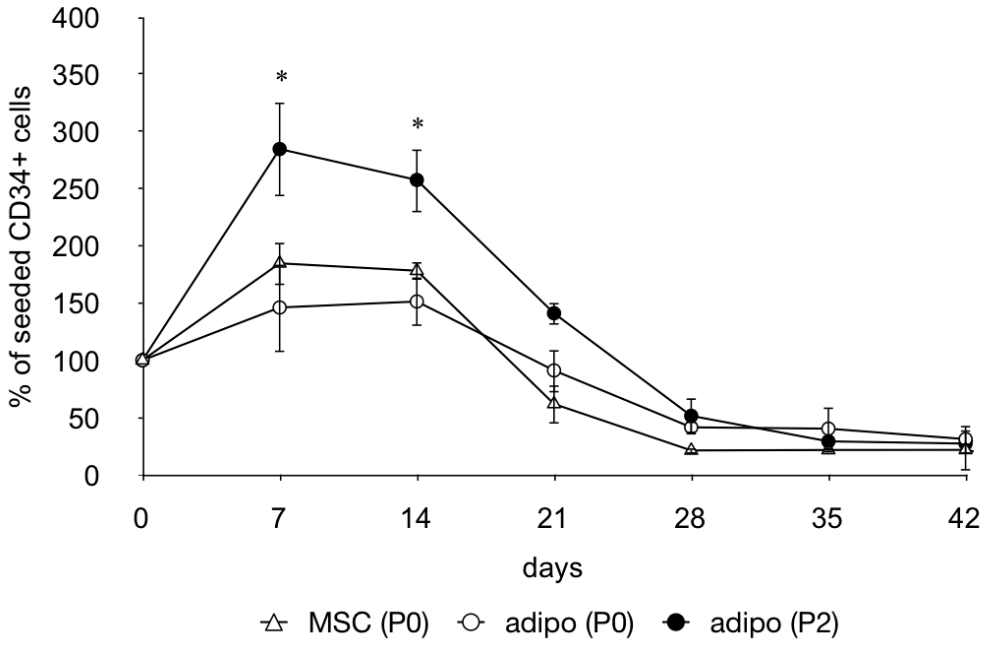

Fig. 4.6. Flow cytometric quantification of $CD34^+$ cells cultured on P0 MSC feeder layers as well as adipogenic feeder layers derived from both P0 and P2 hMSCs. Data are given as means ± SD ($n \geq 3$). A statistically significant difference with respect to adipo (P2) is denoted by an asterisk above the respective time point.

Discussion

The goal of this study was to assess the ability of adipocytes to inhibit hHSC differentiation and therefore prolong hHSC survival in long-term *in vitro* cultures. This is in stark contrast to the many experiments that are focused on rapid short-term expansion of hHSCs *in vitro*. Therefore the rate of expansion is of less interest, versus the duration of stem cell survival *in vitro*. The hypothesis was that *in vitro* cultures of hHSCs in the presence of adipocytes allow for prolonged hHSC survival.

The experiment comparing no feeder, undifferentiated hMSC, osteogenic and adipogenic feeder layers in a minimal medium confirmed this hypothesis. The adipogenic feeder layers showed a significantly higher $CD34^+$ cell survival at all time

points. The choice to not add any additional cytokines to the culture medium in this experiment, did allow demonstration of the unmasked effects of the growth factors released by the feeder cells alone. However the lack of sufficient serum in the medium was detrimental to proliferative capacity of the feeder cells. This is especially visible in that the hMSC feeder layers performed as poorly as the cultures without any feeder cells, which is in contrast to experiments showing improved hHSC proliferation with hMSC feeder layers (Jang 2006; Hofmeister 2007). The lack of sufficient growth factors stimulating proliferation is likely the reason behind the rapid decline in hHSC survival.

In the subsequent experiment, the cultures using a minimal medium showed a similar trend, however with a much less rapid decline. Besides the difference between the use of aspirates of new donors for both the feeder layers as well as the BMMNCs, the biggest difference is the addition of 15% instead of 2% FBS in the culture medium. This lead to the conclusion that a higher FBS content is necessary for long-term hHSC survival, supposedly due to the enhanced proliferative capacity of the feeder cells. More FBS however only reduced the rate of decay. For an increase of $CD34^+$ cells, expansion medium supplemented with a cocktail of growth factors was required. This result was expected, as the composition of the expansion medium closely resembled commercially available hHSC expansion media.

Coinciding with current cultures using these commercial media, maximum expansion was achieved at 2 weeks. However in the context of the goal of this project, to achieve long-term hHSC survival *in vitro*, the initial rapid expansion is of less importance, but instead the percentage of $CD34^+$ cells surviving at later time points is of greater interest. With this in mind the lack of statistical difference in initial proliferation on both the hMSC and adipogenic feeder layers indicates that the presence of adipocytes does not inhibit hHSC expansion, but instead does reduce the rate of $CD34^+$ cell decay, which is visible after 3 weeks. This decay in $CD34^+$ expression can result from either apoptosis or

differentiation. Though the effects of adipocytes on hHSCs *in vivo* suggest that adipocytes inhibit hematopoiesis, further studies will be necessary to elucidate the true mechanism of the adipocytes on the hHSCs.

On the other hand in the comparison of P0 versus P2 feeder layers, initial expansion was significantly lower in P0 feeder cells. Not considering the difference between feeder layer cells derived from different donors, it can be concluded that the use of unpassaged hMSCs creates a more "natural" stem cell niche. In theory the hHSCs should anchor to the niche cells and given the appropriate signals, should remain in a more quiescent state (Li 2005; Wilson 2006). The assumption that the P0 feeder cells do recreate the niche better than the P2 cells leads to the conclusion that the initial expansion of $CD34^+$ cells, stimulated by the cytokines in the culture medium, is inhibited by the presence of a quiescent stem cell niche. Because of the significant difference in initial expansion, as well as the difference in source of feeder cells, further comparison of long-term hHSC survival between P0 and P2 feeder layers is not feasible.

Comparing the undifferentiated hMSC and the adipogenic feeder layers derived from P0 cells, shows no statistically significant difference between the two. Interesting though is the fact that the mean values of the adipogenic feeder layers showed a lower initial expansion up to 2 weeks and a less rapid decay of $CD34^+$ cells after 3 weeks. This coincides with *in vivo* findings in stem cell transplants, where successful repopulation of the bone marrow is inversely related to the rate of adiposity present in the ablated bone marrow (Casamassima 1989). In this case this would be especially true due to the presence of not only more, but also larger adipocytes in the P0 feeder layers. With respect to the goal of the project, the less rapid decay of $CD34^+$ cells in adipogenic versus undifferentiated feeder layers, correlates to the hypothesis of prolonging hHSC survivial.

Therefore, in general, the $CD34^+$ cell survival was prolonged using feeder layers that included adipocytes. The fact that this observation was present in all experiments, and considering the fact that the cells for each experiment were derived from different donors (each experiment had one donor for the feeder layers, except for the last experiment where two separate donors were used for the P0 and P2 feeder layers, and in each experiment a different donor was used for the seeded BMMNCs, leading to a total of 7 different bone marrow donors), leads to the conclusion that this observation is not an artifact of a single donor. Variances in proliferation are though clearly visible between the different donors. This can be demonstrated in comparison of the $CD34^+$ levels at 2 weeks in Fig. 2 and Fig. 5. Both experiments included a condition where the hHSCs were expanded on a P2 adipogenic feeder layers using a culture medium with the same growth factors, however the cells were derived from different donors. In the experiments depicted in Fig. 2 we achieved approx. 6-fold expansion after 14 days, whereas in Fig. 5 we have only a 3-fold expansion after 14-days. Further experiments comparing properties of donors will be necessary to determine the optimal proliferation.

Ultimately, though the prolonged *in vitro* survival gradually diminished in all cultures post 5 weeks. As noted in the results the feeder layers cells started to detach after 3 weeks and contract, which likely led to this decay in survival. This decay is inevitable in 2D cultures, as mentioned in the introduction mitotic inhibition of the feeder cells by irradiation would not have allowed long-term cytokine release by the feeder cells. Another role in the ultimate decay of hHSCs is the fact that these are all 2D cultures and on TCP. This does not truly mimic the complex niche structure found in whole bone marrow. Future plans should therefore include the use of a 3D scaffold biomaterial that would not only better replicate the bone marrow niche, but also avoid the peeling effects of the feeder layers.

Contact requirement of feeder cells

In an attempt to understand the mechanism between the feeder cells and the seeded HSCs, we performed an array of transwell studies. These would allow us to determine if the cytokines secreted by the feeder cells were sufficient for the observed results or if direct contact was necessary.

Materials and Methods

hMSCs were extracted and expanded as previously described. P2 MSCs were grown to confluence in T-185 flasks. Using the same culture media as listed before, half of the flasks were kept undifferentiated, and the other half were differentiated towards adipocytes for 3 weeks. After this time period, all cells were detached using trypsin and re-plated into 6-well plates using the same hMSC expansion medium supplemented with bFGF, to obtain rapid confluence. After 3 days, BMMNC were isolated and seeded at $1x10^6$ cells per well and kept as previously denoted in an hHSC expansion medium. For direct co-cultures BMMNC were seeded directly on top of the feeder layers. For indirect co-cultures BMMNC were seeded into a transwell-insert with a filter membrane out of polyethylene terephthalate (PET), with a pore size of 0.4 μm (Millipore, Billerica, MA, USA). Inserts were placed into 6-well plates and filled with medium. Cells were extracted at weekly time points using trypsin and labeled using CD34-FITC for flow cytometric analysis.

Statistical analysis

All flow cytometric data are expressed as means ± SD and a minimum of six replicates were performed for each assay. Using GraphPad Prism (GraphPad Software, San Diego, CA) a student-t-test was used to compare between two groups and a two-way analysis of variance (ANOVA) was used for statistical analysis of multiple groups. Statistical difference between experimental groups was considered to be significant when the p value was < 0.05.

Results

The cells showed again a rapid expansion of $CD34^+$ cells that peaked at 2 weeks, and then declined again thereafter (Fig. 4.7). Comparing the undifferentiated and adipogenic differentiated feeder layers: the adipogenic feeder cells had a significantly higher amount of $CD34^+$ cells at later time points. The initial peak observed in the direct co-cultures was not observed in the indirect co-cultures using transwells. Instead an increase was observed at 3 weeks. Data acquisition stopped at 4 weeks due to a malfunction of the flow cytometer.

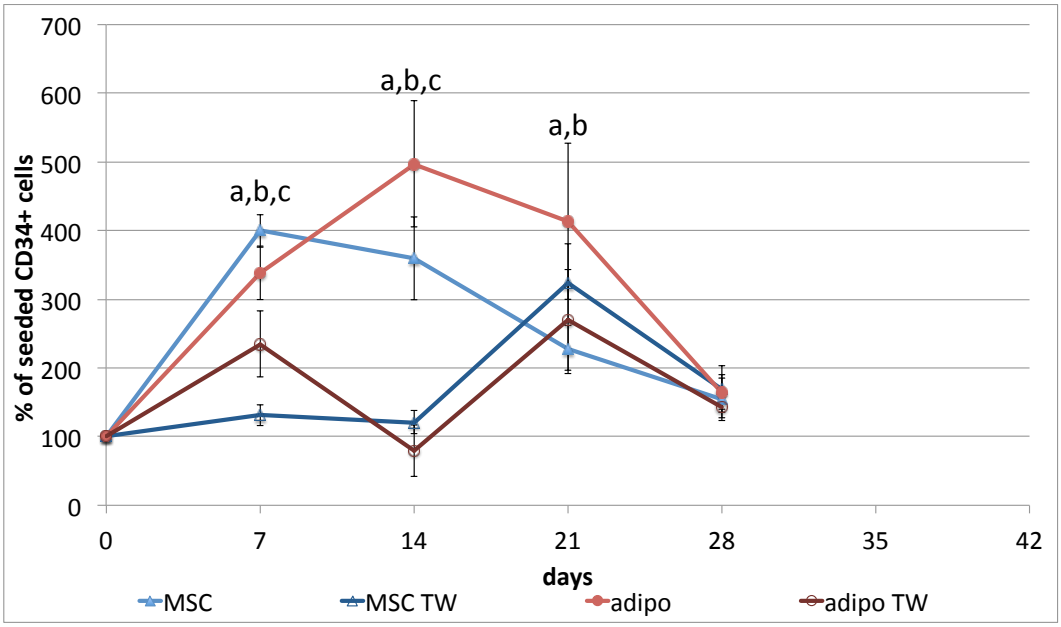

Fig. 4.7. Flow cytometric quantification of $CD34^+$ cells in both hMSC as well as adipogenic feeder cultures. Feeder cultures were additionally maintained in either direct co-culture with HSCs or indirectly using transwells (TW). Data are given as means ± SD ($n \geq 3$) and a statistically significant difference is denoted by a letter above the respective time point (a = MSC vs. adipo, b = MSC vs. MSC TW, c = adipo vs. adipo TW).

Discussion

Though the results of this study showed again an improved maintenance of $CD34^+$ cells in a feeder layer containing adipocytes, long-term effects could not be confirmed due to

the malfunctioning of the analytical machine. Interesting is the observation that the in-direct co-cultures did not show the initial expansive peak that had been previously observed. If one assumes that this effect is not the result of the PET of the culture membrane that the BMMNCs are cultured on, then one can safely state that direct co-culture is necessary for the observed effects. This would coincide with observations made by Koller et al. who performed in-direct co-cultures by adding conditioned medium from stromal cells to the bone marrow cells (Koller 1997). They confirmed the presence of soluble signals, however the conditioned medium did not completely substitute for direct contact. The late increase in the indirect co-cultures at 3 weeks coincides with the observation that in all cultures the feeder layers started detaching from the well around that time point. However due to its close proximity, the feeder cells started attaching to the bottom side of the transwell. This was very obvious when the transwell inserts were removed for flow cytometric analysis.

Varying the amount of adipocytes

To test the hypothesis that the inclusion of adipocytes in the feeder layer can aid in maintaining the HSC population *in vitro* by suppressing differentiation, we wanted to see if varying the amount of adipocytes in the feeder layer would also show a variance in the survival rate. As previously mentioned, we tried to increase the amount of adipocytes in the feeder layer using undifferentiated feeder cells. Though an increase in the amount of adipocytes was seen in the unpassaged feeder layers, this also introduced another variable between the unpassaged and passaged feeder cells as these were forcibly derived from two different donors. Therefore, because increasing the amount of adipocytes was not possible, we attempted to see if we could accurately decrease the amount of adipocytes. For this we first prepared feeder cells as either undifferentiated MSCs or differentiated them towards adipocytes and then passaged them into new cultures. The new cultures contained either just undifferentiated MSCs or just MSCs

differentiated towards adipocytes. As a third variable, we also seeded new cultures with a 1:1 mixtures of both cell types, with the expectation that these cultures would have half the amount of adipocytes as compared to purely adipogenic cultures.

Materials and Methods

hMSCs were extracted and expanded as previously described. Cells were seeded at P2 in 6-well plates and grown to confluence. Using the same culture media as listed before, half of the plates were kept undifferentiated, and the other half were differentiated towards adipocytes for 3 weeks. After this time period, all cells were detached using trypsin and the feeder cells of each cell type were each pooled in a single vial. 1/3 of each vial was mixed together in a separate container and labeled MSC/adipo. Then the cells of each vial were seeded into new 6-well plates using the same hMSC expansion medium supplemented with bFGF, to obtain rapid confluence. After 3 days, BMMNC were isolated and seeded at $1x10^6$ cells per well and kept as previously denoted in an hHSC expansion medium. Cells were extracted at weekly time points using trypsin and labeled using CD34-FITC for flow cytometric analysis.

Statistical analysis

All flow cytometric data are expressed as means ± SD and a minimum of six replicates were performed for each assay. Using GraphPad Prism (GraphPad Software, San Diego, CA) a student-t-test was used to compare between two groups and a two-way analysis of variance (ANOVA) was used for statistical analysis of multiple groups. Statistical difference between experimental groups was considered to be significant when the p value was < 0.05.

Results

The cells showed again a rapid expansion of $CD34^+$ cells that peaked at 2-3 weeks, and then declined again thereafter (Fig. 4.8). Comparing the undifferentiated and adipogenic differentiated feeder layers: the adipogenic feeder cells had a significantly higher amount

of CD34⁺ cells that was at least 50% higher at all time points after 3 weeks. The mean values of the half-half mixture of undifferentiated and adipogenic differentiated cells did lie between the values of the non-mixed feeder cultures, however the large standard deviations of all cultures yielded a lack of statistical significance. This was confirmed by performing a two-way ANOVA test.

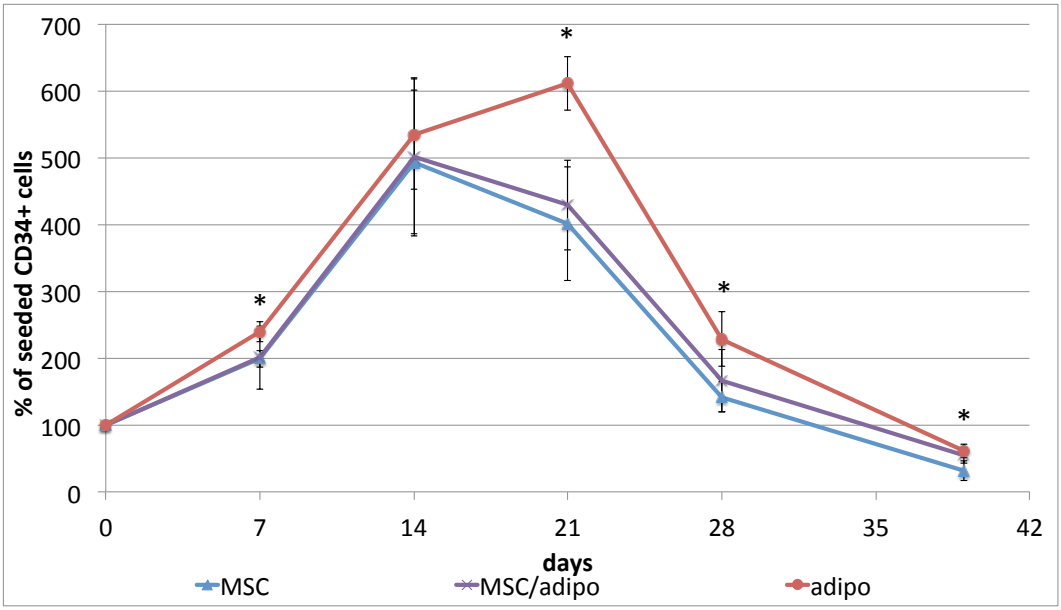

Fig. 4.8. Flow cytometric quantification of CD34⁺ cells in feeder cultures with varying amounts of adipocytes. Feeder cells were first kept either undifferentiated or differentiated towards adipocytes and then detached with trypsin. Feeder cells were then re-plated using just undifferentiated cells (MSC), adipogenic differentiated cells (adipo) or a 1:1 mixture of each cell type (MSC/adipo). Data are given as means ± SD ($n \geq 6$) and a statistically significant difference between MSC and adipo feeder layer is denoted by an asterisk above the respective time point.

Discussion

The results from this study showed again the improved maintenance of CD34⁺ cells when using a feeder layer containing adipocytes. Although the mean values of the mixed cultures did follow the trend by lying between the values of the MSC and adipo cultures, the large variances do not allow one to draw a confident conclusion that the amount of

adipocytes correlate to the *in vitro* survival rate of the HSCs. The large variance has likely to do with a few observations: A. Given that we started differentiation on P2 hMSCs, we did not have a very high percentage of adipocytes within the feeder layers to start off with (see Chapter III). Therefore by cutting the amount of adipocytes in half, the percentage was even lower (approx. 5% adipocytes in mixed cultures). B. To obtain a mixed population required an additional passaging step, using trypsin and centrifugation. This additional step lowered the total amount of cells available for re-seeding that was likely biased against adipocytes, as these are more fragile than undifferentiated hMSCs. C. Although the two different cell conditions were mixed at a 1:1 ratio, there were still differences in adipogenic differentiation visible between cultures of the mixed populations. In future experiments we should investigate methods to increase the amount of adipocytes instead.

CHAPTER V – 3D YELLOW BONE MARROW CULTURE

Limitations of 2D studies

An underlying issue of all 2D feeder layer cultures is the limit as to how long the feeder layers cells can be maintained in culture. In the tests performed in chapter IV, the 2D feeder layers started to detach after 3 weeks and *in vitro* HSC survival gradually diminished in all cultures post 5 weeks. The detachment is due to proliferation of the feeder layer cells that loose their affinity for TCP when they become over-confluent. To inhibit proliferation feeder layers are often irradiated to halt mitosis of the cells. This is however not a viable option in long term cell culture for several reasons mentioned in chapter IV. To reconstitute the bone marrow environment located in the spongy trabecular bone and to overcome the peeling effect in 2D cultures, we decided to culture the bone marrow construct in a 3D porous structure (scaffold). The importance of 3D-culture can be seen in the high cell density of the microenvironment where direct cell-cell interactions are very important (Mayani 1992; Wilson 2006; Zhang 2006). We therefore needed to search for an ideal substrate for 3D bone marrow culture.

Silk as scaffold substrate

As scaffold substrate silk fibroin was chosen for several reasons:

- Using silk as scaffold matrix allows full control over scaffold morphology (Uebersax 2006).

- Silk fibroin is a protein with high biocompatibility and slow degradation and has been successfully used for long-term 3D cell culture without significant structural loss (Altman 2003; Kim 2005).

- Additionally silk scaffolds can easily be modified to be more biomimetic. They have previously been coated with hydroxyapatite (Kim 2008) or implemented with growth factors (Li 2006; Wang 2006; Wang 2009).

- It has proven to be an excellent material not only for osteogenic regeneration (Meinel 2005), but also for reconstruction of adipose tissue (Mauney 2005; Mauney 2007).

- Being a material with a low density, permits the use of several non-invasive techniques to analyze structural changes such as confocal microscopy (Hofmann 2007) or micro-computed tomography (µCT) (Hagenmuller 2007).

- Our group has extensive experience using polymeric scaffolds to reconstruct 3D bone grafts in static and perfusion cultures (Meinel 2004; Marolt 2006; Kim 2007).

General Materials and Methods

Extraction and production of silk scaffolds

Silk fibroin was extracted according to previous publications (Nazarov 2004). Briefly: The silk was derived from stifled silk cocoons of the silkworm (Latin: *bombyx mori*). After removing the dead larvae the cocoons were cut into small pieces and boiled in a 0.02 M Na_2CO_3-solution to remove sericin, a glue type protein that holds the fibroin strands together. Multiple washing steps assured a high purification of the silk fibers. These were then liquefied using a 9.3 M LiBr-solution. The resulting yellowish solution was dialyzed against deionized water (diH_2O) for several days to remove the LiBr, yielding an aqueous silk solution with a silk concentration of ~8%.

Using the salt leaching method, the scaffolds were prepared by first aliquoting the silk solution into containers and then adding salt spheres of 300-400 µm diameter. The containers were sealed and the silk was left to recrystallize for 1 week at room temperature. Then the scaffolds were submersed in diH_2O for several days to leach out

the salt, yielding the porous structure. Scaffolds were then cut into cylinders of the dimensions: 8 mm diameter and 4 mm height.

Before seeding, the scaffolds were washed twice with phosphate buffered saline (PBS), air dried over night and sterilized in an autoclave. To facilitate cell-seeding, they were then submersed in their respective culture medium over night (conditioning), allowing them to soak in the liquid and thereby reducing the hydrophobicity of the silk structure.

Cell seeding

$1x10^6$ cells twice-passaged (P2) MSCs were seeded in a volume of 100 µL hMSC expansion medium, consisting of high glucose DMEM supplemented with 10% fetal bovine serum (FBS), antibiotics (100 U/mL penicillin, 100 µg/mL streptomycin, 0.25 µg/mL fungizone), 0.1 mM nonessential amino acids and 1 ng/mL basic fibroblast growth factor (bFGF). Medium changes occurred bi-weekly and was switched after 3 weeks expansion to an adipogenic medium consisting of DMEM:F12 supplemented with 3% FBS, antibiotics (100 U/mL penicillin, 100 µg/mL streptomycin, 0.25 µg/mL fungizone), 33 µM biotin, 17 µM D-pantothenic acid hemicalcium salt, 1 µM human insulin, 1 µM dexamethasone, 50 mM 3-isobutyl-1-methylxanthine (IBMX) and 5 µM 2,4-thiazolidinedione (TZD). After 3 weeks of adipogenic differentiation BMMNC were seeded at $1x10^6$ cells per scaffold and kept in HSCM, consisting of IMDM supplemented with 15% FBS, antibiotics, 55 µM ß-mercaptoethanol, 10 ng/mL Flt-3, 10 ng/mL IL-6, 10 ng/mL SCF 10 ng/mL and 2 ng/mL IL-3.

Confocal analysis of feeder layers on scaffolds

Prior to seeding of the BMMNC on the scaffolds, additional constructs were analyzed using confocal microscopy. To highlight macroscopic structures, 4',6-diamidino-2-phenylindole (DAPI) was added to visualize nuclei and the silk scaffold, acetomethoxy-calcein (calcein AM) to display live cells, and a commercial solution of Nile Red (AdipoRed) to stain the lipids in adipocytes.

For this scaffolds were first cut in half and then washed 3x with PBS. To each scaffold 1 mL 50 µM DAPI lactate, 1mL 200 µM calcein AM, and 56 µL AdipoRed (Lonza), were added, mixed a few times gently through the scaffold and let incubate for 20 min at room temperature in the dark. Orientation of the scaffold pieces was noted and transferred to a glass cover dish for confocal measurement.

Cell extraction for flow cytometry

For quantitative analysis of the $CD34^+$ population, medium was collected from each scaffold in conical tubes. Scaffolds were subsequently washed 3x with PBS while collecting washes in respective tube. 2 mL 0.25% trypsin-EDTA was perfused multiple times through each scaffold for a total of 10 min and again collected in the respective tube. Finally, scaffolds were vigorously perfused 3x with PBS to collect any remaining cells attached to the scaffold. The cell suspensions were pelleted and resuspended in 100 µL FACS buffer that consisted of PBS supplemented with 0.5% bovine serum albumin (BSA) and 5 mM EDTA. To each cell suspension 10 µg human Immunoglobulin G (IgG) (Sigma, Saint Louis, MO) was added to block binding of nonspecific receptors. Subsequently 10 µL of CD34-FITC antibody (BD Biosciences, San Diego, CA) was added to label the hHSCs. The cells from the remaining well were left unlabeled as a negative control. After incubation in the refrigerator for 30 min the cells were washed twice with 1 mL FACS buffer and finally resuspended in 250 µL FACS buffer for flow cytometric analysis on a standard two-laser FACSCalibur (BD Biosciences, San Jose, CA).

Data analysis was performed using 2D dot plot gating with FlowJo analytical software (Tree Star, Inc., Ashland, OR). This allowed quantification of labeled cells to compare to histological analysis. Since the total cells per scaffold varied strongly depending on the manipulation of the feeder cells, the percentage of $CD34^+$ cells in each well was not an ideal comparison between the different conditions. Therefore the data was plotted as

percent of seeded $CD34^+$ cells remaining in each well at each time point, with 100% being the initial amount of $CD34^+$ cells in the fresh bone marrow.

Statistical analysis

All flow cytometric data are expressed as means ± SD and a minimum of three replicates were performed for each assay. Using GraphPad Prism (GraphPad Software, San Diego, CA) a two-way analysis of variance (ANOVA) was used for statistical analysis of multiple comparisons. Statistical difference between experimental groups was considered to be significant when the p value was < 0.05.

Coating with bone matrix proteins

In a first experiment we decided to coat aqueous derived silk scaffolds with biomaterials that are highly abundant in the bone marrow cavity. Next to bare silk scaffolds we included collagen type I, the most abundant protein in the bone matrix (Glowacki 2008), hydroxyapatite (HA), the most abundant mineral in the bone matrix (Hancox 1972; Yoshikawa 2009), and fibronectin, an adhesion protein believed to play an important role in hematopoiesis (Weinstein 1989).

Materials and Methods

After preparation of the scaffolds, the coatings were performed accordingly:

Collagen I

Scaffolds were autoclaved for sterilization and rehydrated overnight in PBS in a six-well plate. Rat tail collagen type I (Invitrogen) was diluted with 0.02 N acetic acid to obtain a 1 mg/mL solution. Scaffolds were coated by immersion in the solution for 5 minutes and left to dry in a culture hood for 2 hours. Prior to seeding, scaffolds were washed 3x with PBS and rehydrated in culture media for 30 minutes.

Hydroxyapatite

Scaffolds were hydrated overnight in diH_2O in a six-well plate. Scaffolds were fixed in holders and perfused with a 0.2 M calcium chloride solution for 15 min. After excess solution was aspirated, the scaffolds we perfused with 0.12 M sodium hydrogen phosphate solution for 15 min. These steps were repeated for a total of 20 cycles to obtain a confluent coating of hydroxyapatite. Scaffolds were then washed 3x with diH_2O and autoclaved for sterilization. Prior to seeding, scaffolds were washed 3x with PBS and rehydrated in culture media for 30 minutes.

Fibronectin

Scaffolds were autoclaved for sterilization and rehydrated overnight in PBS in a six-well plate. Human plasma fibronectin (Invitrogen) was reconstituted by adding diH_2O to obtain a 1 mg/mL solution. Scaffolds were coated by immersion in the solution for 5 minutes and left to dry in a culture hood for 2 hours. Prior to seeding, scaffolds were washed 3x with PBS and rehydrated in culture media for 30 min.

Culture conditions

Scaffolds were kept throughout the entire experiment in 6-well plates with 4 mL medium to keep the entire scaffold submersed. Culture medium was replenished fully on a bi-weekly basis. Plates were kept in a hypoxic incubator with 5% O_2, 5% CO_2 and 95% humidity.

Results

Confocal analysis

Confocal images of the scaffolds showed that not many feeder cells were present on the scaffolds and that confluence of the feeder layer had high regional differences (Fig. 5.1). DAPI was predominantly present on scaffold structures, and calcein staining appeared to conform to cellular structures. AdipoRed staining of lipid droplets was not only visual as red dots but also as yellow substructures (overlay of AdipoRed and calcein staining)

predominantly within the green cellular structures (Fig. 5.2). Due to a misaligned intensity setting, images of the uncoated scaffolds (Fig. 5.1A) appeared to have a higher abundance of adipocytes. Disregarding this mistake, there was no apparent difference in lipid presence between the scaffolds of different coatings. Scaffold structures were limitedly visible in the HA coated scaffolds.

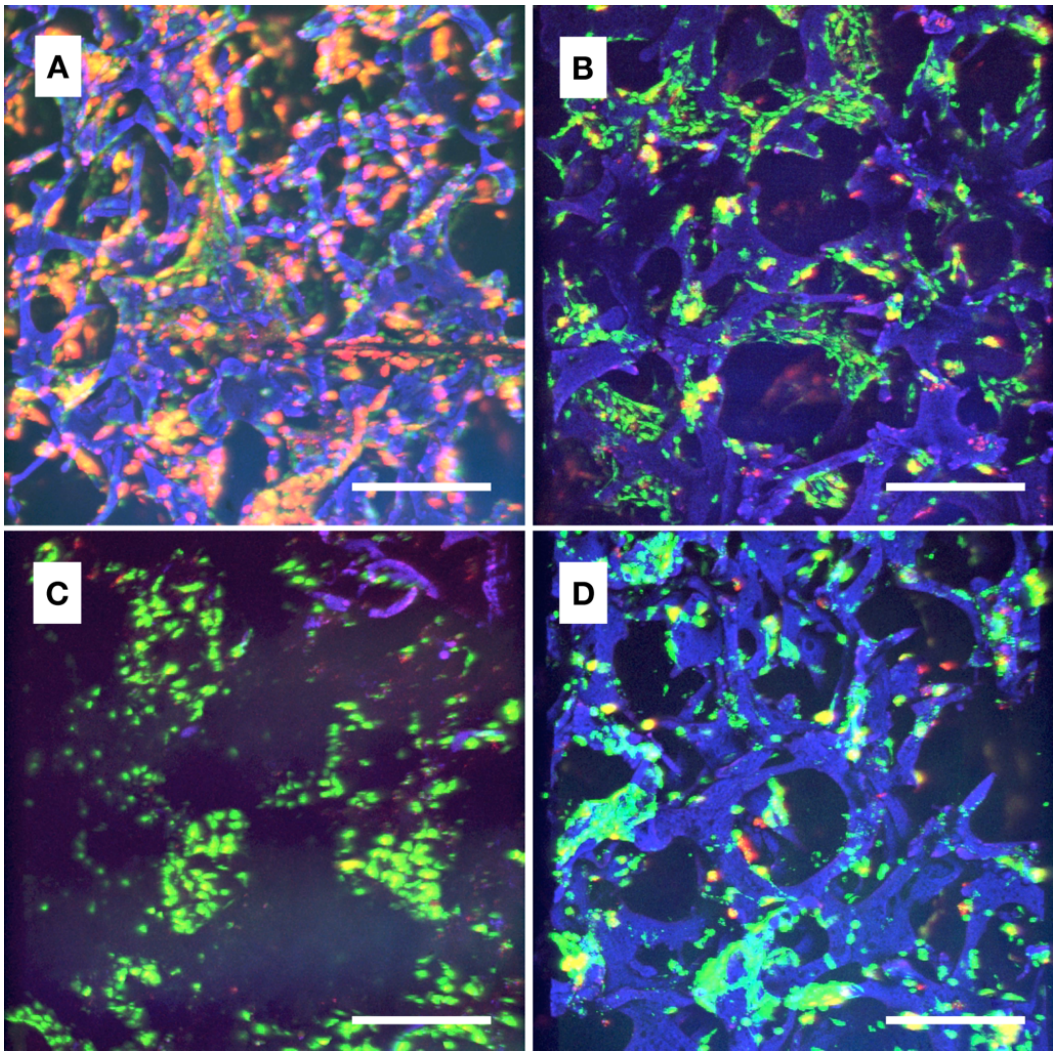

Fig. 5.1. Confocal images of aqueous-derived silk scaffolds, pore-size: 300 - 400 μm, seeded once with hMSCs. (A) uncoated, (B) coated with collagen I, (C) hydroxyapatite, and (D) fibronectin. Blue = DAPI, Green = Calcein, Red/Yellow = AdipoRed. Scale bar = 400μm.

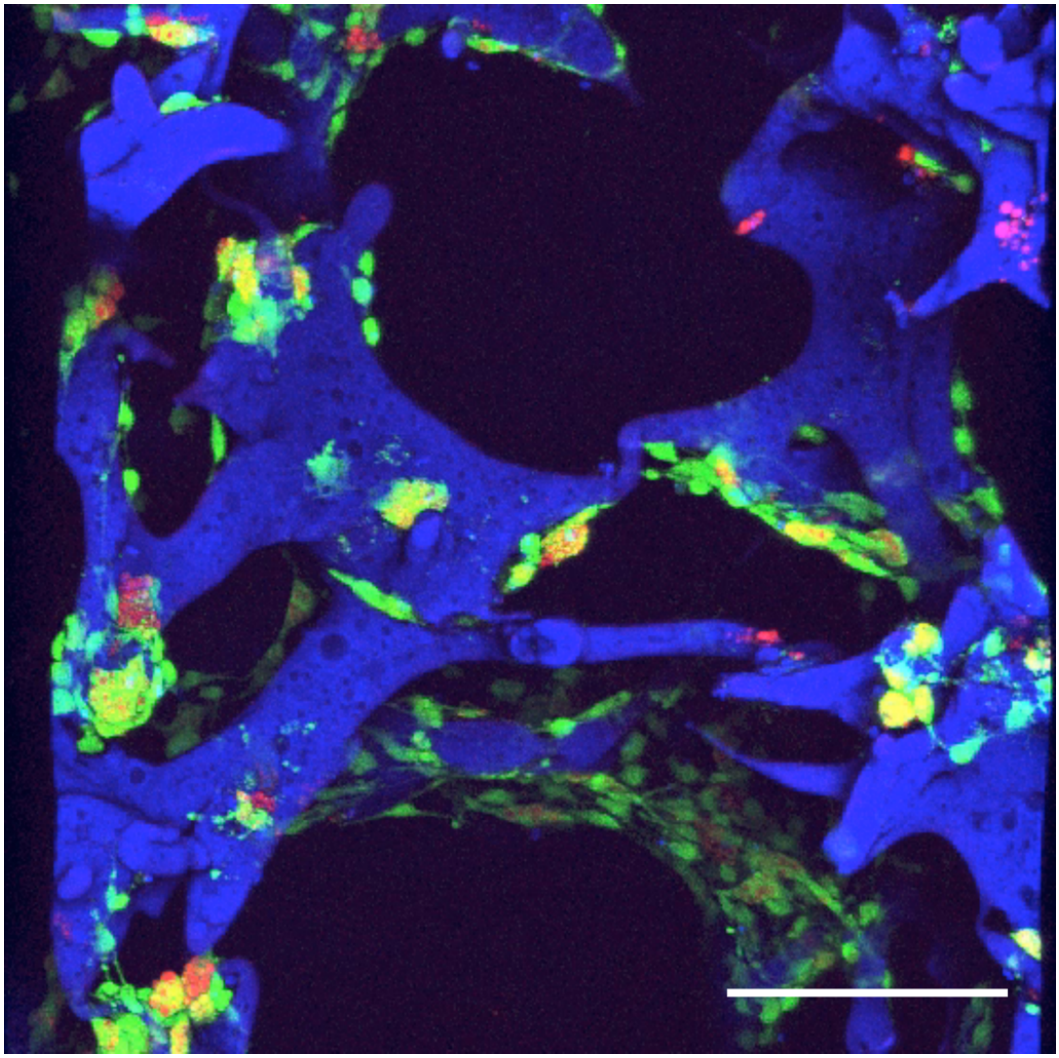

Fig. 5.2. Confocal image at 20x magnification of aqueous-derived silk scaffold, coated with 1mg/mL collagen I, pore-size: 300 - 400 µm, seeded once with P2 hMSCs. Scale bar = 200 µm.

Flow cytometric quantification

Quantification of the $CD34^+$ cells showed no significant differences at most time points when comparing between scaffolds with different coatings (Fig. 5.3). Only HA coated scaffolds at 14 days had a significantly lower $CD34^+$ cell percentage than other conditions. In all conditions cell percentages dropped below 20% at the 3 day time point, but recovered up to 50% after 14 days. Cultures were stopped at 21 days, due to insufficient scaffolds, where all conditions reached about 25% $CD34^+$ cell survival.

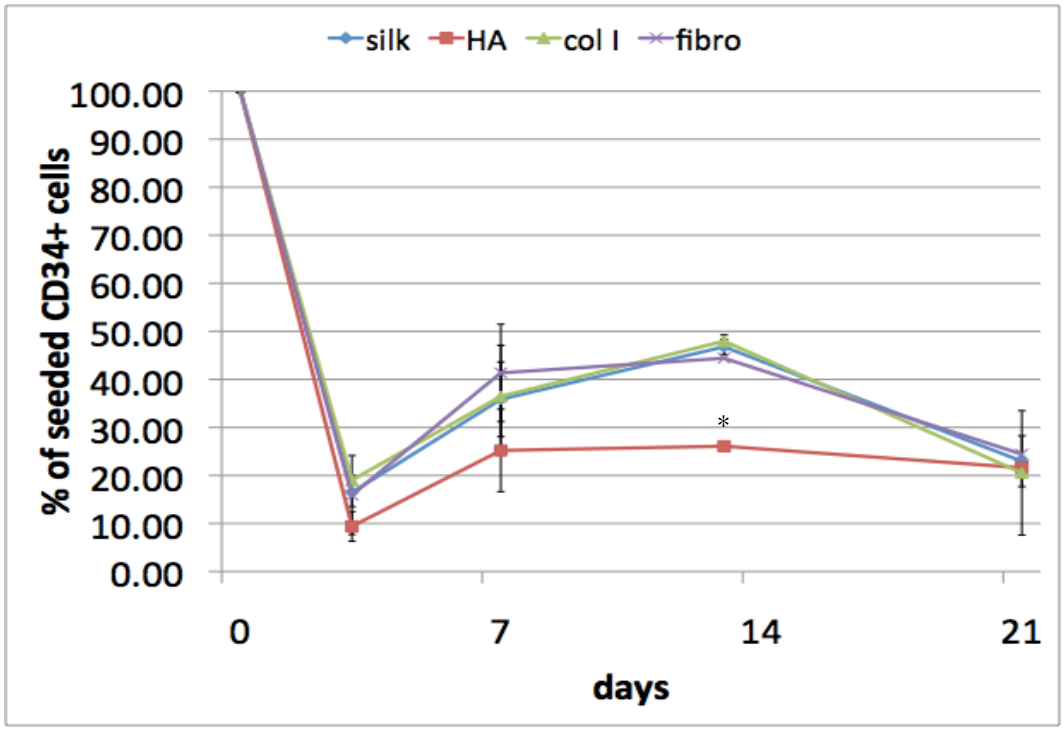

Fig. 5.3. Time-lapsed, flow cytometric quantification of CD34+ population in 3D silk scaffolds kept uncoated (blue), coated with collagen I (green), hydroxyapatite (red) and fibronectin (purple). Data are given as means ± SD (n ≥ 3). A statistically significant difference with respect to uncoated silk scaffolds (silk) is denoted by an asterisk above the respective time point.

Discussion

Confocal images proved effectiveness of the chosen staining method. Nuclei of the individual cells were not visible using the DAPI stain, very likely due to the fact that silk fibroin has a very high affinity for dyes. Likewise, the other two dyes (calcein AM and AdipoRed) were possibly also taken up by the silk, however were not measured in fluorescence, as they require metabolic modification (calcein AM) or affinity binding (AdipoRed) to display a signal at visible wavelengths. DAPI staining provided very detailed imaging of the silk structure, even at a microscopic level (Fig. 5.2). Confluence of the feeder layer was rather low, which is fairly common in silk scaffolds and was appointed to the cell seeding technique. The lower amount of cells in the HA coated scaffolds, and the difficulty to see structures of the silk scaffold, was explained in the

properties of HA. Being a highly dense mineral, HA doesn't permit penetration of light in the visible range. Additionally, the surface properties are very rough on this crystalline material. Cells are likely to bind tightly to these rough surfaces, also making it more difficult for extraction. Therefore, we concluded that the lower number of $CD34^+$ cells in HA scaffolds is not due to an effect of the coating, but rather to do the difficulty of extracting all the cells for quantification. There also seemed no apparent difference in the amount of adipogenic differentiation between the different coatings. Adipogenic differentiation was low in all cases. These findings led us to conclude that the alteration of silk with bone matrix proteins had no clear benefit and that uncoated silk scaffolds are suitable for 3D bone marrow tissue engineering. The initial drop in cell count was likely due to the complete removal of medium during medium exchanges, as non-adherent cells were not actively contained within the scaffolds structure. Half medium exchanges should therefore be performed similar to the 2D studies.

Coating with softer matrix proteins

As a follow up of the first coating experiment, we made an attempt to increase both cell adhesion, but also adipogenic differentiation by coating the scaffolds with softer matrix proteins. In this case the coating should serve two-fold: A. coated silk scaffolds have been shown to improve cell adhesion (Vepari 2007). B. softer scaffold matrices have been shown to increase adipogenic differentiation (Engler 2006; Park 2011). Next to bare silk scaffolds we therefore included collagen type IV, matrigel, and tropoelastin as coating materials.

Collagen IV

Collagen IV was chosen over collagen I for coating as it lacks the regular glycine amino acids in every third residue, which is necessary for a tight collagen triple helix (Khoshnoodi 2008). Because of the higher irregularity in the collagen IV structure, the protein structure is less tightly bound together, yielding a softer matrix. Previous

research suggests, collagen IV is the major matrix component associated with adipogenic differentiation (Mauney 2010). This research showed that collagen IV was more efficient than collagen I as a substrate to improve adipogenic differentiation.

Matrigel

Matrigel is derived from the extracellular matrix (ECM) of mouse sarcomas and is processed as a commercial product. It is composed of laminin (56%), collagen IV (31%), and proteoclygans such as entactin (8%). It includes many growth factors, though the concentration of these is variable between batches. Matrigel is a known stimulant of adipogenesis (O'Connor 2003), and it was shown that Matrigel was better for adipogenic differentiation of hASCs than collagen alone (Park 2009). The laminin in Matrigel should also have a positive effect on cell attachment (Patrick 2003). Increased cell attachment should lead to an increase in cell density, which in turn should again lead to increased adipogenic differentiation (McBeath 2004). While laminin is a key component of Matrigel, it has been shown in previous studies that laminin alone does not promote adipogenic differentiation (Patrick 2003).

Tropoelastin

The natural polymer elastin is made up of tropoelastin subunits; these subunits are cross-linked to form elastin. Tropoelastin is much softer than elastin due to the lack of cross-linking. This characteristic makes tropoelastin a favorable extracellular matrix option for adipogenesis. Additionally, tropoelastin has an $\alpha_v\beta_3$ integrin, which has been shown to induce adipogenesis (Wise 2009; Mauney 2010), Finally, the use of tropoelastin has been shown to aid in HSC expansion due to its elastic properties (Holst 2010). These properties made tropoelastin a coating worth investigating for the project.

CFC

Another attempt was made on using CFC assays for stem and progenitor cell quantification. Due to previous overgrowing of the plates with hMSCs from the feeder layer, the $CD34^+$ population was isolated before colony seeding by FACS.

Materials and Methods

After preparation of the scaffolds, the coatings were performed accordingly. A high protein concentration was chosen allowing the deposition of a thick coating film as opposed to just adsorption of binding proteins. The reasoning behind this was that the cells would truly experience the lower elastic modulus of the culture substrate.

Collagen IV

Collagen IV was obtained commercially (Sigma). A 1.5 mg/mL solution was prepared by dissolving 10 mg of lyophilized collagen IV powder in 6.67 mL 0.1 M acetic acid. Solution was mixed until homogenous, and it was then kept on ice. 1 mL of 0.1 M acetic acid was added to each scaffold placed in 24-well plates. Plates were left in biosafety hood for 2 hours. Excess liquid was aspirated until wells appeared dry. 80 µL of collagen IV solution was added to each scaffold. Scaffolds were then placed in an oven at 60 °C for 4 hours to denature the collagen. Subsequently, 10 µL of 0.5M NaOH solution was added to scaffolds for neutralization and gelation. Scaffolds were then kept in incubator overnight for the collagen to solidify.

Matrigel

Matrigel was obtained commercially (BD Bioscience). The Matrigel (10.6 M) was thawed at room temperature until liquid (heating will change the properties of Matrigel, so a hot water bath was not used). An 1.5 mg/mL aqueous Matrigel solution was fashioned by adding 0.708 mL of Matrigel to 4.3mL of PBS. The solution was mixed until homogeneous, and it was then put on ice. Scaffolds were presoaked in 1 mL of diH_2O in 24-well plates for 2h in a biosafety hood. Excess liquid was aspirated until wells

appeared dry. 80 µL of Matrigel solution was added to each scaffold. Scaffolds were then placed in an incubator overnight for gelation of Matrigel.

Tropoelastin

Tropoelastin was obtained through generous donation from Anthony Weiss at the University of Sydney, Australia. A 1.4 mg/mL aqueous solution of was made by mixing 6 mg tropoelastin in 4.3 mL of PBS until homogeneous. The subsequent solution was kept on ice to prevent the degradation of the tropoelastin. Scaffolds were presoaked in 1 mL of diH_2O in 24-well plates for 2h in a biosafety hood. Excess liquid was aspirated until wells appeared dry. 80 µL of tropoelastin solution was added to each scaffold. Scaffolds were then placed in sterile pouches and kept at 4 °C overnight to promote coacervation of the tropoelastin (Yeo 2011).

Culture conditions

Prior to seeding, scaffolds were washed 3x with PBS to remove excess coating material and rehydrated in culture medium for 30 minutes. Scaffolds were kept throughout the entire experiment in 6-well plates with 4 mL medium to keep the entire scaffold submersed. Culture medium was replenished bi-weekly by slowly exchanging all but 1 mL of the medium from the top of each well to prevent removal of non-adherent cells. Plates were kept in a hypoxic incubator with 5% O_2, 5% CO_2 and 95% humidity.

CFC

The cells were extracted from the scaffolds and labeled with CD34-FITC as previously described for flow cytometry. Using a MoFlo cell sorter (Dako Cytomation), the $CD34^+$ cells were extracted into HSCM medium. The sorted cells were then added to aliquots of Methocult CFC assay medium. Tubes were vortexed for 1 minute and 1.1 mL of the Methocult-cell mixture was expelled evenly into 35mm petri dishes. Each condition was measured in duplicate. Dishes were kept in a 20% O_2 incubator, at 37 °C and 95% humidity. Colonies were counted after 16 days.

Results

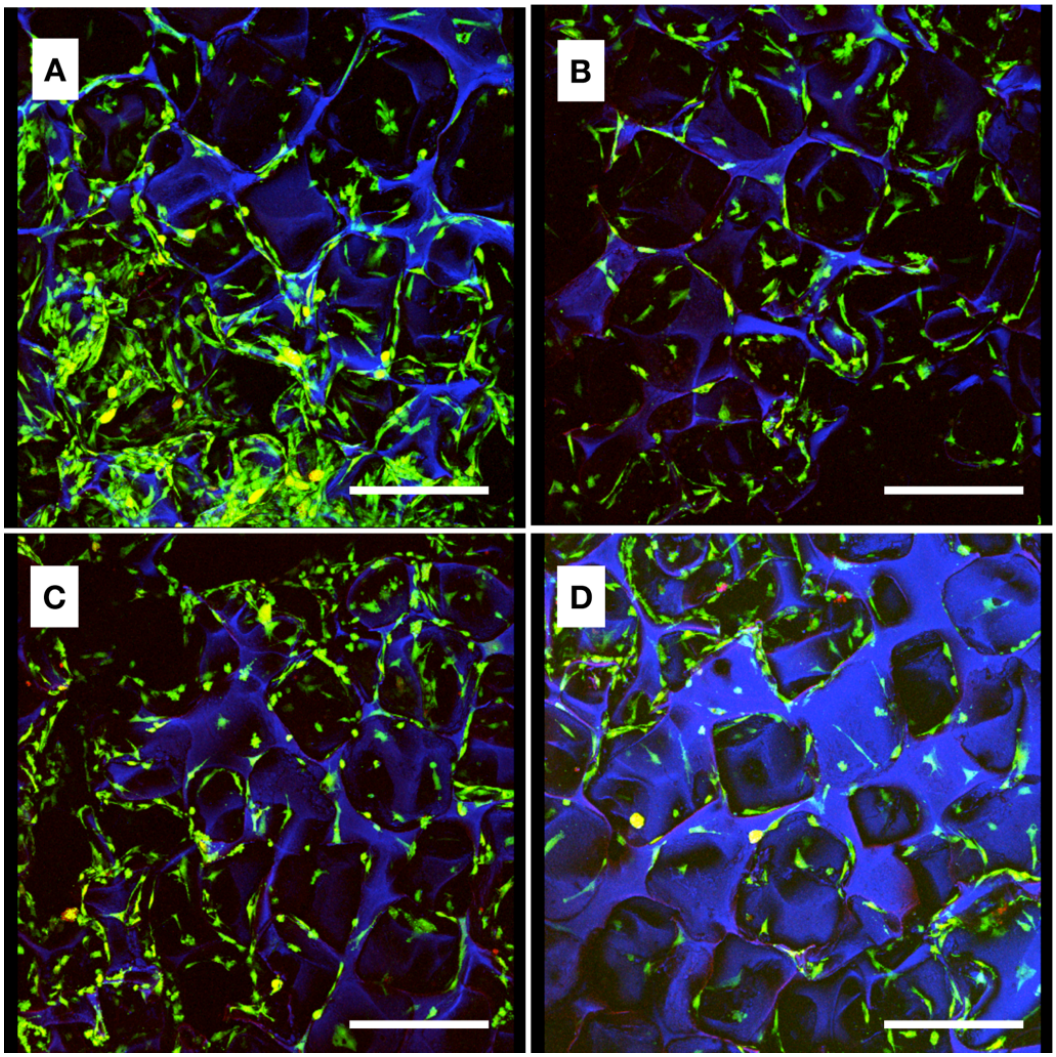

Fig. 5.4. Confocal images of aqueous-derived silk scaffolds, pore-size: 300 - 400 µm, seeded once with hMSCs. (A) uncoated, (B) coated with collagen IV, (C) matrigel, and (D) tropoelastin. Blue = DAPI, Green = Calcein, Red/Yellow = AdipoRed. Scale bar = 400 µm.

Confocal analysis

The non-coated silk scaffold had the greatest cell confluence compared to the coated scaffolds (Fig. 5.4). There were no apparent differences in cell density between the different coatings and confluence was rather low in all cases. Also, no differences could be made out in the number of adipocytes.

Flow cytometric quantification

Quantification of the $CD34^+$ cells showed no significant differences at most time points when comparing between scaffolds with different coatings (Fig. 5.5). Only the Matrigel coating showed a slightly higher $CD34^+$ cell survival at 21 and 28 days when compared to collagen IV and tropoelastin, though this was not significant. Also, instead of an initial drop, cell percentages increased initially and only started to decrease after 21 days.

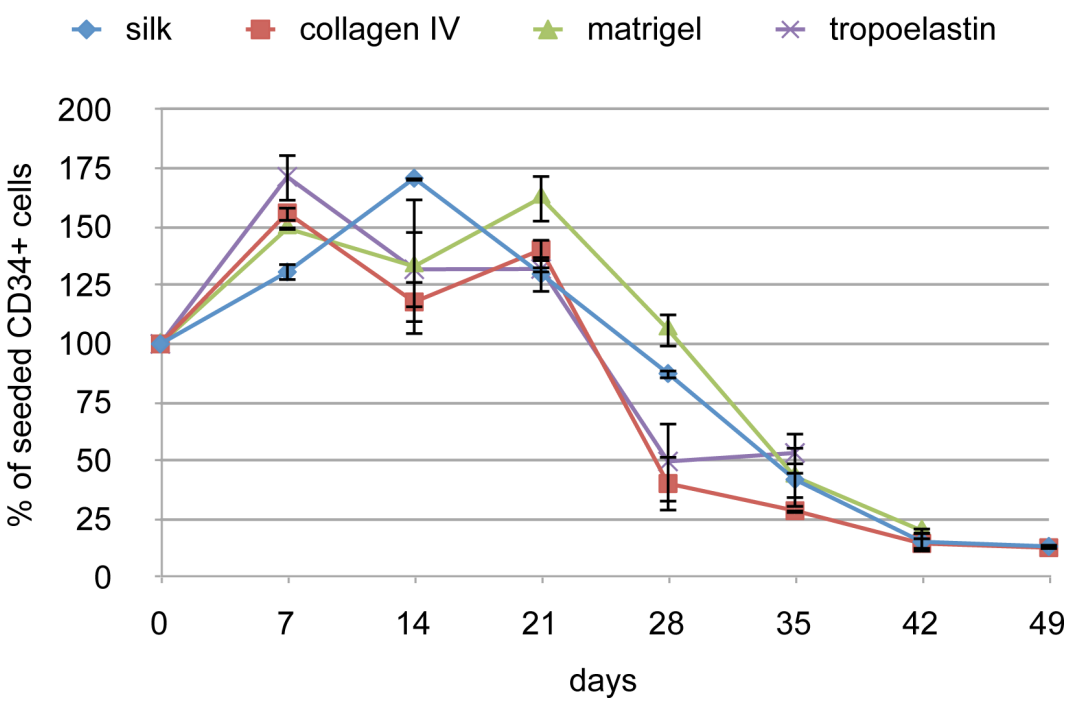

Fig. 5.5. Time-lapsed, flow cytometric quantification of $CD34^+$ population in 3D silk scaffolds kept uncoated (blue), coated with collagen IV (red), matrigel (green), and tropoelastin (purple). Data are given as means ± SD ($n \geq 3$).

CFC

Colony assays provided no significant differences between coated scaffolds (Fig. 5.6). Colony percentages dropped significantly in comparison to fresh bone marrow.

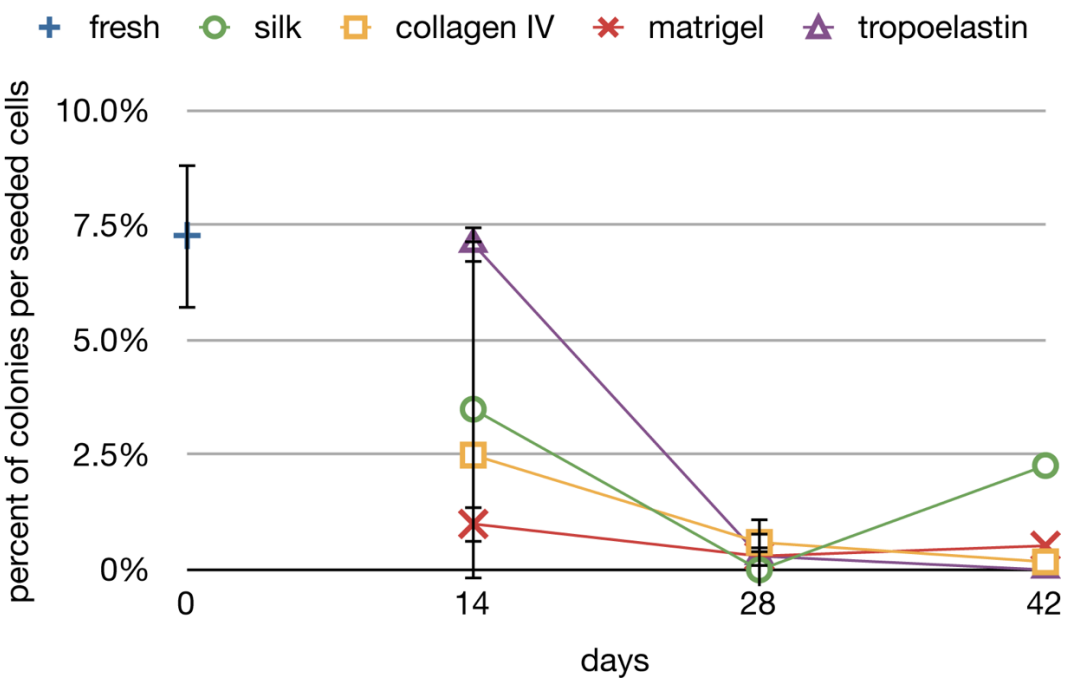

Fig. 5.6. Time-lapsed, CFC assay of $CD34^-$ population in 3D silk scaffolds kept uncoated (green), coated with collagen IV (yellow), matrigel (red), and tropoelastin (purple). Colonies are given as percent of total seeded cells, assuming each colony was derived from 1 stem or progenitor cell. Data are given as means ± SD ($n \geq 2$).

Discussion

As described in the introduction, the purpose of the coating was to increase adipogenic differentiation of the feeder layer, which would in turn help to maintain HSC populations. A proposed conclusion for the general failure of the coating is that the coatings degraded during the long culture period *in vitro*: The coatings used were chosen because they have a low elastic modulus and are therefore softer. A major factor in the softness of a material is a low amount of cross-linking between its subunits. This lack of cross-linking however also generally means that softer materials are more prone to degradation (Weadock 1996). Assuming successful coating, the high protein concentrations used for coating, likely provided at thick layer to which the cells predominantly adhered to. Degradation of the coating proteins could have led to detachment of the feeder cells from the scaffold. Since silk had no coating, cells were

seeded directly onto the scaffold and therefore did not detach due to coating degradation.

Unfortunately, coating efficiency could not be measured due to the previously mentioned high affinity of dyes and matrix specific antibodies to the silk. Alternatively we tried to obtain detection of the coating through fluorescence measurement, however this was unsuccessful due to lack of specific wavelengths of the matrix proteins and a high autofluorescence of the silk (data not shown).

Another reason that might explain the lack of significant differences between the different coatings is the 3D static setup. Though we were able to remove the drop in $CD34^+$ cells after initial seeding by exchanging only half the medium, the non-adherent cells were not contained within the scaffold matrix. Since the scaffolds were surrounded by a large volume of medium, adding medium to the well will have dispersed the non-adherent cells. Following gravity these cells sank to the bottom of the well and covered the entire surface area.

6-well plate:

surface area = 9.6 cm^2

porous scaffold:

$$diameter(d) = 8mm = 2 \times radius(r)$$
$$height(h) = 4mm$$
$$\Rightarrow r^2 \times \pi = 50.27mm^2$$

relative percent:

$$100\% \frac{50.27mm^2}{9.6cm^2} = 5.24\%$$

Therefore the only non-adherent cells to actually be contained within and experience the feeder cells within the scaffold structure will have been at the footprint of the scaffold, which is only 5.2% of the total surface area. This low percentage of cells being subject to the different conditions would result in most cells experiencing bare TCP in all culture plates and the lack of differences between the conditions. To overcome this issue, we would need to place the scaffolds in a container restricting dispersion of the cells outside of the scaffold. This will however also limit the volume of culture medium that the cells have access to, which is approximately just the volume of the scaffold:

6-well plate:

3 mL of medium per well per medium exchange.

porous scaffold:

volume of entire scaffold:

$$diameter(d) = 8mm = 2 \times radius(r)$$
$$height(h) = 4mm$$
$$\Rightarrow r^2 \times \pi \times h = 200mm^3 = 200\mu L$$

assuming close packing of equal spheres, the volume of the pores is:

$$\frac{\pi}{3\sqrt{2}} \approx 0.74$$
$$\Rightarrow 200\mu L \times 0.74 = 148\mu L$$

relative percent:

$$100\% \frac{148\mu L}{3mL} = 4.93\%$$

Therefore the cells will only have access to 4.93% of the medium volume of an entire well. The medium in the scaffolds must therefore be constantly replenished. Manually this would require a medium exchange every 4.2 hours. Ideally though this should provided in an automated fashion using a perfusion bioreactor.

Finally, CFC assays showed very little benefit. Not only were there high variances, but the actual amount of $CD34^+$ cells that could be isolated by FACS was so low after 14 days that it was difficult to even obtain colonies.

Multiple seedings

Since confluence was not obtained by coating the silk scaffolds with different matrices, an increase in cell density was pursued by performing multiple cell seedings over multiple days on the silk scaffolds, as this had been successfully performed in our lab (Mandal 2011). By seeding cells on pre-seeded scaffolds, we expected that the cells of the previous seedings had produced sufficient ECM for the stem cells of subsequent seedings to adhere to. Again the thought was that increased cell attachment would lead to an increase in cell density, which in turn should again lead to increased adipogenic differentiation (McBeath 2004).

Materials and Methods

Cell seeding

After standard preparation and sterilization of the aqueous silk scaffolds, constructs were pre-conditioned in hMSC expansion medium over night. The next day scaffolds were aspirated until all pores appeared dry and subsequently seeded with $1x10^6$ cells of P2 MSCs in a volume of only 15 µL hMSC expansion medium. Constructs were kept in an incubator over the next hour, while intermittently adding 15 µL of medium every 15 min. After 1h the well was filled with expansion medium and kept in an incubator for 3 days. These steps were repeated for second and any subsequent seedings. After an additional 3 days in expansion medium, medium was switched for 3 weeks to an adipogenic medium consisting of DMEM:F12 supplemented with 3% FBS, antibiotics (100 U/mL penicillin, 100 µg/mL streptomycin, 0.25 µg/mL fungizone), 33 µM biotin, 17 µM D-pantothenic acid hemicalcium salt, 1 µM human insulin, 1 µM dexamethasone, 50 mM 3-isobutyl-1-methylxanthine (IBMX) and 5 µM 2,4-thiazolidinedione (TZD). BMMNC

were again seeded after 3 weeks of adipogenic differentiation at $1x10^6$ cells per scaffold and kept in HSCM, consisting of IMDM supplemented with 15% FBS, antibiotics, 55 μM ß-mercaptoethanol, 10 ng/mL Flt-3, 10 ng/mL IL-6, 10 ng/mL SCF 10 ng/mL and 2 ng/mL IL-3.

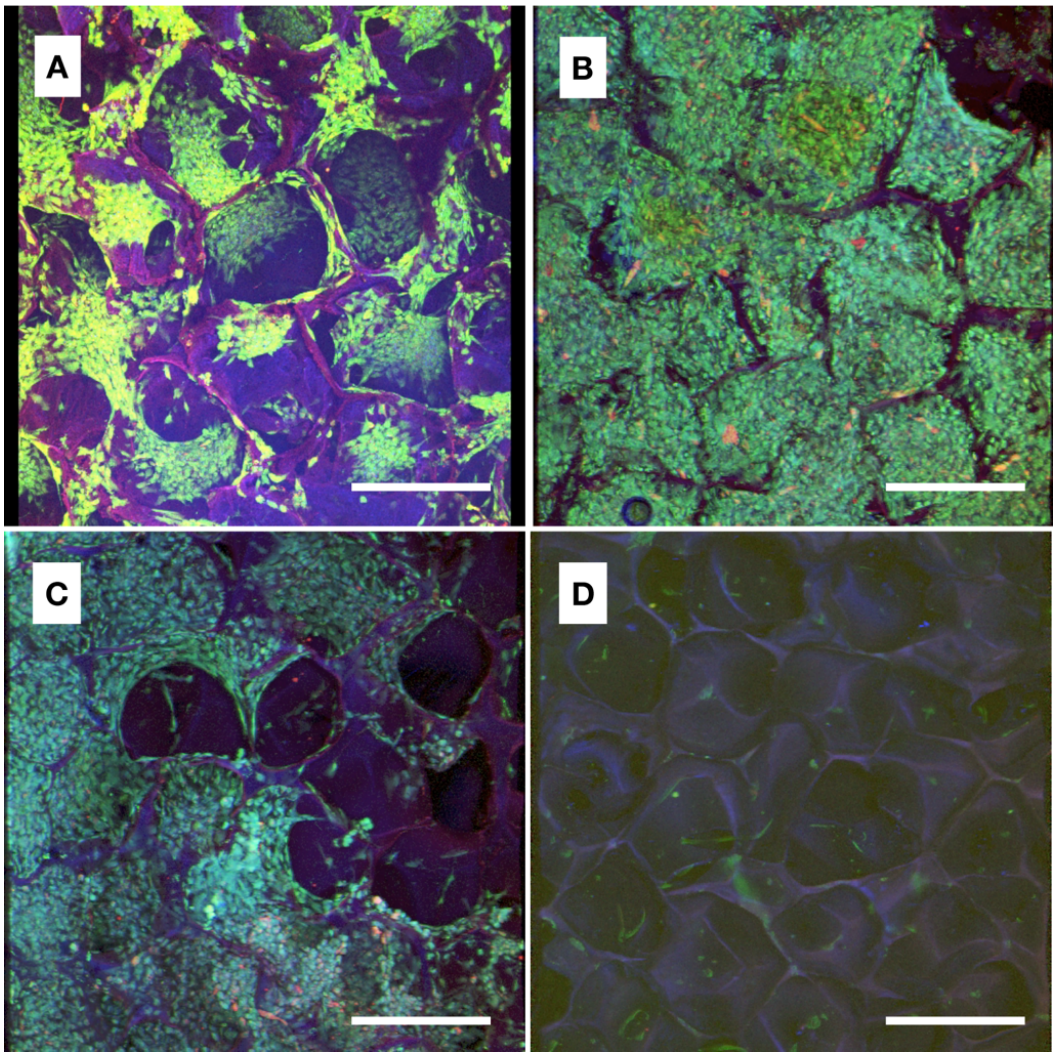

Fig. 5.7. Confocal images of aqueous-derived silk scaffolds, pore-size: 300 - 400 μm, seeded (A) twice and (B-D) three times with hMSCs. Cell density was highest (B) at the top of the scaffold and fairly confluent (C) at the bottom as well. Very few cells were detected (D) in the center of the scaffold. Blue = DAPI, Green = Calcein, Red/Yellow = AdipoRed. Scale bar = 400 μm.

Results

After a second seeding, multiple confluent regions were visible in the pores of the scaffold (Fig. 5.7A) and even higher confluence was detected after a third seeding (Fig. 5.7B-D). Additionally, a large amount of lipid droplets were distributed amongst the confluent layers. Confluence was highest at the top of the scaffold (Fig. 5.7B), where the cells were seeded, and also quite a few cells were present at the bottom of the scaffold (Fig. 5.7C). In the center of the scaffold cell density was very low and almost no AdipoRed staining could be detected (Fig. 5.7D).

Discussion

The additional seedings added significantly to both cell density and adipogenic differentiation (Fig. 5.7). The cell layers conformed very well to the pores of the scaffold creating a lining that is very similar in appearance to the bone marrow stroma. Additionally, regions with higher cell density seemed to have more lipid droplets, which agrees with previous observations (McBeath 2004). The uneven distribution of the cells throughout the scaffold can be traced back to the seeding method. Since cells were seeded at a very high concentration and constantly from the top, most cells adhered there. Cells that did not adhere instantly, likely dropped to the bottom of the scaffold and expanded there on TCP creating another confluent layer. Very few cells were present in the middle of the scaffold, since nothing promoted retention of the cells there. If seeding were to be performed in dynamic perfusion system, a more uniform cell distribution could possibly be achieved.

Another possibility of the lack of cells in the core can be related to the discussion in the previous experiment: because a thick confluent layer of cells formed at the perimeters of the scaffolds, and these were all kept in static cultures, likely very little nutrients reached all the way into the core of the scaffold.

Perfusion Culture

To overcome the difficulty of nutrient delivery to the core of a scaffold, there are several bioreactors available that increase mass transport through the constructs (Martin 2004). Spinner flasks and rotating wall vessels have traditionally been used, and function by stirring the medium to increase diffusion. Unfortunately, these techniques also require a large volume of medium surrounding the scaffolds, which, as previously outlined, does not contain non-adherent cells within the constructs. Therefore perfusion bioreactors need to be used that can perfuse medium at a very controlled rate. This needs to be fast enough to provide nutrients to the core, but slow enough to not flush the non-adherent cells out of the constructs.

Generation I - "U-Tube bioreactor"

The first bioreactors that were used were based on a design generously provided by the group of Ivan Martin at the University Hospital in Basel, Switzerland. The setup was based on a polycarbonate chamber that had polypropylene tubing attached at either side (Wendt 2006). The bottom tubing was connected via a U-shaped PharMed BPT tubing, giving the reactor its "U-tube" name. Constructs were fastened in place in the chambers and using a syringe pump, medium was perfused back and forth from one tube to the other. An access port at the bottom of the chamber provided easy medium changes (Fig. 5.8).

These reactors were updated in several ways:

- Polycarbonate was replaced with Radel, an amber translucent material with much better tensile and impact strength, to overcome the cracks that formed when fastening the chambers.
- 0.45 µm cellulose membrane filters were placed at the top and bottom of the scaffolds, to increase containment of the non-adherent cells within the scaffolds.

- Joints were glued with epoxy and finally sealed by melting to reduce the amount of leaks that occurred when pressure built-up within the chamber.

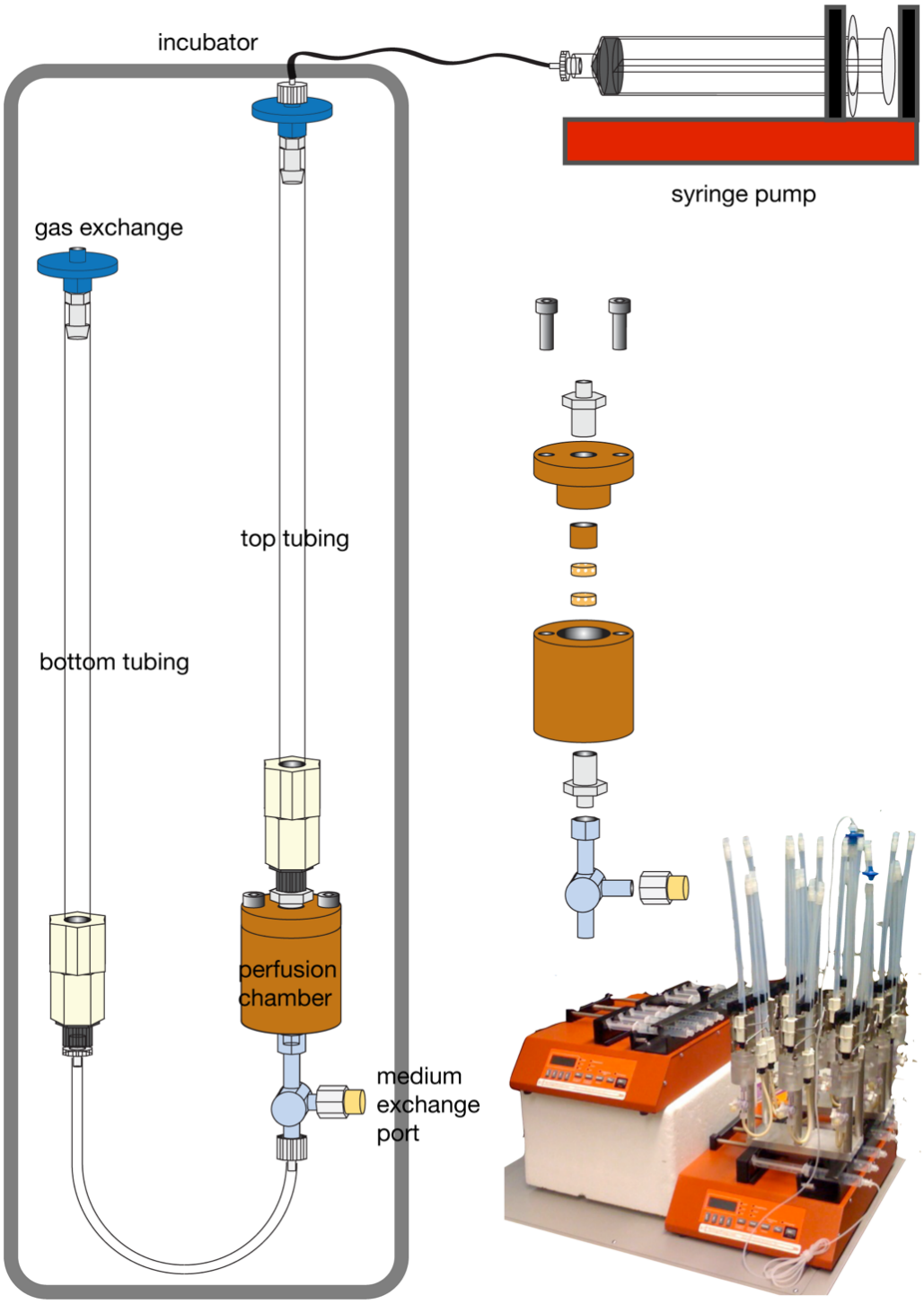

Fig. 5.8. Diagram and photograph of U-tube perfusion bioreactor.

Though with these improvements, the chambers could be completely sealed to eliminate contamination, there were still a few major flaws in the design concept when adapting the reactors for non-adherent cell culture:

- Though cells could be contained within the scaffolds using membrane filters, the rapid expansion of the blood cells led to clogging of the filters and a rapid pressure build-up within the chambers.

- Medium could not be extracted through the chamber during medium changes as this would have resulted in the simultaneous extraction of the non-adherent cells from the scaffolds. The design of the reactors required therefore that medium exchanges be only performed when medium was in the bottom tubing. This not only required precise timing of medium changes, but also required the medium to flow bi-directionally. This bi-directional flow also increased clogging of the filters.

- Perfusion was achieved by a bi-directional syringe pump that was never in direct contact with the medium. There was always an air gap between the medium and the syringes. When cell densities within the scaffolds increased, pathways for perfusion were restricted and caused a rapid increase in pressure. At later time points the restrictions were high enough to allow compression of the air gaps without any medium perfusing through the constructs. In extreme cases this pressure build-up caused leaking at the interfaces of certain components.

- Gas exchange from the reactor could only occur at one end of the tubing and at a small surface area. This area was also in varying distance to the scaffold depending on the level of the medium in the tubing. Given the diffusion limitation of oxygen in water and the low flow rate resulting in a low turbulence of the medium, the scaffolds likely experienced a constant variance of their O_2 environment throughout perfusion.

Generation II - “Unidirectional perfusion bioreactor”

Learning from the experiences with the “U-tube” reactor, we decided to develop a new bioreactor that was optimized for the use of non-adherent cells.

- The system had to be completely sealed to prohibit contaminants of entering and spreading in the chambers.
- Unidirectional flow was a requirement and no air gaps were permitted.
- No filters could be implemented in the fluid stream after the constructs that would otherwise clog when non-adherent cells were washed into the membranes.
- Medium exchange should be time independent.
- Gas exchange, primarily O_2 diffusion should be at constant distance to the constructs.

Figure 5.9 shows a schematic overview of the unidirectional perfusion bioreactor.

- Medium was loaded into the syringe attached to a syringe pump outside the incubator. This allowed one to change medium at any time point without having to open the incubator. This also kept the medium at a lower temperature for a longer time period, reducing the rate of degradation of cytokines.
- Medium flowed unidirectionally through a long 2 m silicone tube to the gas exchange port, where it equilibrated to the environment of the incubator. Two hydrophobic filters were used here: the first provided a barrier for the medium, containing it within the bioreactor, whereas the second one prohibited contact between the medium and any contaminants.

- After equilibration, the medium flowed through the scaffolds contained within a commercially available polypropylene perfusion chamber (P3D-6, Ebers Medical, Zaragoza, Spain).
- A membrane filter at the bottom of the scaffolds prevented cells from sinking below the scaffolds. Unidirectional flow prevented the filters from clogging.
- A low flow rate of 60 µL/h was chosen to not flush the non-adherent cells out of the scaffolds. Due to the low flow rate we could rely on gravity to contain the cells within the scaffold.
- SmartSite injection sites (Smiths Medical, Dublin, OH, USA) at the entrance of the gas exchange port and at the exit of the perfusion chamber allowed one to easily remove and transport the subunits whilst maintaining a sterile environment. This can be helpful for imaging and cell extraction.
- A silicone tube was attached to the exit port of the perfusion chamber, directing the depleted culture medium into a waste container. This waste container was provided by a standard-sized 50 mL conical tube, that could be easily exchanged when the container was full.

Additional benefits:

- The perfusion chamber could be easily exchanged with other chamber types, making the system very modular.
- All parts are commercially available and are either delivered sterile or can be sterilized in an autoclave.
- Very little mechanical modification is necessary and the entire bioreactor can be assembled without any tools.

- The entire system has a small footprint, and is mainly limited only by the amount of syringes that fit the syringe pump (Fig. 5.10).

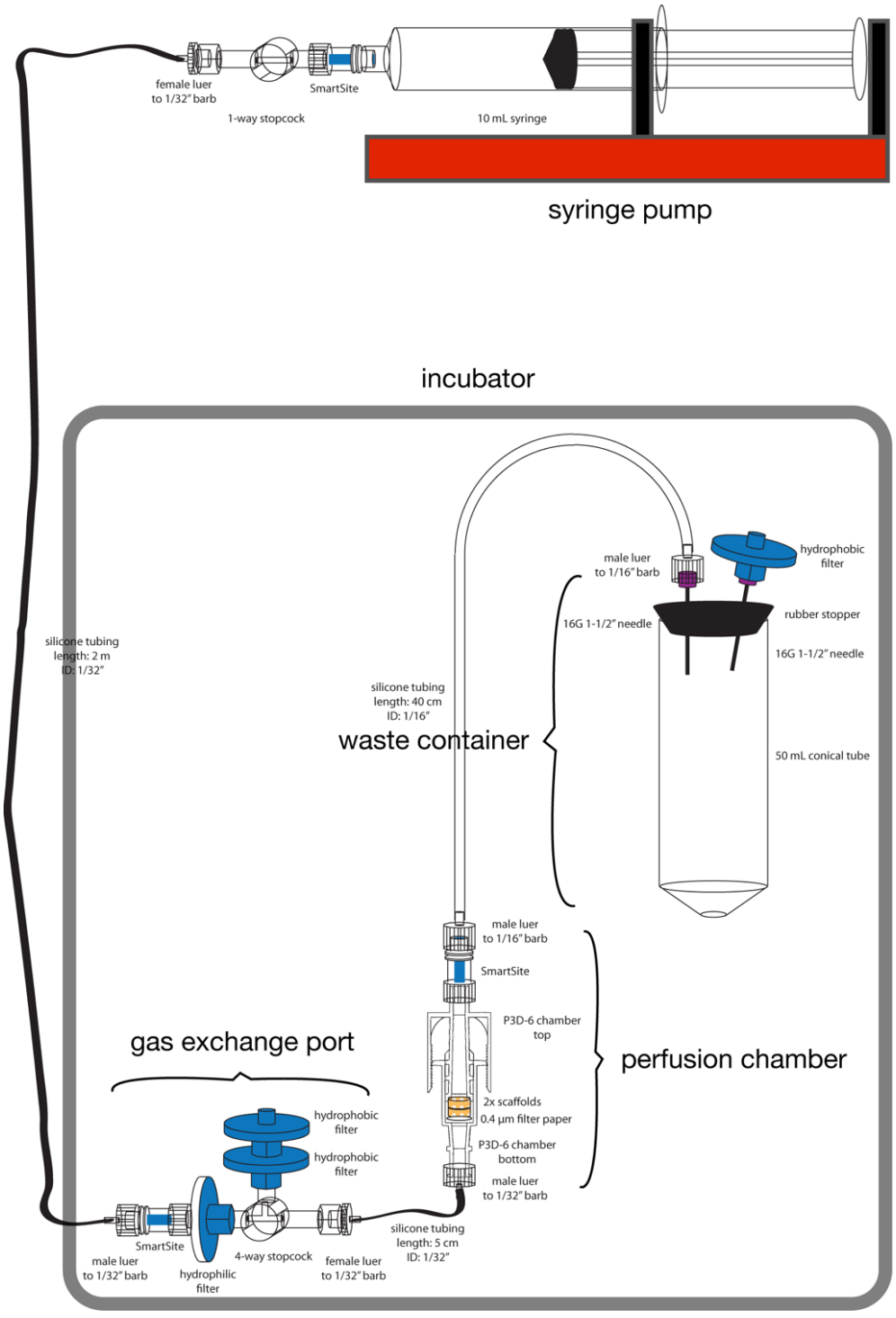

Fig. 5.9. Diagram of new unidirectional perfusion bioreactor.

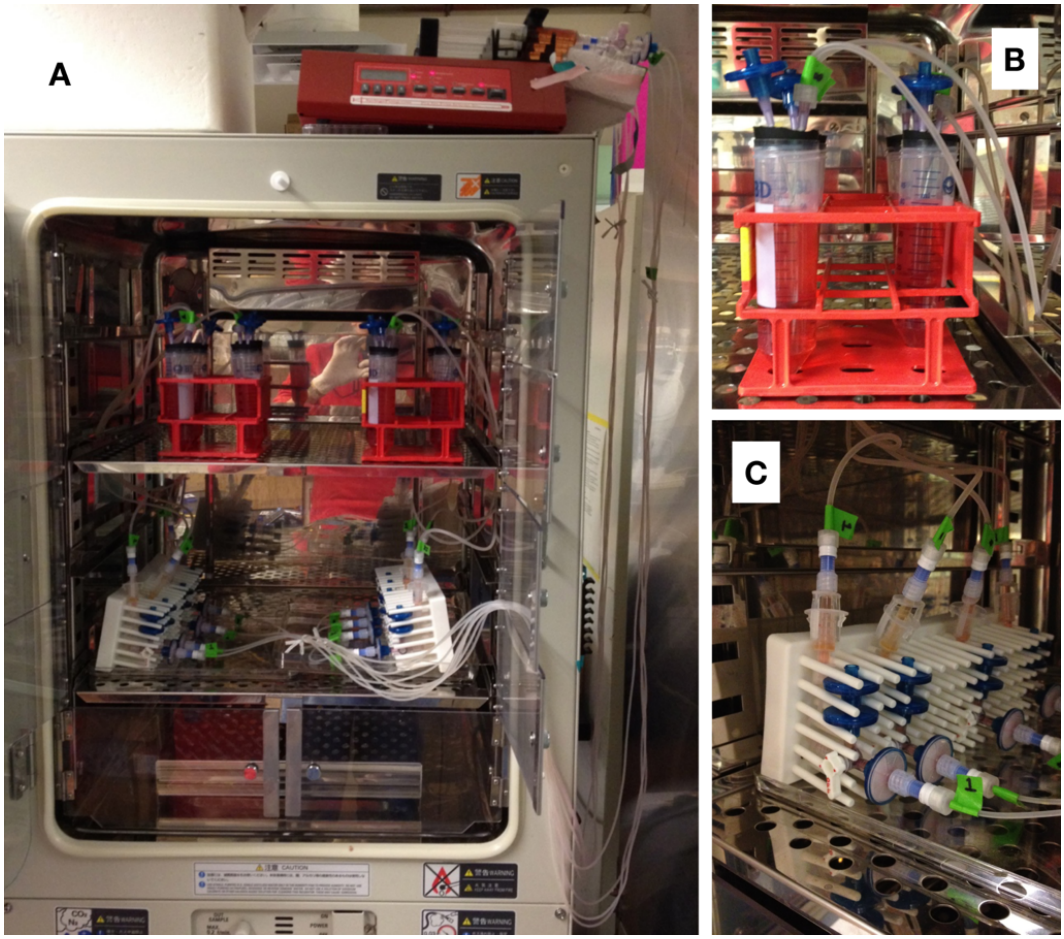

Fig. 5.10. Photographs of new unidirectional perfusion bioreactor in incubator. (A) Entire setup. (B) Waste containers. (C) Gas exchange ports and perfusion chambers.

Comparison of the U-tube and the unidirectional perfusion bioreactor

The following is a comparison of the results obtained when using the two types of perfusion reactors. The data from the U-tube reactor is from the last run using this reactor type, when the system was optimally adjusted for non-adherent cell culture. Though there were many alterations on the reactors over time, the data presented here is still highly representative of all the runs with the U-tube reactor. On the other hand, the data using the unidirectional perfusion bioreactor is only from the first run when it was used.

Materials and Methods

In both bioreactors the same scaffold dimensions and cell numbers were used as previously described.

Scaffolds that were differentiated towards adipocytes were placed in the U-tube bioreactor. Scaffolds were placed with filter membranes into the perfusion chamber the same day as BMMNC were seeded. Due to the previously mentioned clogging of 0.45 µm filters, 3 µm filter membranes were chosen instead and only placed below the scaffold. 8 mL of hHSC expansion medium was injected to the bottom tubing of each reactor. Medium flow rate was set at 1.5 mL / h when flowing from the bottom to the top tubing and 0.3 mL / h in the reverse direction. These flow rates were chosen for two reasons: A. By having a faster flow rate in the direction of the top tubing, one was hoping to retain more cells within the perfusion chamber. B. With a flow volume of 6 mL in each direction, these flow rates would allow the medium to be at the same level every 24 h, allowing precise timing for a medium change from the bottom tubing. Scaffolds were extracted on a bi-weekly basis as previously described.

Scaffolds either kept undifferentiated or differentiated towards adipocytes were kept in individual perfusion chambers of the unidirectional perfusion bioreactors. Scaffolds were placed with 0.45 µm filter membranes into the perfusion chamber the same day as BMMNC were seeded. Medium flow rate was set at 60 µL / h. This flow rate was chosen for two reasons: A. It was slow enough to not flush non-adherent cells out of the scaffold. This was determined by quantifying the amount of cells collected in the waste tube. B. It was fast enough to provide the cells within the chamber with sufficient nutrients. This was both calculated based on the amount of medium required during changes in static culture as well as adjusted based on observation of the pH indicator in the medium below and above the scaffolds. Scaffolds were extracted on a weekly basis as previously described.

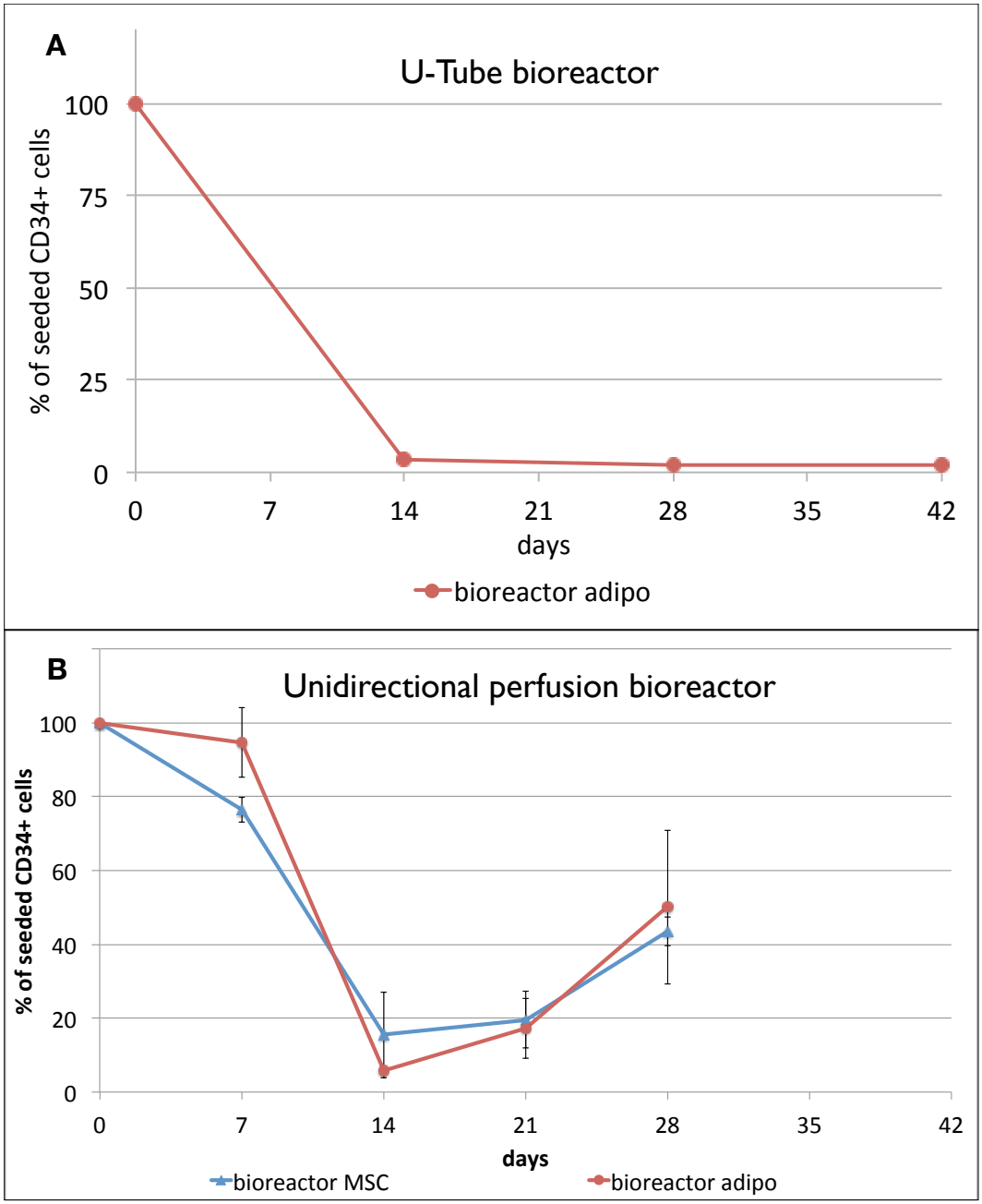

Fig. 5.11. Flow cytometric quantification of $CD34^+$ cells in 3D perfusion cultures, (A) using the U-tube bioreactor and (B) using the unidirectional perfusion bioreactor. Data are given as means ± SD (n ≥ 2).

Results

After seeding in the U-tube reactor, the remaining $CD34^+$ cells dropped to 3.5% at two weeks and remained around 2% at 6 weeks (Fig. 5.11A). In the unidirectional perfusion

bioreactor a drop to almost 6% occurred as well at two weeks, however a gradual increase occurred up to 50% at 4 weeks (Fig. 5.11B). Data acquisition stopped after 4 weeks due to a malfunction of the flow cytometer. No significant differences in $CD34^+$ cell survival were observed between the MSC and adipogenic scaffolds in the unidirectional perfusion bioreactors.

Discussion

Due to the large footprint and the lack of sufficient reactors, only very few data points could be obtained using the U-tube bioreactors. Though these reactors have previously been shown to be beneficial in perfusion cultures of MSCs, the lack of containment within the chamber, likely led to the rapid decrease in $CD34^+$ cells (Wendt 2006). Containment within the chambers was not noticeably improved using the 3 µm membrane filters and this was confirmed by detection of a cell pellet when spinning down the extracted medium during early medium changes. As previously discussed, any filter with a smaller pore size would have rapidly clogged up and interrupted perfusion.

On the other hand, filters of the unidirectional perfusion bioreactors did not clog despite being only 0.45 µm in diameter. This was largely attributed to the unidirectional flow. The smaller footprint of chambers allowed the installment of more chambers in the incubator. Not only was one therefore able to obtain more frequent measurements, but the increase in chambers also allowed comparison of MSC and adipo scaffolds. The lack of significant difference between the two conditions can be attributed to the anatomy of the scaffolds depicted in Figure 5.7B-D. Not only were the feeder layers not evenly distributed throughout the scaffold, but also the amount of adipocytes present was fairly low. Finally, the significant decrease observed at two weeks, may be caused by several different factors: A. The flow rate was indeed too high and did flush cells out of the chamber. These cells might have not been detected when analyzing the waste medium if there were only a few cells in a large volume of medium. B. Improper handling

of the system is another possibility as this was one of the first times this novel system was used for measurements. C. Most of the $CD34^{+}$ cells did not engraft well within the scaffold and either died or differentiated. Further experiments are needed to address these issues.

CHAPTER VI – CONCLUSIONS AND FUTURE DIRECTIONS

In Chapter II we addressed the difficulties that come with HSC research, and highlighted the additional restrictions when using human cells. Though the value of animal research should not be neglected, a greater effort needs to be done to translate these findings to human cells, especially within the hematopoietic field where a lot of the markers and pathways detected in mice have not been identified in humans. In an attempt to add an additional descriptive marker to the identification of human HSCs we've analyzed the characteristics of two populations with different sizes. Based on *in vitro* assays it seems that the smaller cells are more quiescent and possibly more primitive than the larger cells. This would have to be confirmed using a humanized mouse model. No matter the outcome though, this simple method might actually serve as a fast analytical tool to determine the capability of an *in vitro* culture to mimic the bone marrow environment. An ideal environment would provide the appropriate factors to retain the stem cells in their natural state, specifically maintain a small, quiescent "heel" population.

In Chapter III we addressed the issues of in vitro expansion on hMSCs and most notably that differentiation potential rapidly declines when expanding using traditional culture methods. Additionally the use of the conventional markers for hMSCs (CD73, CD90 and CD105) does clearly not suffice in the definition of a true stem cell. The use of the more novel markers CD146 and CD271 would more likely be appropriate markers of stemness and coincide with groups that have observed co-localization of HSCs with $CD146^{+}$ and $CD271^{+}$ cells within the human bone marrow (Tormin 2011). Again, the data shows that these cells are only minimally present in the passaged cultures, therefore culture conditions should be investigated that would improve the expansion of these cell types. Finally, the discovery that hASCs had an increased CD34 expression makes it a very

impractical cell type to use as a feeder layer, despite suggestions that ASCs are the better feeder layers (Nakao 2010).

In Chapter IV we showed an improvement of $CD34^+$ cultures when using a feeder layer. Though the adipogenic feeder layer had the best long-term survival rate, the osteogenic feeder layer also showed an improvement over the current gold standard using an MSC feeder layer. In a future experiment one should therefore combine all three of these feeder layers to observe any synergistic effects. This coincides with observations that there is a three-way co-regulation of hematopoiesis, osteogenesis and adipogenesis within the bone marrow compartment (Botolin 2006; Naveiras 2009).

Another concern regarding the feeder layer was addressed in Chapter IV, where it was decided to not irradiate the feeder culture opposed to widespread use in the literature. This was addressed in the introduction of the chapter and also coincides with the observations of Koller et al. (Koller 1997): their data suggested that an irradiated stroma did not provide discrete niches, but instead acted through soluble signals. This less potent soluble mechanism could also be observed in our transwell studies, where direct cell-cell contact was necessary for the expansion of the hHSCs. However our data was not able to elucidate the role of adipocytes, specifically if direct cell-cell contact is necessary for the adipocytes to maintain the stem cell pool. Due to the belief that adipocytes in the bone marrow down-regulate hematopoiesis by reduced production of GM-CSF and G-CSF, and also by the secretion of TNF-α and adiponectin (Naveiras 2009), one should measure the amount of these soluble factors in the adipogenic cultures. This analysis could be greatly improved if we were able to increase the amount of adipogenic differentiation. Recent research in our lab has shown that the use of an indomethacin based differentiation medium has a great improvement in adipogenic differentiation over the differentiation medium used in this study (data not shown here). Using this medium, differences between feeder layers would likely be large enough to

also obtain statistically significant results when varying the amount of adipocytes present. Caution should be taken though when switching to an alternative differentiation medium, as the resulting adipocytes may be of a different type (e.g. white versus brown adipose tissue) and possibly secrete different growth factors at different levels.

Ultimately though we have shown that the inclusion of adipocytes does have a significant effect on maintaining the $CD34^+$ cell pool *in vitro*. Due to the limitation of human stem cell markers listed in Chapter II, we cannot say for sure if these conditions truly maintain the pool of stem cells or just delay differentiation. For this the suggested measure of soluble factors may also give insight if the feeder layer is also maintaining its secretion in the long-term cultures. Again this is limited by the peeling of the feeder layers where a 3D construct would alleviate this issue.

In Chapter V we've drastically improved our methods to obtain a confluent 3D structure and also a perfusion system that has shown potential for long-term hHSC *in vitro* culture. Using the perfusion system during seeding will likely improve the distribution of the feeder cells throughout the scaffold and using the aforementioned differentiation medium we can possibly obtain a structure that not only shows a confluent stroma, but is also rich in adipocytes. Using such a structure should not only allow us to truly mimic a bone marrow structure but also allow long-term culture of the bone marrow cells. As mentioned in Chapter I this is crucial to:

- assess the effects of new drugs on bone marrow cells for drug screening.
- provide long-term proliferation of whole bone marrow *in vitro* and possibly yield a practical and cost effective source of stem cells. These can then not only be used for further research but can also be used to establish a bank with a wide range of stem cells that may facilitate donor matching for transplants.

ABBREVIATIONS

2D	two-dimensional
3D	three-dimensional
APC	allophycocyanin
ASC	adipose tissue-derived stem cell
BAT	brown adipose tissue
bFGF	basic fibroblast growth factor
BMMNC	bone marrow mono-nuclear cells
bmMSC	bone marrow-derived MSC
BSP	bone sialoprotein
CAR	CXCL12-abundant reticular
CD	cluster of differentiation
CDXX^{+}	positive expression of CDXX
CDXX^{-}	negative expression of CDXX
CFC	colony-forming cell
CFU	colony-forming unit
CML	chronic myelogenous leukemia
COL1A1	collagen type I
DAPI	4',6-diamidino-2-phenylindole
diH2O	deionized water
DMEM	Dulbecco's modified Eagle's medium
DNA	deoxyribonucleic acid
ECM	extracellular matrix
EDTA	ethylenediaminetetraacetic acid
ELISA	enzyme-linked immunesorbent assay
FACS	fluorescence-activated cell sorting
FBS	fetal bovine serum
FDA	Food and Drug Administration of the United State of America
FITC	fluorescein isothiocyanate
FL-1	fluorescence detector 1

Flt-3	fms-like tyrosine kinase 3
FSC	forward scatter
G-CSF	granulocyte colony-stimulating factor
GAPDH	glyceraldehyde 3-phosphate dehydrogenase
GF	growth factor
GLUT4	insulin-responsive glucose transporter 4
GM-CSF	granulocyte–macrophage colony-stimulating factor
HSC	hematopoietic stem cell
HIV	human immunodeficiency virus
HSC	hematopoietic stem cell
IL-3	interleukin 3
IL-6	interleukin 6
IMDM	Iscove's modified Dulbecco's medium
ITRC	intermediate-term repopulating cell
LT-HSC	long-term repopulating hematopoietic stem cell
LTC-IC	long-term culture-initiating cell
MACS	magnetic-activated cell sorting
MDS	Myelodisplastic Syndrome
MEM-α	Minimal essential medium alpha
MPN	myeloproliferative neoplasms
MPP	multipotent progenitor cell
MRI	magnetic resonance imaging
MSC	mesenchymal stem cell
NOD	non-obese diabetic
Px	passage number x
PBS	phosphate buffered saline
PE	phycoerythrin
PerCP	peridinin chlorphyll protein
PET	polyethylene terephthalate
PPARG	perixosome proliferator-activated receptor γ
qPCR	quantitative polymerase chain reaction

RBC	red blood cell
RNA	ribonucleic acid
RUNX2	runt-related transcription factor 2
SCF	stem cell factor
SCID	severe combined immunodeficiency
SNO	specialized niche osteoblast
SSC	side scatter
ST-HSC	short-term repopulating hematopoietic stem cell
SVF	stromal vascular fraction
TCP	tissue culture plastic
TNF-α	tumor necrosis factor alpha
TZD	thiazolidinedione
UCP-1	uncoupling protein 1
VSEL	very small embryonic-like
WAT	white adipose tissue

BIBLIOGRAPHY

Altman, G. H., Diaz, F., et al. (2003). "Silk-based biomaterials." Biomaterials **24**(3): 401-416.

Andrae, J., Gallini, R., et al. (2008). "Role of platelet-derived growth factors in physiology and medicine." Genes & development **22**(10): 1276-1312.

Arai, F. and Suda, T. (2007). "Maintenance of quiescent hematopoietic stem cells in the osteoblastic niche." Ann N Y Acad Sci **1106**: 41-53.

Barry, F. P. and Murphy, J. M. (2004). "Mesenchymal stem cells: clinical applications and biological characterization." Int J Biochem Cell Biol **36**(4): 568-584.

Benveniste, P., Frelin, C., et al. (2010). "Intermediate-term hematopoietic stem cells with extended but time-limited reconstitution potential." Cell stem cell **6**(1): 48-58.

Beresford, J. N. and Owen, M. E. (1998). Marrow stromal cell culture. Cambridge [England]; New York, Cambridge University Press.

Beyer Nardi, N. and da Silva Meirelles, L. (2006). "Mesenchymal stem cells: isolation, in vitro expansion and characterization." Handbook of experimental pharmacology(174): 249-282.

Bianco, P. (2011). "Bone and the hematopoietic niche: a tale of two stem cells." Blood **117**(20): 5281-5288.

Boitano, A. E., Wang, J., et al. (2010). "Aryl hydrocarbon receptor antagonists promote the expansion of human hematopoietic stem cells." Science **329**(5997): 1345-1348.

Botolin, S. and McCabe, L. R. (2006). "Inhibition of PPARgamma prevents type I diabetic bone marrow adiposity but not bone loss." Journal of cellular physiology **209**(3): 967-976.

Botolin, S. and McCabe, L. R. (2007). "Bone loss and increased bone adiposity in spontaneous and pharmacologically induced diabetic mice." Endocrinology **148**(1): 198-205.

Boxall, S. A., Cook, G. P., et al. (2008). "Haematopoietic repopulating activity in human cord blood CD133(+) quiescent cells." Bone Marrow Transplant.

Boyum, A. (1968). "Isolation of mononuclear cells and granulocytes from human blood. Isolation of monuclear cells by one centrifugation, and of granulocytes by combining centrifugation and sedimentation at 1 g." Scandinavian journal of clinical and laboratory investigation. Supplementum **97**: 77-89.

Braccini, A., Wendt, D., et al. (2005). "Three-dimensional perfusion culture of human bone marrow cells and generation of osteoinductive grafts." Stem Cells **23**(8): 1066-1072.

Brookes, M. (1967). "Blood flow rates in compact and cancellous bone, and bone marrow." Journal of anatomy **101**(Pt 3): 533-541.

Casamassima, F., Ruggiero, C., et al. (1989). "Hematopoietic bone marrow recovery after radiation therapy: MRI evaluation." Blood **73**(6): 1677-1681.

Charbord, P. (2010). "Bone marrow mesenchymal stem cells: historical overview and concepts." Human gene therapy **21**(9): 1045-1056.

Clark, B. R., Jamieson, C., et al. (1997). "Human long-term bone marrow culture." Methods Mol Biol **75**: 249-256.

Consortium, T. U. (2011). Ongoing and future developments at the Universal Protein Resource. Nucleic acids research. **39:** D214-D219.

D'Ippolito, G., Schiller, P. C., et al. (1999). "Age-related osteogenic potential of mesenchymal stromal stem cells from human vertebral bone marrow." Journal of bone and mineral research : the official journal of the American Society for Bone and Mineral Research **14**(7): 1115-1122.

da Silva Meirelles, L., Caplan, A. I., et al. (2008). "In search of the in vivo identity of mesenchymal stem cells." Stem Cells **26**(9): 2287-2299.

de Jong, J. L. and Zon, L. I. (2005). "Use of the zebrafish system to study primitive and definitive hematopoiesis." Annual review of genetics **39**: 481-501.

de Wynter, E. A., Buck, D., et al. (1998). "CD34+AC133+ cells isolated from cord blood are highly enriched in long-term culture-initiating cells, NOD/SCID-repopulating cells and dendritic cell progenitors." Stem Cells **16**(6): 387-396.

Dexter, T. M., Allen, T. D., et al. (1977). "Conditions controlling the proliferation of haemopoietic stem cells in vitro." Journal of cellular physiology **91**(3): 335-344.

Di Iorgi, N., Mittelman, S. D., et al. (2008). "Differential effect of marrow adiposity and visceral and subcutaneous fat on cardiovascular risk in young, healthy adults." International journal of obesity **32**(12): 1854-1860.

DiMascio, L., Voermans, C., et al. (2007). "Identification of adiponectin as a novel hemopoietic stem cell growth factor." Journal of immunology **178**(6): 3511-3520.

Dominici, M., Le Blanc, K., et al. (2006). "Minimal criteria for defining multipotent mesenchymal stromal cells. The International Society for Cellular Therapy position statement." Cytotherapy **8**(4): 315-317.

Dubois, S. G., Floyd, E. Z., et al. (2008). "Isolation of human adipose-derived stem cells from biopsies and liposuction specimens." Methods in molecular biology **449**: 69-79.

Dunbar, C. E., Takatoku, M., et al. (2001). "The impact of ex vivo cytokine stimulation on engraftment of primitive hematopoietic cells in a non-human primate model." Annals of the New York Academy of Sciences **938**: 236-244; discussion 244-235.

Ecklund, K., Vajapeyam, S., et al. (2010). "Bone marrow changes in adolescent girls with anorexia nervosa." Journal of bone and mineral research : the official journal of the American Society for Bone and Mineral Research **25**(2): 298-304.

Engler, A. J., Sen, S., et al. (2006). "Matrix elasticity directs stem cell lineage specification." Cell **126**(4): 677-689.

Festy, F., Hoareau, L., et al. (2005). "Surface protein expression between human adipose tissue-derived stromal cells and mature adipocytes." Histochemistry and cell biology **124**(2): 113-121.

Friedenstein, A. J., Gorskaja, J. F., et al. (1976). "Fibroblast precursors in normal and irradiated mouse hematopoietic organs." Experimental hematology **4**(5): 267-274.

Fruhbeck, G. (2006). "Intracellular signalling pathways activated by leptin." The Biochemical journal **393**(Pt 1): 7-20.

Gersbach, C. A., Le Doux, J. M., et al. (2006). "Inducible regulation of Runx2-stimulated osteogenesis." Gene Ther **13**(11): 873-882.

Gimble, J. M. (1990). "The function of adipocytes in the bone marrow stroma." New Biol **2**(4): 304-312.

Gimble, J. M., Robinson, C. E., et al. (1996). "The function of adipocytes in the bone marrow stroma: an update." Bone **19**(5): 421-428.

Gimble, J. M., Zvonic, S., et al. (2006). "Playing with bone and fat." Journal of cellular biochemistry **98**(2): 251-266.

Glatz, J. F., Luiken, J. J., et al. (2010). "Membrane fatty acid transporters as regulators of lipid metabolism: implications for metabolic disease." Physiological reviews **90**(1): 367-417.

Glowacki, J. and Mizuno, S. (2008). "Collagen scaffolds for tissue engineering." Biopolymers **89**(5): 338-344.

Goncalves, R., Lobato da Silva, C., et al. (2006). "A Stro-1(+) human universal stromal feeder layer to expand/maintain human bone marrow hematopoietic stem/progenitor cells in a serum-free culture system." Exp Hematol **34**(10): 1353-1359.

Gothot, A., Pyatt, R., et al. (1997). "Functional heterogeneity of human CD34(+) cells isolated in subcompartments of the G0 /G1 phase of the cell cycle." Blood **90**(11): 4384-4393.

Greenberg, P., Cox, C., et al. (1997). "International scoring system for evaluating prognosis in myelodysplastic syndromes." Blood **89**(6): 2079-2088.

Gregory, C. A., Prockop, D. J., et al. (2005). "Non-hematopoietic bone marrow stem cells: molecular control of expansion and differentiation." Experimental cell research **306**(2): 330-335.

Gurevitch, O., Slavin, S., et al. (2007). "Conversion of red bone marrow into yellow - Cause and mechanisms." Med Hypotheses **69**(3): 531-536.

Hagenmuller, H., Hofmann, S., et al. (2007). "Non-invasive time-lapsed monitoring and quantification of engineered bone-like tissue." Ann Biomed Eng **35**(10): 1657-1667.

Hancox, N. M. (1972). Biology of bone. Cambridge [Eng.], University Press.

Helmy, K. Y., Patel, S. A., et al. (2010). "Stem cells and regenerative medicine: accomplishments to date and future promise." Therapeutic delivery **1**(5): 693-705.

Ho, A. D., Wagner, W., et al. (2008). "Heterogeneity of mesenchymal stromal cell preparations." Cytotherapy **10**(4): 320-330.

Hofmann, S., Hagenmuller, H., et al. (2007). "Control of in vitro tissue-engineered bone-like structures using human mesenchymal stem cells and porous silk scaffolds." Biomaterials **28**(6): 1152-1162.

Hofmeister, C. C., Zhang, J., et al. (2007). "Ex vivo expansion of umbilical cord blood stem cells for transplantation: growing knowledge from the hematopoietic niche." Bone Marrow Transplant **39**(1): 11-23.

Holst, J., Watson, S., et al. (2010). "Substrate elasticity provides mechanical signals for the expansion of hemopoietic stem and progenitor cells." Nature biotechnology **28**(10): 1123-1128.

Howlader, N., Noone, A., et al. (2010) "SEER Cancer Statistics Review, 1975-2008."

Huang, S. and Czech, M. P. (2007). "The GLUT4 glucose transporter." Cell metabolism **5**(4): 237-252.

Iscove, N. N. (1984). Culture of Lymphocytes and Hemopoietic Cells in Serum-Free Medium. New York, NY, Alan R. Liss, Inc.

Ito, M., Hiramatsu, H., et al. (2002). "NOD/SCID/gamma(c)(null) mouse: an excellent recipient mouse model for engraftment of human cells." Blood **100**(9): 3175-3182.

Izadpanah, R., Kaushal, D., et al. (2008). "Long-term in vitro expansion alters the biology of adult mesenchymal stem cells." Cancer Res **68**(11): 4229-4238.

Jang, Y. K., Jung, D. H., et al. (2006). "Mesenchymal stem cells feeder layer from human umbilical cord blood for ex vivo expanded growth and proliferation of hematopoietic progenitor cells." Ann Hematol **85**(4): 212-225.

Jing, K., Heo, J. Y., et al. (2009). "Expression regulation and function of Pref-1 during adipogenesis of human mesenchymal stem cells (MSCs)." Biochimica et biophysica acta **1791**(8): 816-826.

Kershaw, E. E. and Flier, J. S. (2004). "Adipose Tissue as an Endocrine Organ." Journal of Clinical Endocrinology & Metabolism **89**(6): 2548-2556.

Khoshnoodi, J., Pedchenko, V., et al. (2008). "Mammalian collagen IV." Microscopy research and technique **71**(5): 357-370.

Kim, H., Cho, H. J., et al. (2010). "CD31+ cells represent highly angiogenic and vasculogenic cells in bone marrow: novel role of nonendothelial CD31+ cells in neovascularization and their therapeutic effects on ischemic vascular disease." Circulation research **107**(5): 602-614.

Kim, H. J., Kim, U. J., et al. (2008). "Bone tissue engineering with premineralized silk scaffolds." Bone **42**(6): 1226-1234.

Kim, H. J., Kim, U. J., et al. (2007). "Bone regeneration on macroporous aqueous-derived silk 3-D scaffolds." Macromol Biosci **7**(5): 643-655.

Kim, U. J., Park, J., et al. (2005). "Three-dimensional aqueous-derived biomaterial scaffolds from silk fibroin." Biomaterials **26**(15): 2775-2785.

Koller, M. R., Bender, J. G., et al. (1992). "Beneficial effects of reduced oxygen tension and perfusion in long-term hematopoietic cultures." Ann N Y Acad Sci **665**: 105-116.

Koller, M. R., Manchel, I., et al. (1997). "Importance of parenchymal:stromal cell ratio for the ex vivo reconstitution of human hematopoiesis." Stem Cells **15**(4): 305-313.

Kondo, M., Wagers, A. J., et al. (2003). "Biology of hematopoietic stem cells and progenitors: implications for clinical application." Annual review of immunology **21**: 759-806.

Laschober, G. T., Brunauer, R., et al. (2009). "Leptin receptor/CD295 is upregulated on primary human mesenchymal stem cells of advancing biological age and distinctly marks the subpopulation of dying cells." Experimental gerontology **44**(1-2): 57-62.

Laubach, J. P., Mitsiades, C. S., et al. (2009). "Novel therapies in the treatment of multiple myeloma." J Natl Compr Canc Netw **7**(9): 947-960.

Le Blanc, K., Tammik, C., et al. (2003). "HLA expression and immunologic properties of differentiated and undifferentiated mesenchymal stem cells." Experimental hematology **31**(10): 890-896.

Lecka-Czernik, B. (2012). "Marrow fat metabolism is linked to the systemic energy metabolism." Bone **50**(2): 534-539.

Li, C., Vepari, C., et al. (2006). "Electrospun silk-BMP-2 scaffolds for bone tissue engineering." Biomaterials **27**(16): 3115-3124.

Li, L. and Xie, T. (2005). "Stem cell niche: structure and function." Annual review of cell and developmental biology **21**: 605-631.

Liu, F., Akiyama, Y., et al. (2008). "Changes in the expression of CD106, osteogenic genes, and transcription factors involved in the osteogenic differentiation of human bone marrow mesenchymal stem cells." J Bone Miner Metab **26**(4): 312-320.

Locasciulli, A., Oneto, R., et al. (2007). "Outcome of patients with acquired aplastic anemia given first line bone marrow transplantation or immunosuppressive treatment in the last decade: a report from the European Group for Blood and Marrow Transplantation (EBMT)." Haematologica **92**(1): 11-18.

Lodish, H. F. (2008). Molecular cell biology. New York, W.H. Freeman.

Mandal, B. B., Park, S. H., et al. (2011). "Stem cell-based meniscus tissue engineering." Tissue engineering. Part A **17**(21-22): 2749-2761.

Marieb, E. N. (2009). Essentials of human anatomy & physiology, Pearson/Benjamin Cummings.

Marolt, D., Augst, A., et al. (2006). "Bone and cartilage tissue constructs grown using human bone marrow stromal cells, silk scaffolds and rotating bioreactors." Biomaterials **27**(36): 6138-6149.

Martin, I., Wendt, D., et al. (2004). "The role of bioreactors in tissue engineering." Trends in biotechnology **22**(2): 80-86.

Mauney, J. and Volloch, V. (2010). "Human bone marrow-derived stromal cells show highly efficient stress-resistant adipogenesis on denatured collagen IV matrix but not on its native counterpart: implications for obesity." Matrix biology : journal of the International Society for Matrix Biology **29**(1): 9-14.

Mauney, J. R., Nguyen, T., et al. (2007). "Engineering adipose-like tissue in vitro and in vivo utilizing human bone marrow and adipose-derived mesenchymal stem cells with silk fibroin 3D scaffolds." Biomaterials **28**(35): 5280-5290.

Mauney, J. R., Volloch, V., et al. (2005). "Matrix-mediated retention of adipogenic differentiation potential by human adult bone marrow-derived mesenchymal stem cells during ex vivo expansion." Biomaterials **26**(31): 6167-6175.

Mayani, H., Dragowska, W., et al. (1993). "Characterization of functionally distinct subpopulations of CD34+ cord blood cells in serum-free long-term cultures supplemented with hematopoietic cytokines." Blood **82**(9): 2664-2672.

Mayani, H., Guilbert, L. J., et al. (1992). "Biology of the hemopoietic microenvironment." Eur J Haematol **49**(5): 225-233.

McBeath, R., Pirone, D. M., et al. (2004). "Cell shape, cytoskeletal tension, and RhoA regulate stem cell lineage commitment." Developmental cell **6**(4): 483-495.

Meinel, L., Fajardo, R., et al. (2005). "Silk implants for the healing of critical size bone defects." Bone **37**(5): 688-698.

Meinel, L., Hofmann, S., et al. (2006). "Osteogenesis by human mesenchymal stem cells cultured on silk biomaterials: comparison of adenovirus mediated gene transfer and protein delivery of BMP-2." Biomaterials **27**(28): 4993-5002.

Meinel, L., Karageorgiou, V., et al. (2004). "Bone tissue engineering using human mesenchymal stem cells: effects of scaffold material and medium flow." Ann Biomed Eng **32**(1): 112-122.

Mendez-Ferrer, S., Michurina, T. V., et al. (2010). "Mesenchymal and haematopoietic stem cells form a unique bone marrow niche." Nature **466**(7308): 829-834.

Meunier, P., Aaron, J., et al. (1971). "Osteoporosis and the replacement of cell populations of the marrow by adipose tissue. A quantitative study of 84 iliac bone biopsies." Clin Orthop Relat Res **80**: 147-154.

Mishima, S., Nagai, A., et al. (2010). "Effective ex vivo expansion of hematopoietic stem cells using osteoblast-differentiated mesenchymal stem cells is CXCL12 dependent." European journal of haematology **84**(6): 538-546.

Mitchell, J. B., McIntosh, K., et al. (2006). "Immunophenotype of human adipose-derived cells: temporal changes in stromal-associated and stem cell-associated markers." Stem Cells **24**(2): 376-385.

Moen, M. D., McKeage, K., et al. (2007). "Imatinib: a review of its use in chronic myeloid leukaemia." Drugs **67**(2): 299-320.

Murray, L. J., Young, J. C., et al. (1999). "Thrombopoietin, flt3, and kit ligands together suppress apoptosis of human mobilized CD34+ cells and recruit primitive CD34+ Thy-1+ cells into rapid division." Experimental hematology **27**(6): 1019-1028.

Nakao, N., Nakayama, T., et al. (2010). "Adipose tissue-derived mesenchymal stem cells facilitate hematopoiesis in vitro and in vivo: advantages over bone marrow-derived mesenchymal stem cells." The American journal of pathology **177**(2): 547-554.

Naveiras, O., Nardi, V., et al. (2009). "Bone-marrow adipocytes as negative regulators of the haematopoietic microenvironment." Nature **460**(7252): 259-263.

Nazarov, R., Jin, H. J., et al. (2004). "Porous 3-D scaffolds from regenerated silk fibroin." Biomacromolecules **5**(3): 718-726.

NIH (2001). Stem Cells: Scientific Progress and Future Research Directions., Department of Health and Human Services.

O'Connor, K. C., Song, H., et al. (2003). "Extracellular matrix substrata alter adipocyte yield and lipogenesis in primary cultures of stromal-vascular cells from human adipose." Biotechnology letters **25**(23): 1967-1972.

Palsson, B. O., Paek, S. H., et al. (1993). "Expansion of human bone marrow progenitor cells in a high cell density continuous perfusion system." Biotechnology (N Y) **11**(3): 368-372.

Park, I. S., Han, M., et al. (2009). "The correlation between human adipose-derived stem cells differentiation and cell adhesion mechanism." Biomaterials **30**(36): 6835-6843.

Park, J. S., Chu, J. S., et al. (2011). "The effect of matrix stiffness on the differentiation of mesenchymal stem cells in response to TGF-beta." Biomaterials **32**(16): 3921-3930.

Patrick, C. W., Jr. and Wu, X. (2003). "Integrin-mediated preadipocyte adhesion and migration on laminin-1." Annals of biomedical engineering **31**(5): 505-514.

Pearson, T., Greiner, D. L., et al. (2008). "Humanized SCID mouse models for biomedical research." Current topics in microbiology and immunology **324**: 25-51.

Petzer, A. L., Hogge, D. E., et al. (1996). "Self-renewal of primitive human hematopoietic cells (long-term-culture-initiating cells) in vitro and their expansion in defined medium." Proceedings of the National Academy of Sciences of the United States of America **93**(4): 1470-1474.

Pittenger, M. F., Mackay, A. M., et al. (1999). "Multilineage potential of adult human mesenchymal stem cells." Science **284**(5411): 143-147.

Pruitt, K. D., Tatusova, T., et al. (2009). "NCBI Reference Sequences: current status, policy and new initiatives." Nucleic acids research **37**(Database issue): D32-36.

Quirici, N., Soligo, D., et al. (2002). "Isolation of bone marrow mesenchymal stem cells by anti-nerve growth factor receptor antibodies." Experimental hematology **30**(7): 783-791.

Reyes, J. M., Fermanian, S., et al. (2006). "Metabolic changes in mesenchymal stem cells in osteogenic medium measured by autofluorescence spectroscopy." Stem Cells **24**(5): 1213-1217.

Reyes, M., Dudek, A., et al. (2002). "Origin of endothelial progenitors in human postnatal bone marrow." The Journal of clinical investigation **109**(3): 337-346.

Rice, W. L., Kaplan, D. L., et al. (2010). "Two-photon microscopy for non-invasive, quantitative monitoring of stem cell differentiation." PLoS One **5**(4): e10075.

Riley, R. S., Ben-Ezra, J. M., et al. (2008) "An Illustrated Guide to Performing the Bone Marrow Aspiration and Biopsy."

Robak, T. and Wierzbowska, A. (2009). "Current and emerging therapies for acute myeloid leukemia." Clinical Therapeutics **31**(Part 2): 2349-2370.

Robinson, S., Niu, T., et al. (2005). "Ex vivo expansion of umbilical cord blood." Cytotherapy **7**(3): 243-250.

Rocha, V., Cornish, J., et al. (2001). "Comparison of outcomes of unrelated bone marrow and umbilical cord blood transplants in children with acute leukemia." Blood **97**(10): 2962-2971.

Romanov, Y. A., Darevskaya, A. N., et al. (2005). "Mesenchymal stem cells from human bone marrow and adipose tissue: isolation, characterization, and differentiation potentialities." Bulletin of experimental biology and medicine **140**(1): 138-143.

Rosen, C. J., Ackert-Bicknell, C., et al. (2009). "Marrow fat and the bone microenvironment: developmental, functional, and pathological implications." Critical reviews in eukaryotic gene expression **19**(2): 109-124.

Rozman, C., Feliu, E., et al. (1989). "Age-related variations of fat tissue fraction in normal human bone marrow depend both on size and number of adipocytes: a stereological study." Exp Hematol **17**(1): 34-37.

Sass, M. D. (1979). "Effect of ammonium chloride on osmotic behavior of red cells in nonelectrolytes." Am J Physiol **236**(5): C238-243.

Seita, J. and Weissman, I. L. (2010). "Hematopoietic stem cell: self-renewal versus differentiation." Wiley interdisciplinary reviews. Systems biology and medicine **2**(6): 640-653.

Sera, Y., LaRue, A. C., et al. (2009). "Hematopoietic stem cell origin of adipocytes." Experimental hematology **37**(9): 1108-1120, 1120 e1101-1104.

Shockley, K. R., Lazarenko, O. P., et al. (2009). "PPARgamma2 nuclear receptor controls multiple regulatory pathways of osteoblast differentiation from marrow mesenchymal stem cells." Journal of cellular biochemistry **106**(2): 232-246.

Smyth, M. J. and Wharton, W. (1992). "Differentiation of A31T6 proadipocytes to adipocytes: a flow cytometric analysis." Experimental cell research **199**(1): 29-38.

Sotiropoulou, P. A., Perez, S. A., et al. (2006). "Characterization of the optimal culture conditions for clinical scale production of human mesenchymal stem cells." Stem Cells **24**(2): 462-471.

Sovalat, H., Scrofani, M., et al. (2011). "Identification and isolation from either adult human bone marrow or G-CSF-mobilized peripheral blood of CD34(+)/CD133(+)/CXCR4(+)/ Lin(-)CD45(-) cells, featuring morphological, molecular, and phenotypic characteristics of very small embryonic-like (VSEL) stem cells." Experimental hematology **39**(4): 495-505.

Suga, H., Matsumoto, D., et al. (2009). "Functional implications of CD34 expression in human adipose-derived stem/progenitor cells." Stem cells and development **18**(8): 1201-1210.

Sul, H. S. (2009). "Minireview: Pref-1: role in adipogenesis and mesenchymal cell fate." Mol Endocrinol **23**(11): 1717-1725.

Suva, D., Garavaglia, G., et al. (2004). "Non-hematopoietic human bone marrow contains long-lasting, pluripotential mesenchymal stem cells." Journal of cellular physiology **198**(1): 110-118.

Tapp, H., Hanley, E. N., Jr., et al. (2009). "Adipose-derived stem cells: characterization and current application in orthopaedic tissue repair." Experimental biology and medicine **234**(1): 1-9.

Tavassoli, M., Watson, L. R., et al. (1979). "Retention of hemopoiesis in tail vertebrae of newborn rats." Cell and tissue research **200**(2): 215-222.

Tefferi, A. and Vainchenker, W. (2011). "Myeloproliferative neoplasms: molecular pathophysiology, essential clinical understanding, and treatment strategies." Journal of clinical oncology : official journal of the American Society of Clinical Oncology **29**(5): 573-582.

ten Dijke, P., Korchynskyi, O., et al. (2003). "Controlling cell fate by bone morphogenetic protein receptors." Molecular and cellular endocrinology **211**(1-2): 105-113.

Tormin, A., Li, O., et al. (2011). "CD146 expression on primary nonhematopoietic bone marrow stem cells is correlated with in situ localization." Blood **117**(19): 5067-5077.

Travlos, G. S. (2006). "Normal structure, function, and histology of the bone marrow." Toxicologic pathology **34**(5): 548-565.

Tuljapurkar, S. R., McGuire, T. R., et al. (2011). "Changes in human bone marrow fat content associated with changes in hematopoietic stem cell numbers and cytokine levels with aging." Journal of anatomy **219**(5): 574-581.

Tyler, D. T. (2005). Components of Bone Marrow**:** Poster.

Uebersax, L., Hagenmuller, H., et al. (2006). "Effect of scaffold design on bone morphology in vitro." Tissue Eng **12**(12): 3417-3429.

Van Epps, D. E., Bender, J., et al. (1994). "Harvesting, characterization, and culture of CD34+ cells from human bone marrow, peripheral blood, and cord blood." Blood cells **20**(2-3): 411-423.

Vater, C., Kasten, P., et al. (2011). "Culture media for the differentiation of mesenchymal stromal cells." Acta biomaterialia **7**(2): 463-477.

Vepari, C. and Kaplan, D. L. (2007). "Silk as a Biomaterial." Progress in polymer science **32**(8-9): 991-1007.

Vunjak-Novakovic, G., Tandon, N., et al. (2010). "Challenges in cardiac tissue engineering." Tissue engineering. Part B, Reviews **16**(2): 169-187.

Wagner, W., Wein, F., et al. (2005). "Comparative characteristics of mesenchymal stem cells from human bone marrow, adipose tissue, and umbilical cord blood." Exp Hematol **33**(11): 1402-1416.

Wang, X., Wenk, E., et al. (2009). "Growth factor gradients via microsphere delivery in biopolymer scaffolds for osteochondral tissue engineering." J Control Release **134**(2): 81-90.

Wang, Y., Singh, A., et al. (2006). "Expansion and osteogenic differentiation of bone marrow-derived mesenchymal stem cells on a vitamin C functionalized polymer." Biomaterials **27**(17): 3265-3273.

Watson, R. T. and Pessin, J. E. (2001). "Intracellular organization of insulin signaling and GLUT4 translocation." Recent progress in hormone research **56**: 175-193.

Weadock, K. S., Miller, E. J., et al. (1996). "Effect of physical crosslinking methods on collagen-fiber durability in proteolytic solutions." Journal of biomedical materials research **32**(2): 221-226.

Weinstein, R., Riordan, M. A., et al. (1989). "Dual role of fibronectin in hematopoietic differentiation." Blood **73**(1): 111-116.

Weissman, I. L. and Shizuru, J. A. (2008). "The origins of the identification and isolation of hematopoietic stem cells, and their capability to induce donor-specific transplantation tolerance and treat autoimmune diseases." Blood **112**(9): 3543-3553.

Wendt, D., Stroebel, S., et al. (2006). "Uniform tissues engineered by seeding and culturing cells in 3D scaffolds under perfusion at defined oxygen tensions." Biorheology **43**(3-4): 481-488.

Wilson, A. and Trumpp, A. (2006). "Bone-marrow haematopoietic-stem-cell niches." Nat Rev Immunol **6**(2): 93-106.

Wise, S. G., Mithieux, S. M., et al. (2009). "Engineered tropoelastin and elastin-based biomaterials." Advances in protein chemistry and structural biology **78**: 1-24.

Yeo, G. C., Keeley, F. W., et al. (2011). "Coacervation of tropoelastin." Advances in Colloid and Interface Science **167**(1-2): 94-103.

Yin, A. H., Miraglia, S., et al. (1997). "AC133, a novel marker for human hematopoietic stem and progenitor cells." Blood **90**(12): 5002-5012.

Yin, T. and Li, L. (2006). "The stem cell niches in bone." J Clin Invest **116**(5): 1195-1201.

Yoshikawa, H., Tamai, N., et al. (2009). "Interconnected porous hydroxyapatite ceramics for bone tissue engineering." J R Soc Interface **6 Suppl 3**: S341-348.

Zhang, H., Chen, J., et al. (2012). "A Meta-Analysis of Unrelated Donor Umbilical Cord Blood Transplantation versus Unrelated Donor Bone Marrow Transplantation in Acute Leukemia Patients." Biology of blood and marrow transplantation : journal of the American Society for Blood and Marrow Transplantation.

Zhang, Y., Chai, C., et al. (2006). "Co-culture of umbilical cord blood CD34+ cells with human mesenchymal stem cells." Tissue Eng **12**(8): 2161-2170.

Zhang, Y., Harada, A., et al. (1995). "Tumor necrosis factor (TNF) is a physiologic regulator of hematopoietic progenitor cells: increase of early hematopoietic progenitor cells in TNF receptor p55-deficient mice in vivo and potent inhibition of progenitor cell proliferation by TNF alpha in vitro." Blood **86**(8): 2930-2937.